

DISSERTATION FOR THE DEGREE OF DOCTOR OF PHILOSOPHY (PHD)

ARID1A mediates the antiproliferative effects of bexarotene  
and carvedilol combination treatment in normal and transformed  
breast cells

by Sham Jdeed

UNIVERSITY OF DEBRECEN

DOCTORAL SCHOOL OF MOLECULAR CELLULAR AND IMMUNE BIOLOGY

DEBRECEN, 2022

DISSERTATION FOR THE DEGREE OF DOCTOR OF PHILOSOPHY (PHD)

ARID1A mediates the antiproliferative effects of bexarotene  
and carvedilol combination treatment in normal and transformed  
breast cells

by Sham Jdeed, PharmD, MSc

Supervisor: Iván P. Uray, MD, PhD



UNIVERSITY OF DEBRECEN

DOCTORAL SCHOOL OF MOLECULAR CELLULAR AND IMMUNE BIOLOGY

DEBRECEN, 2022

## Table of Contents

List of Tables.....	7
List of Figures.....	9
List of Abbreviations.....	11
1. Abstract.....	17
2. Introduction.....	18
2.1 Cancer Biology.....	18
2.1.1. Origin of cancer cells.....	18
2.1.2. Hallmarks of cancer.....	18
2.2 Breast Cancer.....	21
2.2.1. Breast Cancer incidence.....	21
2.2.2. Breast cancer definition and classification.....	22
2.2.3. Main pathways activated in breast cancer.....	23
2.2.4. Breast Cancer treatment.....	26
2.2.5. Breast Cancer Chemoprevention.....	27
2.3 Retinoids and Reginoids.....	27
2.3.1. Retinoid metabolism.....	27
2.3.2. Retinoid/Reginoid signaling.....	27
2.3.3. Retinoids/ Reginoids in Medicine.....	29
2.3.4. Retinoids/ Reginoids in Cancer.....	29
2.4 The Sympathetic System.....	30
2.4.1. The adrenergic signaling.....	30
2.4.2. The adrenergic signaling role in cancer.....	32
2.4.3. Carvedilol.....	33
2.5 Chromatin Remodeling.....	33
2.5.1. DNA Packaging.....	33
2.5.2. Chromatin remodeling and the regulation of biological processes.....	33
2.5.3. SWI/SNF.....	35
2.5.4. ARID1A.....	36
2.6 Hypothesis and Aim of the study.....	40
3. Materials.....	41
3. 1 Equipment.....	41
3. 2 Consumable.....	42
3. 3 Chemicals and Reagents.....	42

3. 4 Drugs.....	44
3. 5 Buffers.....	44
3. 6 Kits.....	45
3. 7 Enzymes.....	46
3. 8 Oligonucleotides.....	46
3. 9 Primary and Secondary Antibodies.....	48
3. 10 Human cell lines.....	50
3. 11 Cell culture media and Supplements.....	50
3. 12 Software.....	51
3. 13 Tools and software used for ChIP-Seq data analysis and visualization.....	51
3. 14 Accession numbers of available ChIP-Seq datasets generated in this study...	53
4. Methods.....	55
4. 1 Cell cultivation system.....	55
4.1.1. Cell culture and treatment.....	55
4.1.2. siRNA transfection.....	55
4.1.3. Escherichia. Coli transformation with ARID1A cDNA plasmid and further plasmid extraction procedure from the bacterial stock .....	57
4.1.4. Transfecting human cell lines with cDNA plasmids.....	57
4.1.5. Proliferation assay.....	58
4.1.6. Colony formation assay.....	58
4.1.7. Wound healing assay.....	59
4.1.8. Studying the effect of IGF-1R neutralization on MCF-7 cell proliferation	59
4. 2 Protein Biochemical technologies.....	60
4.2.1. Protein extraction and protein concentration measurement.....	60
4.2.2. Western-blotting.....	60
4.2.3. Protein samples preparation for sequencing.....	61
4.2.4. Immunocytochemistry/Immunofluorescence.....	61
4. 3 Genomics and Analysis of nucleic acids.....	62
4.3.1. RNA isolation.....	62
4.3.2. RT-qPCR.....	62
4.3.3. Chromatin immunoprecipitation (ChIP).....	64
4.3.4. ChIP-qPCR.....	65
4. 4 Data analysis and Bioinformatics.....	65
4.4.1. Fluorescent image analysis.....	65
4.4.2. ChIP-Seq data processing.....	66

4.4.3. Statistical analysis.....	66
5. Results.....	67
5. 1 Bexarotene and carvedilol (Bex+Carv) combination treatment decreased normal and transformed breast cell's proliferation.....	67
5. 2 Bexarotene and carvedilol combination treatment induced ARID1A protein levels in HME-hTert cells.....	68
5. 3 Overexpression of ARID1A protein levels.....	69
5. 4 Identifying putative ARID1A target genes through in Silico analysis of publicly available CHIP-Seq and RNA-Seq datasets.....	71
5. 5 Optimization of ARID1A chromatin immunoprecipitation protocol in breast cell lines.....	72
5. 6 ARID1A genomic characterization in MCF-7 cells upon Bex+Carv combination treatment.....	74
5. 7 ARID1A is enriched to regulatory elements assigned to genes involved in cell proliferation and IGF1 signaling pathway upon Bex+Carv treatment in MCF-7 cells.....	77
5. 8 Insulin like growth factor receptor 1 (IGF-1R) and Insulin receptor substrate (IRS1) protein levels are downregulated upon Bex+Carv treatment.....	81
5. 9 ARID1A knock down increased IGF1R protein expression and MCF-7 cell growth.....	82
5. 10 ARID1A ChIP optimization in HME-hTert cells.....	83
5. 11 ARID1A is recruited to regulatory elements assigned to genes involved in transforming growth factor Beta pathway upon bexarotene and carvedilol combination treatment in HME-hTert cells.....	85
5. 12 ARID1A enrichment to its target regions upon Bex+Carv treatment is associated with a change in the expression of the corresponding genes in HME-hTert cells.....	87
5. 13 ARID1A knock-down affects its target gene expression in HME-hTert cells	88
5. 14 ARID1A controls SMAD4 nuclear translocation upon Bex+Carv treatment	89
5. 15 ARID1A mediates the suppression effects of Bex+Carv on gene and protein expression of the mesenchymal markers.....	90
6. Discussion.....	93
6. 1 Bex+Carv treatment induced ARID1A protein expression levels in a transcriptional in dependent manner.....	95
6. 2 Bex+Carv treatment affects ARID1A genomic occupancy in MCF-7 cells to be more enriched to regulatory elements assigned to genes involved in epithelial cell proliferation.....	95
6. 3 ARID1A is recruited to regulatory elements assigned to genes involved in IGF-1 signaling pathway upon Bex+Carv treatment in MCF-7 cells.....	96

6. 4ARID1A enrichment to regulatory elements assigned to genes involved in transforming growth factor Beta pathway is associated with a change in the expression of target genes upon Bex and Carv combination treatment in HME-hTert cells.....	97
6. 5 ARID1A mediates the suppression effects of Bex+Carv on gene and protein expression of the mesenchymal markers.....	99
7. Summary.....	100
8. List of Main New Scientific results.....	104
9. Reference.....	105
10. List of Publications related to the dissertation.....	114
11.Acknowledgment.....	115
12.Keywords.....	116

## **List of tables:**

Table 2-1: Breast cancer molecular classification.....	22
Table 3-1: List of equipment used.....	41
Table 3-2: List of consumables.....	42
Table 3-3: List of chemicals.....	43
Table 3-4: List of the used drugs.....	44
Table 3-5: List of the used buffers.....	44
Table 3-6: List of used kits.....	45
Table 3-7: List of used enzymes.....	46
Table 3-8: List of primers used for RT-qPCR.....	46
Table3-9: List of primers used for ChIP-qPCR during ChIP optimization step.....	47
Table3-10: List of primers used for ChIP-qPCR against the selected regions .....	47
Table 3-11: List of used primary antibodies.....	48
Table 3-12: List of used conjugated secondary antibodies.....	49
Table 3-13: List of used cell lines.....	50
Table 3-14: List of used culture media and supplements.....	50
Table 3-15: List of used software.....	51
Table 3-16: List of tools used for ChIP-Seq using Linux server .....	51
Table 3-17: List of tools used for ChIP-Seq using Galaxy server .....	51
Table 3-18: List of software used for ChIP-Seq analysis and visualization.....	53
Table 3-19: List of publicly available datasets.....	53
Table 3-20: List of tools used for RNA-Seq using Galaxy server.....	54
Table 4-1: siRNA transfection protocol in HME-hTert and MCF-7 breast cells.....	56
Table 4-2: HEK293 cells transfection protocol with cDNA plasmid using TransIT-BrCa reagent.....	58
Table 4-3: Reverse transcription reaction for Taq-man assay.....	63
Table 4-4: quantitative polymerase chain reaction qPCR reaction for Taq-man assay.....	63

Table 4-5: Reverse transcription reaction for SYBR GREEN assay.....64

Table 4-6: quantitative polymerase chain reaction qPCR reaction for SYBR GREEN assay.....64

## **List of Figures:**

Figure 2-1: Schematic diagram illustrating tumor development stages.....	18
Figure 2-2: Cancer hallmarks and therapeutic targets that interfere with each of the acquired capability.....	21
Figure 2-3: IGF-1/IGF-1R signaling pathway.....	25
Figure 2-4: TGF- $\beta$ SMAD and non-SMAD dependent signaling pathway.....	26
Figure 2.5: Molecular signaling pathway mediated by retinoids and rexinoids in target cells.....	29
Figure 2-6: alpha 1 and Beta1 adrenergic signaling pathway.....	32
Figure 2-7: The process of chromatin remodeling through ATP-dependent complexes or histone modification.....	35
Figure 2-8: SWI/SNF chromatin remodeling complex.....	36
Figure 4-1: Steps of the colony formation assay.....	59
Figure 4-2: wound healing assay using culture insert.....	59
Figure 4-3: Chromatin immunoprecipitation procedure .....	65
Figure 5-1: Bex+Carv treatment is associated with antiproliferative effects in HME-hTert cells and MCF-7 cells.....	68
Figure 5-2: Bexarotene and carvedilol combination treatment induced ARID1A protein but not transcript levels in HME-hTert cells.....	69
Figure 5-3: ARID1A overexpression in HEK293 cell line.....	71
Figure 5-4: Identifying putative ARID1A target genes through in silico analysis of publicly available ChIP-Seq and RNA-Seq datasets.....	72
Figure 5-5: ARID1A ChIP-Seq optimization in breast cancer cell lines.....	74
Figure 5-6: ARID1A genomic occupancy upon Bex+Carv treatment in MCF-7 cells.....	76
Figure 5-7: ARID1A motif enrichment analysis in MCF-7 cells.....	77
Figure 5-8: Validation of ARID1A ChIP-Seq in MCF-7 cells.....	78
Figure 5-9: Functional analysis of ARID1A genomic occupancy in MCF-7 cells upon Bex+Carv treatment.....	80
Figure 5-10: Determination of IGF-1R and IRS1 protein levels upon Bex+Carv treatment and the effect of ARID1A behind it.....	82

Figure 5-11: ARID1A knockdown induces IGF1R protein expression associated with an increase in MCF-7 cell proliferation.....	83
Figure 5-12: ARID1A ChIP optimization in HME-hTert cells.....	85
Figure 5-13: ARID1A is recruited to regulatory elements assigned to genes involved in TGF- $\beta$ signaling pathway and proliferation regulation upon Bex+Carv combination treatment in HME-hTert cells.....	87
Figure 5-14: ARID1A target's gene expression is changing upon Bex+Carv treatment in HME-hTert cells.....	88
Figure 5-15: ARID1A KD affects the expression of its putative target genes.....	89
Figure 5-16: Bexarotene and carvedilol combination affects TGF- $\beta$ signaling pathway activation, mediated by ARID1A.....	90
Figure 5-17: Bexarotene and carvedilol combination treatment affects the downstream signaling of ARID1A target genes.....	92
Figure 6-1: Schematic diagram showing a summary of the detected effects of Bex+Carv treatment on MCF-7 transformed cells mediated by ARID1A actions...	97
Figure 6-2: Schematic diagram showing a summary of the detected effects of Bex+Carv treatment on HME-hTert normal cells mediated by ARID1A and BRG1 actions.....	100
Figure 7-1: Schematic diagram representing the effects of Bex+Carv treatment on MCF-7 cells .....	103
Figure 7-2: Schematic diagram representing the effects of Bex+Carv treatment on HME-hTert cells .....	104

## **List of Abbreviations**

### **Units and sizes**

°C: degree Celsius  
bp: base pair  
g: gram  
kb: kilobasepairs  
kD: kilodalton  
kg: kilogramm  
l: liter  
M: molar  
mA: milliamperere  
min: minute  
mL: milliliter  
mm: millimeter  
mM: millimolar  
rpm: rotations per minute  
RT: room temperature  
s: second  
SD: standard deviation  
SEM: standard error of the mean  
T<sub>m</sub>: average melting temperature  
UV: ultraviolet  
Volt: unit for voltage  
x g: multiplied by gravity force  
µg: microgram  
µl: microlitre  
µm: micrometer  
µM: micromolar

### **Chemical and Biochemical compounds**

aa: amino acids  
ACN: Acetonitrile  
ADP: Adenosine diphosphate  
AI: Aromatase inhibitors  
AP: Ammonium per sulfate  
ATP: adenosine-5'-triphosphate  
BCA: bicinchoninic acid assay  
Bex: Bexarotene  
BSA: bovine-serum-albumin  
cAMP: cyclic adenosine monophosphate  
Carv: Carvedilol  
cDNA: complementary deoxyribonucleic acid  
DAPI: 4',6-diamidino-2-phenylindole

DMEM: dulbecco's modified Eagle's medium  
DMSO: dimethylsulfoxide  
DNA: deoxyribonucleic acid  
dNTP: deoxynucleotide triphosphates  
DTT: Dithiothreitol  
EDTA: ethylene diaminetetraacetic acid  
FA: Formaldehyde  
FBS: fetal bovine serum  
H<sub>2</sub>O<sub>2</sub>: Hydrogen Peroxide  
HCl: Hydrochloric acid  
IAA: Indole-3-acetic acid  
LB: Lysogeny broth  
MEBM: Mammary Epithelial Basal Medium  
MgCl<sub>2</sub>: Magnesium chloride  
mRNA: messenger ribonucleic acid  
NaAc: Sodium acetate  
NaCl: Sodium Chloride  
NaDoc: Sodium deoxycholate  
NaHCO<sub>3</sub>: Sodium Bicarbonate  
PBS: phosphate-buffered saline  
PBST: phosphate buffered saline containing 10 % tween 20  
RNA: ribonucleic acid  
Rpm: rotations per minute  
RPMI: Roswell Park Memorial Institute  
SDS: sodium dodecyl sulfate  
SERMs: Selective estrogen receptor modulators  
siARID1A: small interfering RNA against ARID1A  
siNT: small interfering RNA non-targeted  
siRNA: Small interfering RNA  
TBS: Tris buffered saline  
TBST: Tris-buffered saline –Tween  
TE: Tris EDTA  
TEMED: Tetramethylethylenediamine  
TFA: Trifluoroacetic acid  
Veh: Vehicle

### **Proteins and peptides**

AKT: Protein kinase B  
AP-1: Activator protein 1  
ARID1A: AT rich interactive domain 1A  
ARID1B: AT rich interactive domain 1B  
ARID2: AT rich interactive domain 2

ATM: ataxia teleangiectasia mutated  
ATR: ATM and Rad3-related  
BAD: BCL2 Associated Agonist Of Cell Death  
BAF: BRG1/BRM-Associated Factor  
Bcl2: B-cell lymphoma 2  
BMP6: Bone Morphogenetic Protein 6  
B-Raf: proto-oncogene, serine/threonine kinase  
BRCA1: BReast CAncer gene 1  
BRG1: Brahma-related gene-1  
BRM: BRAHMA  
C/ebpa: CCAAT Enhancer Binding Protein Alpha  
CBP: CREB-binding protein  
CCNB2: Cyclin B2  
CCND1: Cyclin D1  
Cdc2: Cyclin-dependent kinase 1  
CDH1: E-cadherin  
CDKN1A: Cyclin dependent kinase inhibitor 1 A  
CHD: Chromodomain helicase DNA binding protein  
Cldn4: Claudin 4  
COUP-TF: COUP Transcription Factor  
CREB: cAMP-response element binding protein  
DHRS3: dehydrogenase/reductase superfamily  
EGFR: epidermal growth factor receptor  
EPAC: exchange protein directly activated by cAMP  
ER: Estrogen receptor  
ErbB: erythroblastic leukemia viral oncogene  
ERK: Extracellular signal-regulated kinase 1/2  
EZH2: Enhancer Of Zeste 2 Polycomb Repressive Complex 2 Subunit  
FGF: Fibroblast growth factors  
FN1: Fibronectin  
FOXA1: Forkhead box A1  
FOXM1: Forkhead box M1  
FOXO3: Forkhead box o3  
FOXQ1: Forkhead box Q1  
FXR: Farnesoid X receptor  
GPCR: G-protein-coupled receptors  
GRHL2: Grainyhead like transcription factor 2  
Gsk-3 $\beta$ : Glycogen synthase kinase 3 beta  
H: Histone  
H2AX: H2A histone family member X  
H3K4,6,9,or 27: Histone 3 lysine 4,6,9,or 27  
HAT: Histone acetyltransferases  
HDAC: Histone deacetylases

HDMs: Histone Demethylases  
Her-2: Human epidermal growth factor receptor  
HMOX1: Heme Oxygenase 1  
HMT: Histone methyltransferases  
Hnf4: Hepatocyte Nuclear Factor 4 Alpha  
hTert: Telomerase reverse transcriptase  
IGF1: Insulin growth factor 1  
IGF-1R: Insulin growth factor 1 receptor  
IGFBP: insulin growth factor binding protein  
IL6: Interleukin 6  
IL8: Interleukin 8  
INSR: Insulin Receptor  
IRS1: insulin receptor substrate 1  
ISWI: Imitation SWItch  
KLF4: Kruppel like Factor 4  
KRAS: Kirsten rat sarcoma virus  
KRT18: Keratin 18  
LXR: liver X receptor  
MAPK: Mitogen-activated protein kinase  
MEK: Mitogen-activated protein kinase kinase  
MKK: Mitogen-activated protein kinase kinase  
MMP: Matrix metalloproteinases  
mTOR: Mammalian target of rapamycin  
N-CAD: N-cadherin  
NCOR: nuclear receptor corepressor  
NF-kB: nuclear factor kappa-light-chain-enhancer of activated B cells  
PARP: Poly (ADP-ribose) polymerase  
PBAF: Polybromo-associated BAF complex  
PDK1: 3-Phosphoinositide-dependent kinase 1  
PI3K: Phosphoinositide 3-kinases  
PIK3IP1: Phosphoinositide-3-Kinase Interacting Protein 1  
PIP2: Phosphatidylinositol 4,5-bisphosphate  
PIP3: Phosphatidylinositol (3,4,5)-trisphosphate  
PKA: protein kinase A  
PNS: parasympathetic nervous system  
PPAR: peroxisome proliferator-activated receptors  
PPARG: Peroxisome Proliferator Activated Receptor Gamma  
PTEN: Phosphatase and TENsin homolog  
RA: Retinoic acid  
RALDH: Retinaldehyde dehydrogenase  
RAR: Retinoic acid Receptor  
Ras: Rat sarcoma virus  
RBPs: RNA-binding proteins  
RNAPII: RNA polymerase II

RTK: Receptor tyrosine kinases  
RXR: retinoid X receptor  
SIN3A: SIN3 Transcription Regulator Family Member A  
SMAD: small mothers against decapentaplegic  
SMAD4: SMAD family member 4  
SMART: silencing mediator of retinoid and thyroid hormone receptor  
SNS: sympathetic nervous system  
SP1: specificity protein 1  
STAT: Signal transducer and activator of transcription  
STRA6: Signaling receptor and transporter of retinol  
SWI/SNF: SWItch/Sucrose Non-Fermentable  
T3: Triiodothyronine  
T4: thyroxine  
TAK1: Transforming growth factor beta-activated kinase 1  
TBR1/TBRI: TGF- $\beta$  receptor  
TCF/LEF: T-cell factor/lymphoid enhancer factor  
TFF1: Trefoil Factor 1  
TGF- $\beta$ : transforming growth factor beta  
TGFBR2: transforming growth factor beta receptor 2  
TR: Thyroid hormone receptors  
TRAF6: TNF Receptor Associated Factor 6  
TRE: TPA response elements  
TSS: Transcription start site  
VDR: vitamin D receptor  
VEGF: Vascular endothelial growth factor

### **Other abbreviations**

ANOVA: Analysis of variance  
AtRA: All-trans retinoic acid  
BED: Browser Extensible Data  
BWA: Burrows-Wheeler Alignment  
ChIP: Chromatin Immunoprecipitation  
ChIP-qPCR: Chromatin immunoprecipitation-quantitative Polymerase Chain Reaction  
COPD: Chronic obstructive pulmonary disease  
CTCL: Cutaneous T-cell lymphoma  
DCIS: Ductal carcinoma in situ  
EMT: epithelial–mesenchymal transition  
ENCODE: Encyclopedia of DNA Elements  
FDA: Food and Drug Administration  
FDR: False Discovery rate  
 $\gamma$ : gamma  
GREAT: Genomic Regions Enrichment of Annotations Tool  
h: human  
HEK: human embryonic kidney cells

hg19: Homo sapiens (human) genome assembly GRCh37  
HMEC: Human mammary epithelial cell  
HPLC-MS: High Performance Liquid chromatography–mass spectrometry  
hs: human sample  
ICC: Immunocytochemistry  
IDC: Invasive ductal carcinoma  
IGV: Integrative Genomics Viewer  
ILC: Invasive Lobular carcinoma  
IP: Immunoprecipitation  
KD: knock down  
KO: Knock Out  
LBD: ligand-binding domain  
LCIS: Lobular carcinoma in situ  
MACS2: Model-based Analysis of CHIP-Seq  
MQ: Milli-Q  
NB: Neuroblastoma  
NFW: Nuclease free water  
NSCLC: non-small-cell lung carcinoma  
PCR: polymerase chain reaction  
PVDF: Polyvinylidene fluoride  
QC: Quality Control  
RPPA: Reverse phase proteomic assay  
RT: Reverse Transcriptase  
RT-PCR: reverse transcription-polymerase chain reaction  
Seq: Sequencing  
SRA: Sequence Read Archive  
TNM: Tumor, Node, Metastasis  
WB: Western Blotting  
Wnt: Wingless-related integration site  
WT: wild type  
 $\alpha$ : alpha  
 $\beta$ : Beta

## 1. Abstract:

Drug synergy is the usage of a combination of agents to produce an effect that is greater than the sum of the effects generated through the administration of each drug individually. That could help reduce toxicity due to high doses beside that targeting various pathways simultaneously reduces the chance of developing drug resistance. Retinoid X receptor (RXR) selective agonist, bexarotene (Bex), in combination with the non-selective beta blocker, carvedilol (Carv), showed synergistic antiproliferative effects on normal epithelial breast cells (HME-hTert) and on the breast cancer cell line (MCF-7). In order to identify the molecular mechanism underlying these effects, we studied the proteomic profile and gene expression signature upon the combination treatment of Bex +Carv. The results demonstrated that the protein levels of ARID1A, AT-rich interactive domain 1 A, are induced upon the combination treatment in normal breast cells but not in the cancer cells. We hypothesized that ARID1A modulate nucleosome organization upon Bex+Carv treatment to regulate the expression of genes related to cell transformation and proliferation regulation. To test our hypothesis, we performed chromatin immunoprecipitation followed by deep sequencing to identify ARID1A target regions under Bex+Carv treatment in normal and transformed cells. We also investigated the correlation between ARID1A enrichment and its target genes' transcript and protein levels through RT-qPCR, Western-blotting, or immunostaining assays. Moreover, we knocked down ARID1A using a specific siRNA pool to study the impact of ARID1A on its target genes. The results revealed that ARID1A was enriched to regulatory elements assigned to genes involved in the insulin-like growth factor signaling pathway upon Bex+Carv treatment in MCF-7 cells. ARID1A enrichment was associated with downregulation in IGF-1R and IRS1 protein expression upon Bex+Carv treatment, these effects were abolished upon ARID1A knockdown. The results refer that one of the mechanisms underlying the antiproliferative effects of Bex+Carv treatment in MCF-7 cells is through suppressing the expression of IGF-1 signaling pathway related genes which was orchestrated by ARID1A actions. Furthermore, ARID1A and BRG1 were identified to be recruited to regulatory elements assigned to genes involved in the transforming growth factor beta (TGF- $\beta$ ) signaling pathway upon Bex+Carv in HME-hTert cells. Bex+Carv treatment was associated with an alteration of TGF- $\beta$  downstream activity reflected in the suppression of the EMT program regulator's gene and protein expression including fibronectin-1 and N-cadherin. Overall, the results showed that bexarotene and carvedilol combination treatment behaves differently in normal or transformed cells targeting TGF- $\beta$  or IGF-1 signaling pathways, respectively. These effects were mediated by the actions of the tumor suppressor ARID1A.

## 2. Introduction

### 2.1 Cancer Biology

#### 2.1.1. Origin of cancer cells:

Cancer development is a multistep process, in which a normal cell acquires tumor-promoting mutations (such as activation of oncogenes or suppression of tumor suppressor genes) after being exposed to carcinogens or under the effect of environmental factors (**Figure 2-1**). On the other hand, cancer-promoting mutations can be inherited. Studies have shown that the accumulation of at least 2-3 mutations is required for tumor initiation, which might take years. Tumors are heterogenic on different levels including the expression profile, cell morphology and treatment response. Heterogeneity can be between tumors within the same organ (Intertumoral heterogeneity) such as the distinct isotypes of breast cancers with different expression markers. On the other hand, heterogeneity can be within the same tumor (intratumoral heterogeneity), for instance, breast cancer cells expressing estrogen receptors varied from 1 to 100% of the cells in an individual tumor. Moreover, cancer can be monoclonal; arising from one cell origin, or polyclonal, in which a tumor is composed of subpopulations arising from different cell origins [1, 2].

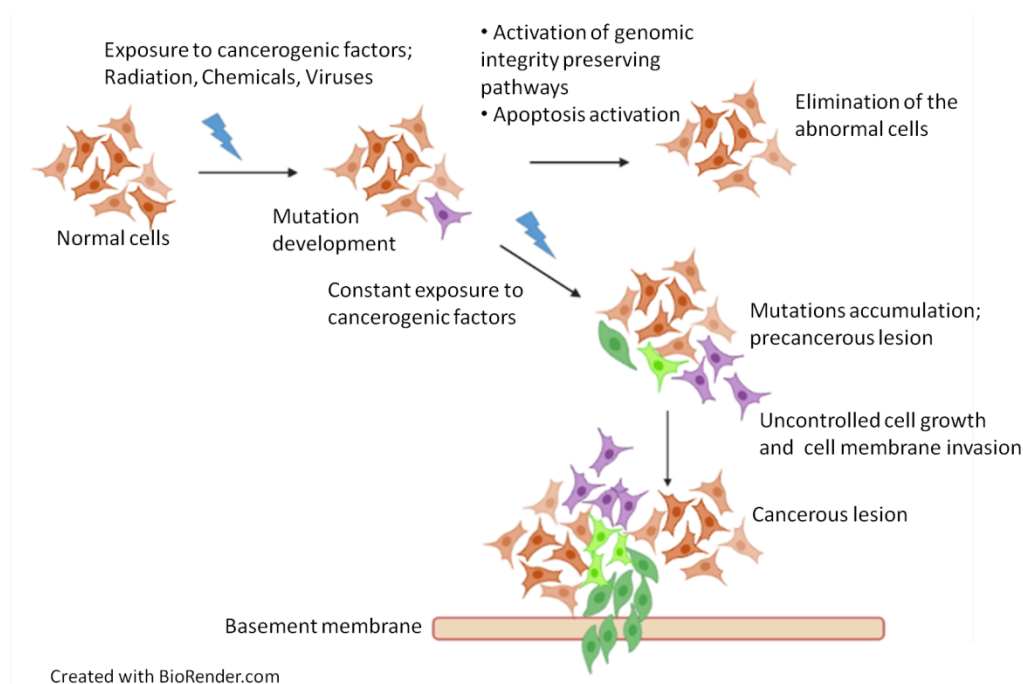


**Figure 2-1:** Schematic diagram illustrating tumor development stages.

#### 2.1.2. Hallmarks of cancer:

Cancer cells during the multistep formation process acquire certain biological capabilities that enable them to survive; these features are called cancer hallmarks. To maintain proliferative signaling, cancer cells could produce and release growth signals or they might increase the expression of growth receptors. Moreover, mutations in the structure of some proteins in a growth signaling pathway may lead to its constitutive activation. For instance, activating mutation in the structure of B-Raf protein leads to

sustained activation of B-Raf to mitogen-activated protein kinase (MAPK) pathway [3]. In addition, a mutation in the catalytic subunit of phosphoinositide-3-kinase leads to constitutive stimulation of the AKT/PI3K signaling pathway [4]. Cancer cells acquire the ability to resist the programmed cell death signals, through either activating anti-apoptosis proteins or suppressing the pro-apoptotic factors [5].

Normal cells have a limited number of divisions due to the presence of telomere repeats which are DNA sequences that protect the ends of chromosomes and are shortened after each DNA replication cycle. In the next step, cells enter a non-proliferative but viable state called senescence. Telomerase is a DNA polymerase enzyme that elongates the telomeric DNA through the addition of telomere repeats. Usually, in normal cells, the expression of the telomerase gene is not activated. However, one of the hallmarks of cancerous cells is to acquire a mutation leading to telomerase enzyme gene expression activation giving cancer cells replicative immortality characteristics [6, 7].

Angiogenesis is the process of blood vessel formation to deliver nutrients and oxygen to the proliferating cells. Angiogenic molecules include VEGFs (vascular endothelial growth factors) which produce MMPs (matrix metalloproteinases). MMPs degrade the extracellular matrix in order to provide space for the endothelial cells to migrate. Endothelial cells are then assembled in tube forms with the help of integrin  $\alpha$ - $\beta$  adhesion proteins to form blood vessels [8].

Metastasis is a late but a life-threatening stage during cancer development. In which tumor cells dissociate from the primary tumor, evade the surrounding tissue, and enter the blood vessels (intravasation), traveling through the blood vessels followed by extravasation when they reach a suitable environment in adjacent or distant organs to form a secondary tumor [9]. Epithelial to mesenchymal transition (EMT) is a process in which epithelial cancer cells acquire mesenchymal characteristics and become mesenchymal cells, which are considered the leading cells during the migration process [10]. Signaling pathways that activate the EMT process, promote metastasis such as the transforming growth factor beta (TGF- $\beta$ ) pathway, Wnt/ $\beta$ -catenin and Notch signaling [11].

During biological processes such as DNA replication and because of exposure to environmental factors, DNA damage can be induced in the cell at a rate that might reach thousands of molecular lesions per cell per day [12], depending on the inducing factor. However, cells have several DNA monitoring mechanisms including DNA repair machinery, DNA damage checkpoint and others to keep the genetic material error-free [13]. Genomic instability is an enabling cancer characteristic that was identified recently. This could happen through defects or mutations affecting molecules or systems that participate in detecting and activating DNA damage repair machinery, directly participating in repairing DNA lesions, and/or antagonizing the effects of mutagens in producing DNA damage [14, 15].

Within normal cells there is an accurate balance in the expression of growth driver genes, which are referred to as proto-oncogenes, and tumor suppressor genes coding for proteins that play critical roles in monitoring cell proliferation and DNA damage repair [16]. Proto-oncogenes have important roles in stimulating normal cell growth; however, a mutation in one allele of the gene is enough to transform it to an oncogene, which stimulates cell growth in an uncontrolled manner. On the other hand, mutations in the two copies of the tumor suppressor genes are needed to inactivate its function in controlling cell behavior. The activation of oncogenes and inactivation of tumor suppressors are implicated in cancer development [17, 18]. P53 is one of the most important tumor suppressors that participates in maintaining the genetic material intact, and it is labeled as the "guardian of the genome" [19]. Mutations in p53 are frequently detected in different cancer types [20]. Moreover, BRCA1 is a gene that plays a role in double-strand DNA damage repair, which is also mutated in a wide range of tumors leading to genomic instability.

The cancer microenvironment is a critical factor in tumor development which can be infiltrated with immune cells that play distinct roles in tumor progression based on their type. While helper T cells and cytotoxic T lymphocytes have anti-tumor effects [21, 22], the monocytes which differentiate to tumor-associated macrophages in the tumor environment produce cytokines and growth factors that have immunosuppressive effects and enhance tumor proliferation, angiogenesis and invasion [23]. Thus cancer cells could evade immune destruction signals through enhancing tumor-promoting inflammation.

Mammalian cells to proliferate and survive need energy in the form of adenosine triphosphate (ATP). Glucose is one of the main sources of ATP production. In differentiated cells, in the presence of adequate nutrients and oxygen, the main pathway in producing energy is through oxidative phosphorylation. However, in the absence of oxygen, cells follow the anaerobic glycolysis to produce ATP through the production of lactate. In proliferative or tumor cells, with or without oxygen presence, cells rely on aerobic glycolysis in order to generate building blocks needed for cell growth and proliferation such as amino acids, fatty acids and nucleotides as well as producing ATP. They rely on glycolysis to produce energy even with adequate oxygen (aerobic glycolysis) is called the "Warburg effect" [24].

All the previously mentioned hallmarks can be targeted on different levels. For instance, growth factor receptor inhibitors to decline growth rate, inhibitors for cell cycle triggering molecules such as cyclin-dependent kinase inhibitors, telomerase inhibitors, anti-inflammatory agents, immune-activating drugs, inhibitors of vascular endothelial growth factor signaling to prevent angiogenesis, inhibitors of molecules participating in the EMT process, aerobic glycolysis suppressors, and pro-apoptotic analogues [25] (**Figure 2-2**).

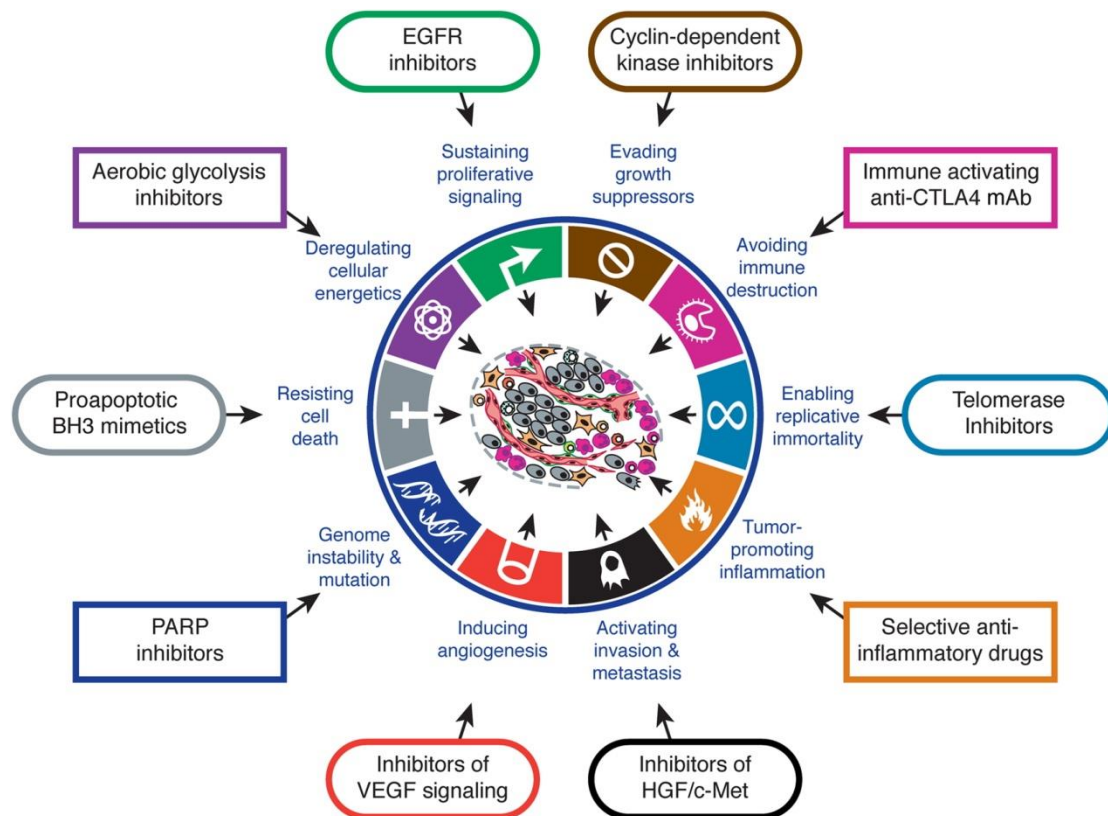


**Figure 2-2:** Cancer hallmarks and therapeutic targets that interfere with each of the acquired capabilities [25].

## 2.2 Breast Cancer

### 2.2.1. Breast Cancer incidence:

Breast cancer is one of the most commonly occurring cancers and the second leading cause for cancer-related deaths among women after lung cancer [26]. In 2020, 2.3 million women were diagnosed with breast cancer with about 685 thousand death cases worldwide [27]. Breast cancer is responsible for 23% of all cancer patients, associating with 14% of cancer deaths [28].

Breast cancer occurs mainly in women, with a small percentage of men who can be diagnosed with the disease (0.5-1%). A number of risk factors might play a role in disease development including; age over 40, not having children, not breastfeeding, family history, alcohol harmful consumption, tobacco smoke exposure, radiation exposure and obesity. Certain genetic mutations could increase the chance of developing the disease including, mutations in BRCA1/BRCA2 genes, mutations in the p53 gene (the guardian of the genome), the tumor suppressor PTEN, which can provide a level of early detection of breast cancer and its prevention [29]. Although breast cancer development is associated with modern life, most incidence and death cases are reported in developing countries. The reason might be due to the lack of education and awareness of the importance of regular screening as well as the shortage of treatment availability [30].

### 2.2.2. Breast cancer definition and classification:

Breast cancer can be defined as the abnormal growth of breast cells to form a tumor, which is considered malignant when cells start to invade the basal membrane toward neighboring tissues. Breast cancer is a heterogeneous disease due to a series of genetic and epigenetic changes that occur during the process of tumor formation and development [31]. It can be classified based on different criteria. The histological classification depends on the type of cells in which the disease arose as well as on cells' behavior. Ductal carcinoma in situ (DCIS), lobular carcinoma in situ (LCIS), invasive ductal carcinoma (IDC) or invasive lobular carcinoma (ILC) the second most common breast cancer accounts for 10-15% of all cases. There are other subtypes of breast cancer that are less common to happen including inflammatory breast cancer, Paget disease, and Papillary carcinoma. Another common category to classify breast cancer is based on the molecular signature including Luminal A or B breast cancer with positive expression of estrogen and progesterone receptors, basal-like or triple-negative breast cancer with negative expression of estrogen, progesterone and epidermal growth factor receptor-2 (Her-2), Her-2 enriched breast cancer with high expression of Her-2 receptor and negative expression of estrogen and progesterone receptors [32-35] (Table 2-1). The disease can also be classified based on the stage (TNM classification) of the disease taking into consideration tumor size (T) lymph nodes status (N) and distant metastasis (M) [36].

Table 2-1: Breast cancer molecular classification:

<b>Molecular Subtype</b>	<b>Incidence</b>	<b>Hormone status</b>	<b>HER2/neu status</b>	<b>Ki67 expression</b>	<b>Response to treatment</b>
Luminal A	40%	ER/PR positive	Negative	Low	Endocrine therapy (tamoxifen and aromatase inhibitors)
Lumina B	10-20%	ER/PR positive	Negative variable	High	Endocrine therapy (tamoxifen and aromatase inhibitors)
Her-2 enriched breast cancer	5-15%	ER/PR negative	Positive	High	Response to trastuzumab (Antibody-dependent cellular toxicity)
Basal-like or triple-negative breast cancer	15-20%	ER/PR negative	Negative	High	Chemotherapy and PARP inhibitors

### 2.2.3. Main pathways activated in breast cancer:

Distinct regulatory signaling pathways participate in the determination of breast cells' fate. The imbalance between the activation and suppression of the leading growth regulators is considered one of the cancer hallmarks and plays a role in the development of cancerous cells. The main pathways participating in the regulation of breast cancer progression include estrogen receptor, human epidermal growth factor receptor, canonical Wnt/ $\beta$ -catenin, transforming growth factor beta and/or insulin-like growth factor receptor signaling pathways [37-41].

Estrogen receptors are transcription factors that belong to the nuclear hormone receptor super-family. Estrogen receptors are present in the cytoplasm, upon estrogen ligand exposure the receptors form homodimers or heterodimers (ER $\alpha$ /ER $\alpha$ , ER $\beta$ /ER $\beta$ , or ER $\alpha$ /ER $\beta$ ) and are translocated to the nucleus to activate or suppress transcription through binding to estrogen response element or other genomic regions with cooperation with transcription regulators. Estrogen signaling participates in the regulation of breast cancer development through nuclear and extranuclear actions [38]. ER regulates the expression of genes related to cancer growth such as IL6 and Cyclin D in addition to genes involved in the EMT process and metastasis development including Snail and Slug [37, 38].

Another family that participates in the determination of cell behavior is the human epidermal growth factor receptor family, referred to as ErbB or HER. HER family consists of 4 members. HER receptor contains three domains; extracellular, transmembrane and intracellular domains with tyrosine kinase activity. Ligand binding causes dimerization of HER receptors and autophosphorylation of the tyrosine residues associated with subsequent activation of downstream signaling pathways including; mitogen-activated protein kinase (MAPK) and PI3K/AKT pathways which eventually lead to cell survival and proliferation. The HER2 receptor is amplified in different types of breast cancer causing over-expression of HER2 protein which is linked to breast tumorigenesis [42].

The Wnt/ $\beta$ -catenin pathway has a pivotal role in the regulation of cell-cell adhesion, embryonic development and tissue homeostasis. The binding of Wnt, glycosylated and secreted, proteins to the frizzled receptor lead to the dimerization with Low-density lipoprotein receptor-related protein 5 and 6. That would lead to the accumulation of Axin protein to the cell membrane, from the intracellular side, and inhibition of glycogen synthesis kinase (GSK-3 $\beta$ ), a negative regulator of the  $\beta$ -catenin pathway, causing the accumulation of  $\beta$ -catenin in the cytoplasm.  $\beta$ -catenin is then translocated to the nucleus to contribute to the regulation of transcription regulation in association with other transcription factors including CREB binding protein and T-cell factor/lymphoid enhancing factor (TCF/LEF).  $\beta$ -catenin regulates the expression of many oncogenes including MYC and CCND1 leading to cell proliferation [43]. High levels of  $\beta$ -catenin are identified in about 50% of clinical breast cancer cases[44]. The positive

regulator of  $\beta$ -catenin (DV1) is amplified in around 50% of breast cancers whereas (FRP1), a  $\beta$ -catenin inhibitor, is lost in more than 70% of metastatic breast cancers [45, 46].

PI3K/AKT/mTOR is a highly activated pathway during breast cancer progression; it is a downstream signaling pathway of several tyrosine kinase receptors such as EGFRs, which are involved in cell proliferation, survival and apoptosis inhibition. Activating mutations of the oncogene phosphatidylinositol 3 kinase (PI3K) are common in breast cancer[47]. PI3K activation leads to the phosphorylation of phosphatidylinositol 4,5-bisphosphate (PIP2) to phosphatidylinositol 3,4,5-trisphosphate (PIP3). PIP3 binds to AKT (protein kinase B), a threonine/serine kinase, leading to the phosphorylation of the latter through the PDK1 enzyme. The serine/threonine kinase mTOR is a downstream effector of AKT, contributing to the regulation of intracellular signaling including cell survival and motility. PTEN is a tumor suppressor that reverses PI3K effects through dephosphorylating PIP3 to PIP2, inhibiting the activation of downstream signaling [48-50].

The mitogen-activated protein kinase pathway (MAPK) is a critical signaling pathway that plays a role in controlling cell proliferation and apoptosis. The pathway is activated through an external signal that activates membrane-bound receptor tyrosine kinase (RTK). The MAPK pathway consists of several protein kinase molecules that activate one another. Ras protein kinase gets phosphorylated by RTK leading to the recruitment of Raf protein kinase to the membrane, activated Raf phosphorylates MEK protein that in turn activates ERK. ERK regulates the transcriptional regulation of genes related to cell proliferation, differentiation and survival regulation [51]. Gain of function mutation in the Ras gene leads to constant activation of this pathway which is implicated in the pathogenesis of many tumors [52].

Insulin-like growth factor receptor family consists of 3 membrane receptors including insulin receptor (INSR), insulin-like growth factor 1, and 2 receptors (IGF-1R, and IGF2R). Their ligands include insulin, IGF1 and IGF2 proteins, their levels and availability are determined by the presence of insulin-like growth factor binding proteins (IGFBP 1-6). The activation of the IGF-IGF-1R axis leads to the autophosphorylation of tyrosine residues of IGF-1R and subsequent phosphorylation of IRS1 adaptor protein, leading to the activation of the PI3K/AKT pathway and MAPK pathway. The consequences include the induction of protein synthesis, inhibition of apoptosis and enhancing cell survival and proliferation [53] (**Figure 2-3**).

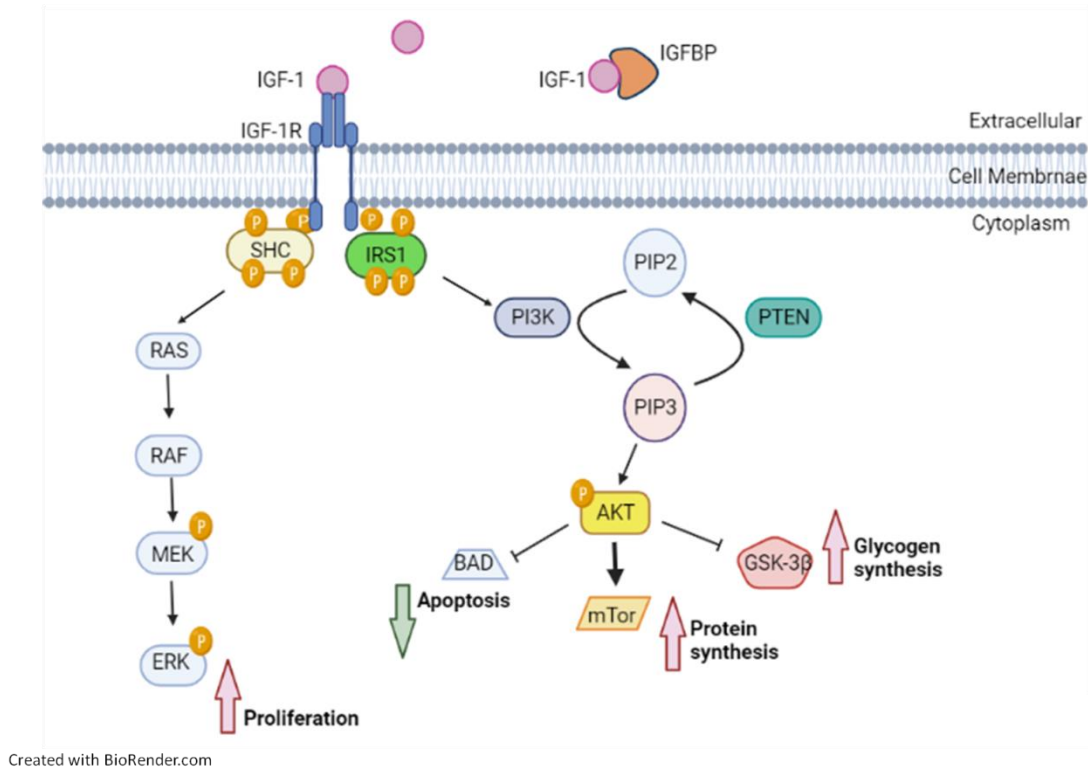


**Figure 2-3:** IGF-1/IGF-1R signaling pathway.

Transforming growth factor beta (TGF- $\beta$ ) conducts its effect through Transforming growth factor receptors (TBRII/TBRI), through Smad or non-Smad signaling pathways. The Smad pathway is activated through the bindings of TGF- $\beta$  to TBRII which leads to TBRI phosphorylation at serine and threonine residues, and subsequent phosphorylation and activation of receptor-regulated Smads (R-Smads) including Smad2 and Smad3 proteins, which form with common-Smads (co-Smad); Smad4, R-Smads- co-Smad complex. The complex interacts with other transcriptional regulators and translocates to the nucleus to regulate the expression of target genes leading to the promotion of epithelial-to-mesenchymal transition (EMT) [54, 55]. At the late stages of tumor, TGF- $\beta$  signaling initiated through TBR phosphorylation at tyrosine residues activates the non-Smad mediated signaling pathway, leading to the activation of AKT/PI3K, JNK/P38, and MAPK pathways[56] (**Figure 2-4**).

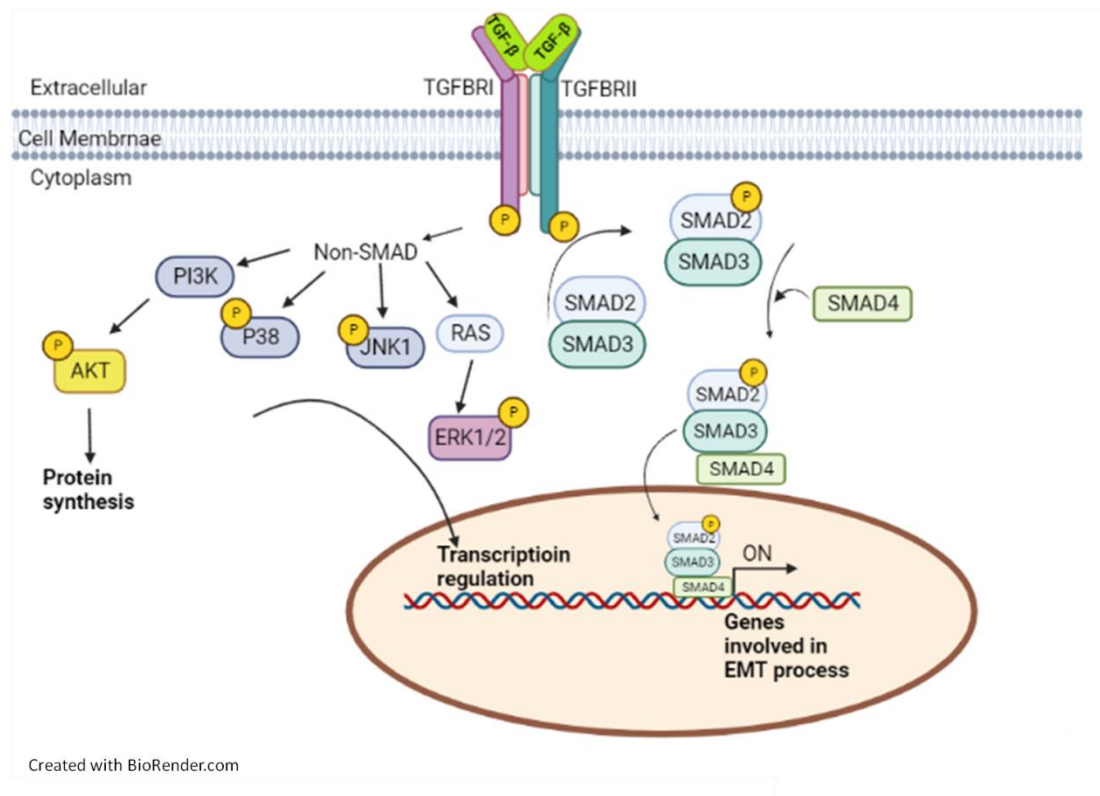


**Figure 2-4:** TGF-β SMAD and non-SMAD dependent signaling pathway.

#### 2.2.4. Breast Cancer treatment:

Breast cancer can be treated through various methods depending on its type and stage. The surgical removal of the tumor mass is usually associated with radiotherapy and chemotherapy to enhance the removal of any cancerous lesion [57].

Targeted therapy has been used successfully to treat different types of breast cancer based on the expression pattern of certain genes. Hormone therapy includes the usage of estrogen receptor modulators, such as SERMs (Selective estrogen receptor modulators) or (AI) aromatase inhibitors which are widely used to treat ER-positive breast cancers [58]. On the other hand, HER-2 enriched breast tumors can be treated by targeting either the human epidermal growth factor receptor using monoclonal antibodies (such as Herceptin) or through kinase inhibitors targeting proteins involved in the downstream signaling pathway [37]. Triple-negative breast cancer can be treated through a combination of surgery, radiation and chemotherapy. Synthetic lethality is a term referring to targeting a pathway related to a certain physiological process, such as DNA repair, while a defect in another pathway related to the same biological process is detected. Thereby enforcing cells to go to the programmed death (apoptosis). For instance, poly (ADP-ribose) polymerase is a family of proteins that participates in several biological processes such as DNA damage repair [59]. BRCA1 is a gene encoding for a protein that plays a major role in double-strand DNA repair machinery [60]. PARP inhibitors showed effectiveness in treating BRCA1 mutated breast cancer cases, these effects are referred to as synthetic lethality [61].

### 2.2.5. Breast Cancer Chemoprevention

Cancer chemoprevention concept was firstly introduced in 1970s referring to the usage of synthetic or natural compounds for the purpose of preventing or delaying the occurrence of malignancy in people at high risk to develop the disease [62]. Clinical studies have shown the effectiveness of tamoxifen (Estrogen receptor modulator) in reducing the odds of breast cancer formation [63]. However, due to the side effects associated with tamoxifen usage as well as that ER modulators are not effective in ER-negative breast cancer cases, there is a strong need for identifying more tolerable new cancer preventive agents with fewer side effects whose actions are independent of the hormone status. Preclinical studies have shown cancer-preventive effects of rexinoids, and synthetic retinoids, in an ER- independent manner [64]. Moreover, clinical studies demonstrated promising results regarding the cancer-preventive effects of rexinoids in combination with other agents such as ER modulators [65] or kinase inhibitors [66].

## 2.3 Retinoids and Rexinoids

### 2.3.1. Retinoid metabolism

Retinoids are fat-soluble molecules that include all vitamin A derivatives. Vitamin A is found in leafy vegetables in the form of carotenoids or animal sources such as the liver in the form of preformed vitamin A [67]. In the intestinal epithelium,  $\beta$ -carotenoid is converted into Retinal by dioxygenase enzyme which can be reversibly converted into Retinol by Retinol dehydrogenase, which can be absorbed through the intestinal to the bloodstream. Moreover, retinol can be re-esterified in the epithelium mucosal cells and secreted in chylomicrons into the lymphatic and blood circulation [68]. The liver captures the retinoids from chylomicron remnants where they can be converted into retinol and other bioactive forms. Vitamin A is stored in the liver in the form of Retinyl esters which can be released into the circulation whenever it is needed in the form of retinol or retinoic acid where retinol-binding proteins (RBPs) carried it out through the bloodstream to the target tissues [69]. Retinol is taken up through the STRA6 receptor to the cells within the target tissues, where retinaldehyde dehydrogenase (RALDH) enzymes are considered the rate-limiting step to produce retinoic acid [70]. The degradation of retinoic acid happens through the CYP26A1 system, while the nuclear receptors RAR/RXR are ubiquitinated and then degraded in the proteasome [71].

### 2.3.2. Retinoid/Rexinoid signaling:

Retinoic acid (RA) is an essential signaling molecule for cell metabolism and tissue homeostasis. All-trans retinoic acid and 9-cis retinoic acid bind to retinoic acid nuclear hormone receptors (RARs) and trigger the expression of various RA target genes involved in the regulation of cell proliferation, differentiation and apoptosis. RARs are also considered transcription factors as they can activate transcription. There are 3 isoforms of RAR receptors ( $\alpha$ ,  $\beta$ ,  $\gamma$ ) which can interact as homodimers (RAR/RAR) or heterodimers with retinoid X receptors (RAR/RXR). The binding of the RAR agonist is essential for RAR/RXR full response [72, 73].

Retinoid X receptors (RXRs) are nuclear hormone receptors whose ligands were not identified when they were discovered. 9-cis retinoic acid, Docosahexaenoic acid, and phytanic acid are natural compounds that bind to RXR. There are 3 types of RXR receptors; RXR- $\alpha$ , RXR- $\beta$ , and RXR- $\gamma$ . RXR can form dimers with other nuclear hormone receptors including RARs, PPARs, LXR, FXR, TR, or VDR [74]. The partner option determines which genes to regulate and which co-regulators to bind. The binding of RXR agonist can activate transcription mediated by RXR heterodimers which can also be activated through the binding of other partners' ligands such as 1 $\alpha$ , 25-dihydroxy vitamin D3 in case of VDR and T3 or T4 in case of TRs. [75, 76]. RXR could also dimerize with orphan nuclear receptors with no identified ligands including COUP-TFI and COUP-TFII [77]

In the absence of ligand, RXR dimer binds to the DNA at hormone response element, the dimer is bound also by a number of co-repressor factors including HDAC, NCoR and SMART that forms a repressor complex to inhibit transcription of target genes [78, 79]. Ligand binding causes conformational changes in the ligand binding domain (LBD) of the nuclear receptor leading to the dissociation of the co-repressors and the binding of co-activators including HAT and HMT which causes transcriptional activation of target genes [80].

Besides their genomic effects, Retinoids show extra-nuclear signaling [81, 82]. Studies showed that retinoids could activate several kinase pathways within minutes of their administration, including the activation of PI3K and MAPKs. Cytokine-dependent retinol capture causes the activation of STAT5 and immune modulation [83]. Retinoids can induce epithelial cell differentiation through the receptor-independent activation of protein kinase c and the subsequent phosphorylation of Erk1/2 and the P90S6 kinase in a CREB-dependent manner of transcriptional regulation of retinoids target genes [82].

The biological functions of retinoids are widely diverse including vision, embryonic development, and immunity modulation [84-86]. As retinoids have played a major role in regulating cell proliferation and differentiation, they have been widely investigated for their anti-tumor activities as single agents or in combination [87-89]. Figure 2-5.

Rexinoids are synthetic retinoids that bind selectively to RXR nuclear hormone receptors which are associated with fewer side effects. Studies have demonstrated the role of rexinoids in the regulation of lipid metabolism [90]. Moreover, the dimer RAR/RXR induces the expression of fibroblast growth factors 21 and 19 (FGF21 and FGF19) which has a role in fatty acids oxidation [91]. In addition, DHRS3 (Dehydrogenase/reductase SDR family member 3) and DEC2 (Basic-helix-loop-helix family member 4e1) which participate in the regulation of embryonic development and cell cycle regulation respectively, are genes regulated by rexinoids [92, 93].

Rexinoids promote epithelial cell differentiation through inducing the expression of genes involved in maintaining epithelial cell characteristics such as integrin  $\beta$ 4, integrin  $\alpha$ 6 and E-cadherin in human mammary epithelial cells (HMEC) [94].

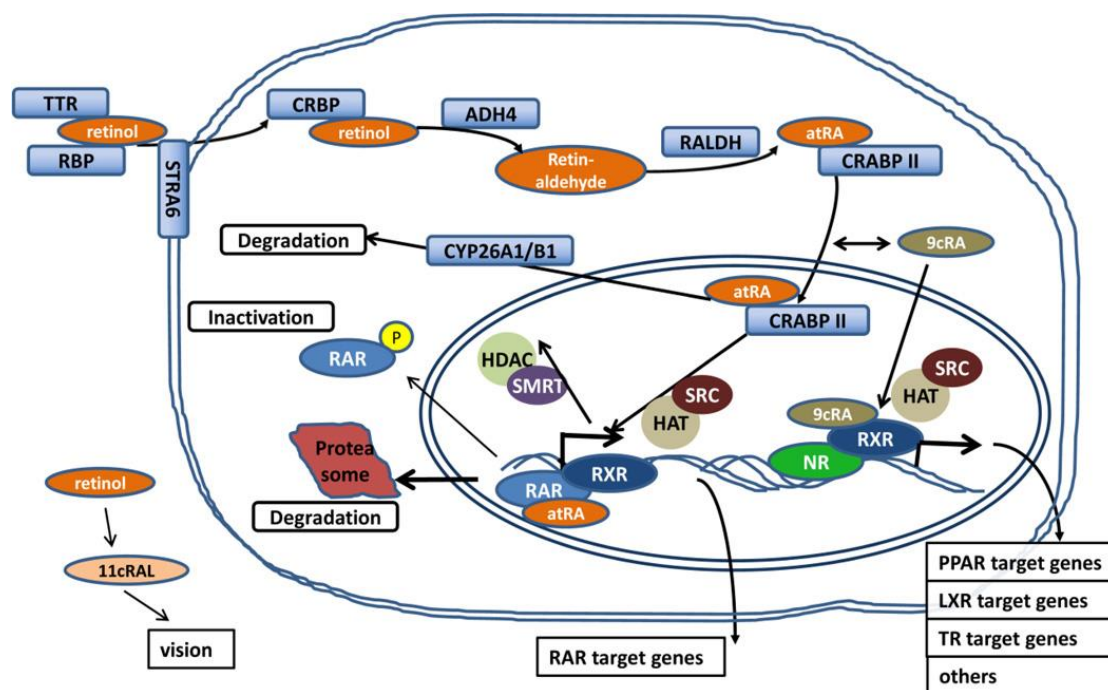


**Figure 2.5:** retinoids and rexinoids metabolism in target cells [70].

### 2.3.3. Retinoids/ Rexinoids in Medicine:

Retinoids have a wide range of medical applications. As these agents were found to promote cell differentiation and have anti-inflammatory properties, retinoids have application in skin disorders such as acne and psoriasis [95]. On the other hand, as retinoids participate in lung development during embryogenesis, it was shown that they enhance alveolar regeneration in chronic obstructive pulmonary disease (COPD) patients [96, 97]. Moreover, studies have illustrated that targeting certain nuclear receptors such as RXR, and PPAR $\gamma$  have improving effects on neurodegenerative diseases. Bexarotene was found to affect the clearance of soluble amyloid- $\beta$  (Beta) in mice models, with more studies being conducted in that context [98]. In addition, bexarotene was found to enhance the growth of dopaminergic neurons giving it the potential to be a beneficial indication in the case of Parkinson's disease [99].

### 2.3.4. Retinoids/ Rexinoids in Cancer:

All trans-retinoic acid induces leukemic cell differentiation in acute promyelocytic leukemia lesions [100]. Clinical studies showed increased progression-free survival in patients with skin, cervical and renal cancers treated with a combination of 13-cis-RA and interferon- $\alpha$ 2a [101]. Phase III clinical trials showed that 13-cis-RA treatment was associated with improved survival of high-risk neuroblastoma patients [102]. In a phase II trial, the addition of atRA to chemotherapy for patients with non-small cell lung cancer (NSCLC) showed progression-free survival [103].

Retinoids were shown to be associated with some side effects including teratogenicity, dry skin, hair loss and cutaneous toxicity. To reduce the side effects, synthetic selective RXR agonists were designed including bexarotene and LGD100268. Bexarotene belongs to the synthetic retinoids family, rexinoids, it binds selectively to RXR nuclear

receptor and triggers the expression of a number of genes involved in differentiation regulation and apoptosis including Caspase 3, COX2, MMP9, VEGF and EGFR [104-106].

Bexarotene has got FDA approval for the treatment of cutaneous T-cell lymphoma (CTCL) [107]. Clinical studies showed promising results for the combination of bexarotene and tyrosine kinase inhibitor erlotinib in a particular group of NSCLC patients with certain mutations such as EGFR and KRAS with high expression of cyclinD1 protein [108].

Although retinoids and rexinoids showed curative effects in certain human cancers, clinical studies showed that they are more effective in precancerous lesions [109, 110] suggesting their usage as cancer preventive agents [111]. In vivo studies showed that bexarotene and LGD100268 were more effective in preventing the development of estrogen-receptor negative mammary tumors than 9-cisRA [64].

Although rexinoids showed good tolerability when it comes to clinical usage even minor side effects should be taken into consideration. Studies reported that rexinoid usage was associated with hyperlipidemia and osteoporosis. Therefore, the concept of combination treatment with agents from other families gives a chance to reduce the dose and thereby the associated side effects. Drug repurposing is a strategy to use agents that are already approved by the FDA to cure or prevent certain medical conditions that are different from their original indication[112]. The combination of rexinoids (RXR agonist) and rosiglitazone (PPAR $\gamma$  agonist), the later is indicated for the treatment of type-2 diabetes[113] showed synergistic antiproliferative and apoptosis-inducing effects in cancer cells mediated by the heterodimer PPAR $\gamma$ /RXR activation leading to Nitric Oxide (NO) production [114]. Moreover agents that participate in the regulation of the adrenergic system showed promising results in treating and/or preventing cancer development [115, 116].

## 2.4 The Sympathetic System

### 2.4.1. The adrenergic signaling:

In the human body the autonomic nervous system, consisting of the sympathetic and parasympathetic nervous systems (SNS and PNS), monitors the involuntary physiological processes including heart rate, blood pressure, digestion, and respiration [117]. The sympathetic system activation is responsible for the fight or flight response to danger, whereas the parasympathetic system is responsible for the stimulation of the rest and digest activities [118].

The sympathetic or adrenergic system is mediated through adrenaline or noradrenalin endogenous neurotransmitters, which bind to 7-transmembrane receptors named adrenoceptors. Adrenoceptors are G protein-coupled receptors (GPCR) that are classified into 3 major classes; alpha 1, alpha 2 and beta receptors. The  $\alpha$ 1 adrenoceptor is coupled to Gq protein which leads to the activation of phospholipase c, increased inositol 3 phosphate and diacylglycerol, leading to an elevation in the intracellular

calcium levels leading to smooth muscle contraction. Alpha 1 adrenoceptors are located mainly in the smooth muscle of the peripheral vessels; their activation caused vasoconstriction meaning that their blockade leads to vasodilation; alpha 1 agonists can be used to treat hypotension, vasodilatory shock and heart failure [119]. Moreover, the alpha 1 antagonist class is indicated for hypertension and benign prostate hypertrophy cases [120] [121].

Alpha 2 receptors are coupled to Gi protein which by activation leads to an inhibition of adenylate cyclase and a decrease in cellular cyclic AMP levels associated with smooth muscle contraction, and though alpha 2 agonists can be used to treat high blood pressure. Alpha 2 receptors are located in the central nervous system and regulate the sympathetic system tone. In addition, presynaptic  $\alpha_2$  receptors are responsible for inhibiting neurotransmitter release [122]. As alpha 2 antagonists increase the secretion of adrenergic and dopamine neurotransmitters they are indicated as antidepressant agents [123].

$\beta$  adrenoceptors can be classified into 3 subclasses including  $\beta_1$ ,  $\beta_2$  and  $\beta_3$ . The activation of  $\beta$  adrenoceptors leads to an increase in cAMP levels.  $\beta_1$  adrenoceptors are coupled to Gs protein and are mainly located in the heart. Their activation stimulates adenylate cyclase and leads to an increase in cyclic AMP and heart rate and contractility [124].  $\beta_2$  adrenoceptors are widely distributed mainly in smooth muscles of the bronchi. They are coupled to Gs and Gi proteins. Their stimulation caused an increase in cAMP leading to smooth muscle relaxation and bronchodilation. Therefore,  $\beta_2$  agonists are indicated for asthma patients [125].  $\beta_3$  adrenoceptors are located mainly in the metabolic organs and their stimulation leads to glycogenolysis and lipolysis [126, 127]. Moreover, Beta-3 adrenoceptors are found in smooth muscle tissue, particularly in the gastrointestinal tract and urinary bladder smooth muscle.  $\beta_3$  agonist causes relaxation of urinary bladder smooth muscles and is used in overactive bladder cases [128]. Non-selective beta blockers are indicated in chronic heart failure and high blood pressure. In general, beta receptors have inhibitory effects on smooth muscles leading to their relaxation. On the other hand, their activation in the heart and in metabolic tissues has stimulatory effects.

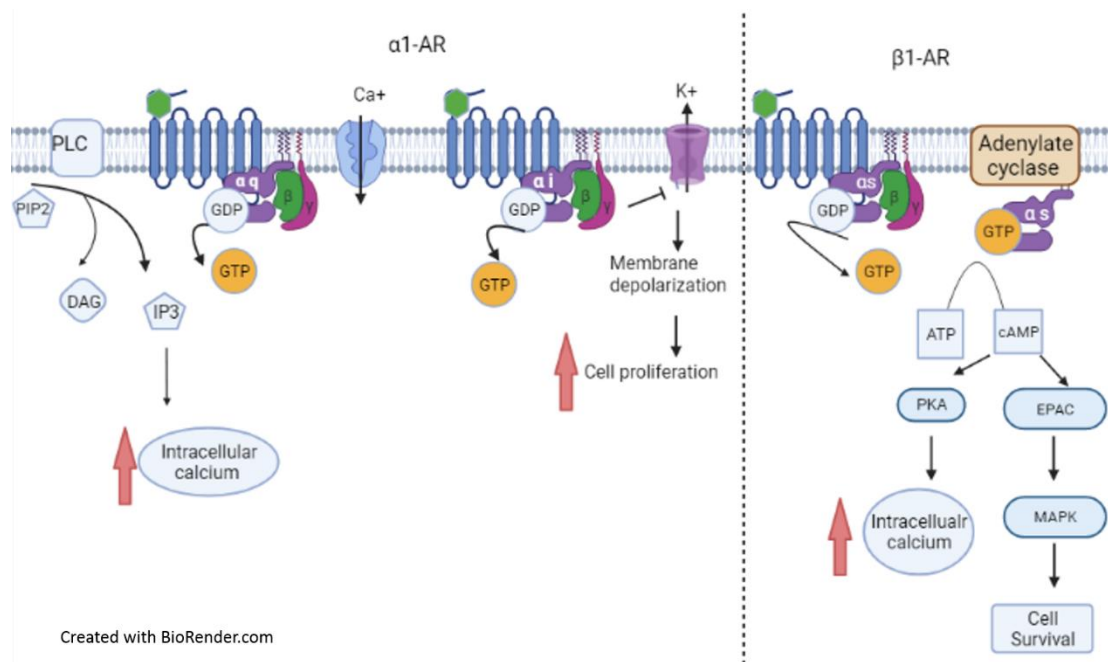


**Figure 2-6:** alpha 1 and Beta1 adrenergic signaling pathway

#### 2.4.2. The adrenergic signaling role in cancer:

The adrenergic signaling pathway is implicated in tumor initiation and progression through promoting cellular processes such as inflammation, angiogenesis and epithelial to mesenchymal transition (EMT). Targeting the adrenergic system showed beneficial effects in cancer patients [129]. Supporting evidence showed that beta-adrenergic antagonists suppress the activation of NF-κB. NF-κB is a transcription factor that is implicated in chronic inflammatory and cancer progression [130] [131]. Tumor-promoting factors including IL-6, IL-8, MMP2, MMP9, and VEGF were found to be upregulated in response to the adrenergic signaling, on the other hand, genes involved in epithelial cells' anti-tumor response were downregulated. Adrenoceptor signaling activation induces metastasis through activating protein kinase A (PKA) and the exchange protein activated by adenylate cyclase (EPAC) signaling pathways. Epidemiological studies have shown that the consumption of non-selective Beta-blockers was associated with a reduction in solid tumor progression rates [132]. Clinical benefits were reported in breast, ovarian, melanoma, and non-small cell lung cancer patients treated with beta-blockers. Moreover, studies have shown that beta-adrenoceptor antagonists are more effective in suppressing micro-metastasis spread in early-stage tumors [133]. On the other hand, a study showed that the usage of selective beta-blockers might increase the risk of breast cancer[134]. A study has shown that strong expression of alpha 1 adrenoceptor is associated with increased proliferation, decreased apoptosis, poor cancer-specific survival and tumor recurrence [135]. The results of the studies point out that the anti-tumor effect behind targeting the adrenergic system is probably mediated by antagonising the alpha-1 adrenergic receptors.

### 2.4.3. Carvedilol:

Carvedilol is a non-selective beta blocker with alpha 1 blocking activity. It is indicated for the treatment of congestive heart failure and high blood pressure, although the contribution of alpha 1 blockade in the therapeutic effects is not known yet [136]. A cohort study showed that patients treated with carvedilol had a 26% lower risk to develop gastrointestinal and lung cancer [137]. Moreover, carvedilol reduces breast primary tumor progression in mouse models [138]. These studies suggest a cancer preventive effect of carvedilol.

Studies have shown that carvedilol has antiproliferative and cytotoxic effects on various types of cancer cell lines. Preclinical studies have demonstrated that carvedilol exhibit the most anti-proliferative and antiangiogenic characteristics compared with other beta-blockers in neuroblastoma cells. Carvedilol was found to arrest cells at the G0/G1 phase in glioma cells. A study showed that carvedilol reduced the expression of the matrix metalloproteinases MMP2 and MMP9, which are important factors in tumor cell invasion and metastasis [139]. Moreover, it was shown that the long-term use of carvedilol decreased cancer risk in the upper gastrointestinal tract and lung cancer [137]. The results of the mentioned studies refer to the role of carvedilol in suppressing tumor development. Regarding patient's response to beta-blockers, studies have shown that epigenetic, which refers to the inherited characteristic on gene expression profile without modifications on the genetic material, could play an important role [140]. Epigenetic modifications can take place through various mechanism including chromatin remodeling [141].

## 2.5 Chromatin Remodeling

### 2.5.1. DNA Packaging:

The human cell nucleus is about 3-10 microns in diameter and the genomic DNA is about 2 meters long, therefore there should be a biological system to arrange the DNA to fit in the nucleus [142]. DNA is organized and packed around nuclear proteins called histones to form the basic unit in chromatin which is the nucleosome. The nucleosome consists of approximately 146bp of DNA wrapped around an octamer of 8 histone proteins (two of each of H2A, H2B, H3, and H4) [143]. Chromatin consists of nucleosomes connected by linker DNA and linker histone H1. It can be found in two structural positions, heterochromatin where the chromatin is condensed and euchromatin with an open structure [144].

### 2.5.2. Chromatin remodeling and the regulation of biological processes:

Chromatin remodeling is the process in which nucleosome structure is reorganized to make the DNA accessible or compacted, depending on the cells' need, to regulate several biological processes including DNA replication, gene transcription or DNA damage repair. This process can be performed through either chromatin remodeling complexes, enzymes that modify histones or DNA methylation [145] [146].

Chromatin remodeling complexes use the energy from ATP hydrolysis to modulate the chromatin structure. They participate in two roles, including packaging the DNA into

nucleosomes or releasing the DNA from the histones. There are 4 families of chromatin remodeling complexes in human cells, including SWI/SNF (SWItching defective/Sucrose NonFermenting), ISWI (Imitation SWItch), CHD (Chromodomain, Helicase, DNA binding), and INO80 (INOsitol requiring 80)[147, 148].

Histone modification can be done through methylation, acetylation, phosphorylation [149], adenosine diphosphate ribosylation, glycosylation, sumoylation or ubiquitylation [150]. The most common post-translational modifications on histones include acetylation and methylation. Histone acetylation can be performed on lysine residues through histone acetyl-transferase enzymes (HATs) including HAT1, CBP/p300. DNA strand carries on a negative charge because of the phosphate-sugar backbone, whereas histones are enriched with basic amino acids with a positive charge including lysine and arginine. The acetylation process on lysine neutralizes histones' positive charge and loosens the histone-DNA interaction making the DNA more accessible. Histone deacetylase (HDAC) is an enzyme that removes the acetyl group, restoring histones' positive charge and enhancing the interaction with DNA [151].

Histone methylation can be done through histone methyltransferases enzymes (HMTs) [152]. The methyl group can be added to the lysine or arginine amino acid residues as mono-, di- or trimethylation. Histone methylation does not change histone charge, contrary to histone acetylation, therefore, does not affect DNA-histone interaction directly. The effect of methylated histone on DNA accessibility can be diverse; for instance, H3K4 and H3K6 methylation lead to more open DNA and active gene transcription. Whereas H3K9 and H3K27 methylation are associated with more compacted DNA and thereby transcription repression [153, 154]. Histone demethylases (HDMs) are enzymes that perform demethylation reactions over histones [155].

Another important example of histone modification is phosphorylation. Whenever DNA damage lesions happen, the H2AX variant is phosphorylated at serine 139 residues by ATM or ATR kinase proteins. This modification makes DNA accessible and recruits DNA repair machinery to the lesion[156].

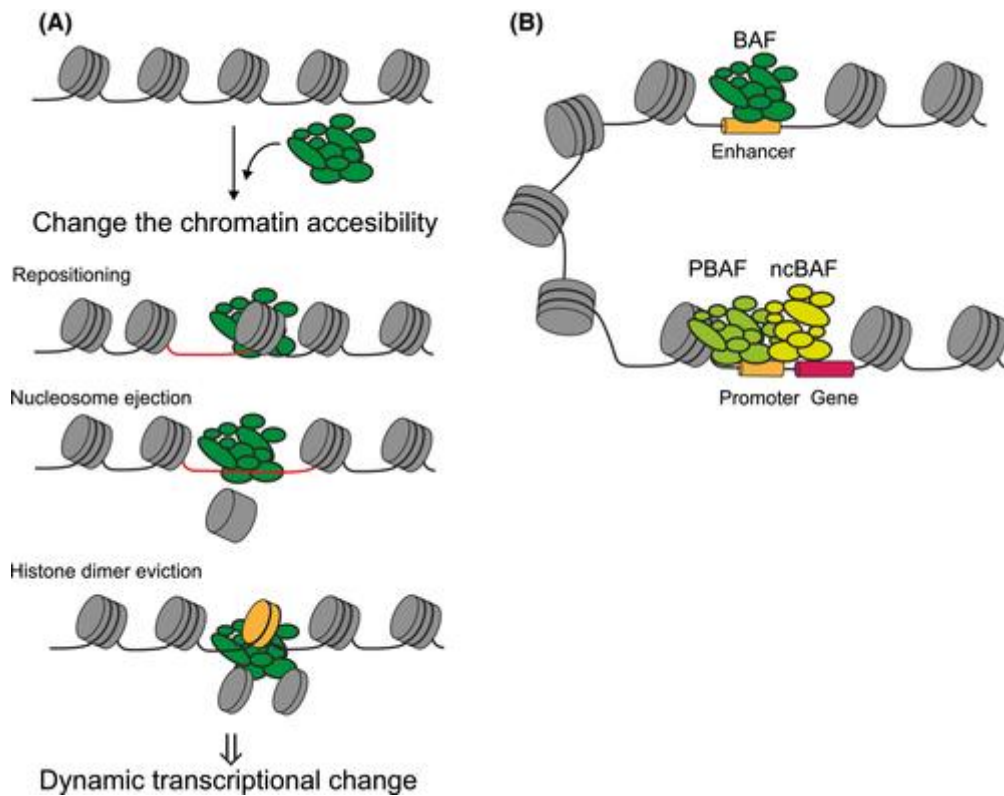


**Figure 2-7:** The process of chromatin remodeling through ATP-dependent complexes[157]

### 2.5.3. SWI/SNF:

SWItch/Sucrose Non-Fermentable complex is a conserved chromatin remodeling complex identified in different organisms including yeast, *Drosophila* and humans. SWI/SNF complex is an ATP-dependent chromatin remodeling complex which utilizes the energy from ATP hydrolysis to alter nucleosome organization to facilitate chromatin accessibility to transcription activators or suppressors [158].

SWI/SNF complex comprises about 15 subunits. This complex can be divided into two groups including the BAF (BRG1-Associated Factor) and PBAF (Polybromo BRG1-Associated Factor) families. Within the core of the complex, there is an ATPase subunit either BRG1 or BRM. Common subunits between the two groups are; BAF45, BAF53, BAF57, BAF60, BAF155, BAF170, and Actin. The ATPase subunit in the BAF complex might be either BRG1 or BRM, whereas, in the PBAF complex it is only BRG1. On the other hand, the ARID subunit is also different in the two complexes; either ARID1A or ARID1B are present in the BAF complex, whereas the ARID2 subunit is specific to the PBAF complex [159].

Studies have shown that SWI/SNF subunits are the most frequently mutated chromatin remodelers in different types of tumors [160]. Moreover, they have an essential role during embryonic development by facilitating cell differentiation through their chromatin remodeling function [161].

## THE MAMMALIAN SWI/SNF COMPLEXES

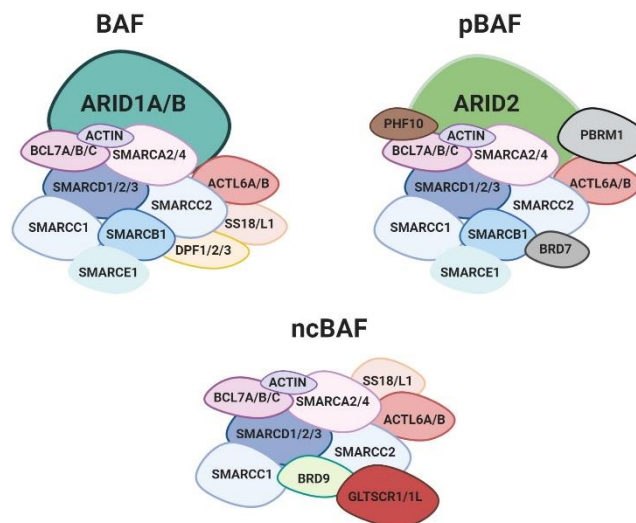


**Figure 2-8:** Schematic diagram of the SWI/SNF complex[162]

### 2.5.4. ARID1A:

AT rich interactive domain 1A protein is a subunit of the SWI/SNF chromatin remodeling complex. Either ARID1A or ARID1B is present exclusively in the BAF complex. Studies have shown that ARID1A is frequently mutated in different types of cancers including ovarian clear cell carcinoma, uterine endometrioid carcinoma, gastric carcinoma, hepatocellular carcinoma, breast cancer and pancreatic cancer, and is considered a tumor suppressor [163-165]. ARID1A is considered a prognostic marker in breast cancer with a higher level of metastatic incidence in patients with ARID1A mutations [166, 167].

The mechanisms behind ARID1A tumor suppressor activity are under investigation., It was demonstrated that ARID1A has a key role in cell cycle regulation. Moreover, it was found that ARID1A knock-out was lethal to mice in the embryonic state as it plays an essential role in cell differentiation. On the other hand, ARID1A is suppressed during certain physiological processes such as wound healing, suggesting that ARID1A is an inhibitor of tissue regeneration as it promotes differentiation and suppresses proliferation in mammals [168]. ARID1A DNA binding motifs overlap with motifs recognized by C/ebpα and Hnf4α transcription factors which regulate cell differentiation. Upon ARID1A loss the binding of these factors to their target genes was reduced. Moreover, it was found that cell cycle markers are elevated upon ARID1A KO. E2F4 is a transcription factor that regulates and suppresses the expression of key regulators of cell cycle entry. The binding of E2F4 to the promoter regions of its target genes was reduced upon ARID1A loss suggesting that there might be an interaction between ARID1A and E2F4 in mouse liver cells [168].

ARID1A participates in maintaining genomic stability. A study showed that ARID1A interact with ATR, DNA damage sensor, and recruited to DNA damage lesions. Moreover, supporting the synthetic lethality concept it was found that ARID1A

deficiency increased the anti-tumor effects of PARP inhibitors in colorectal and breast cancer cell lines [169].

Another study investigating the role of ARID1A in preserving genomic stability showed that ARID1A plays a key role in telomere cohesion through directly regulating the expression of STAG1 protein, a subunit in the cohesion complex. Moreover, they found that the distance between the two sister chromatids increased upon ARID1A inactivation in ovarian clear cell carcinoma cell lines (RMG1 and OVCA429). On the other hand, they mentioned that ARID1A inactivation participates in maintaining genomic stability by eliminating cells with defective telomere cohesion, as maintaining telomere cohesion is essential for mitotic integrity [170].

ARID1A participates in the maintenance of chromatin accessibility primarily at enhancer regions. Gene ontology studies revealed that ARID1A targets are involved in pathways correlated to cancer development such as TGF- $\beta$  signaling, Hedgehog signaling and epithelial-mesenchymal transition [171]. ARID1B is an alternative subunit for ARID1A and the study suggested that targeting ARID1B in ARID1A-mutant cancers could be a therapeutic strategy.

ARID1A is frequently mutated in different types of cancers including ovarian, colorectal, pancreatic, and breast cancers, which is associated with a decrease in its protein levels. The re-expression of ARID1A in T47D cell line, harboring a non-sense mutation with ARID1A gene, significantly inhibited colony formation, supporting the tumor suppression activity of ARID1A [165].

ER-positive breast cancer patients with relatively higher ARID1A expression levels had a better clinical outcome. On the other hand, ARID1A inactivation was associated with treatment resistance [172]. The study demonstrated that ARID1A and SWI/SNF complex are recruited to ER target genes even before ligand activation, meaning in an ER-independent manner. The study revealed that ARID1A binding events were increased upon tamoxifen treatment, suggesting that ARID1A is involved in cell response to ER antagonists. ARID1A recruitment at ER target regulatory elements was mediated through the transcription factor FOXA1, with a significant reduction in ARID1A binding events upon FOXA1 KO. Moreover, ARID1A binding was repressive and associated with HDAC1 (histone deacetylase) recruitment to the target regions. This mechanism, stating that upon ER antagonist treatment ARID1A and HDAC1 are recruited to ER target regions through FOXA1 and form a suppressive complex was suggested to be responsible for the involvement of ARID1A KO in resistance to ER antagonists [173].

Another study showed that ARID1A binds to the active promoter and enhancer regions. ARID1A loss was associated with a reduction of RNA polymerase II (RNAPII) at transcription start sites which were restored upon ARID1A expression. Moreover, ARID1B gene expression is upregulated upon ARID1A depletion and could compensate its role in monitoring the physiological function of RNAPII [174].

Moreover, it was found that ARID1A and EZH2 methyltransferase regulates PIK3IP1, an inhibitor for PI3K activity, expression in an antagonistic manner in ovarian clear cell carcinoma (OCCC). ARID1A promotes PIK3IP1 expression whereas EZH2 silenced the gene. As ARID1A and EZH2 compete to bind to PIK3IP1 regulatory elements, ARID1A effects are dominant and are associated with gene activation. In ARID1A mutated cells EZH2 suppression effects of PIK3IP1 take place, leading to PI3K-AKT pathway activation and positive regulation of cell growth. In this study, they found that targeting the EZH2 enzyme in ARID1A-mutated cells represents a novel therapeutic strategy based on the synthetic lethality principle in OCCC cells [175]. A study showed that ARID1A loss of function sensitizes breast cancer cells to mTOR inhibitors [167].

ARID1A is mutated in over 50% of ovarian cancers. A study focusing on investigating ARID1A tumor suppressive activity revealed that restoring ARID1A expression in ARID1A mutated cell lines; HEC-1-A, uterine endometrioid carcinoma cell line, and OVISE, ovarian clear cell carcinoma, was associated with a decrease in cell proliferation. Moreover, the in vivo study showed that ARID1A expression in Tet-On inducible HEC-1-A tumor xenograft was associated with a significant decrease in tumor weight compared to the control group. Gene expression studies revealed that genes related to cell cycle regulation were differentially expressed upon ARID1A KO, including CDKN1A (P21) and SMAD3. In addition, they found that ARID1A and BRG1 directly interact with p53, a well-established regulator for P21 and SMAD3. ARID1A regulates the expression of p21 in a p53-dependent manner, suggesting a mechanism behind ARID1A tumor suppressive activity [176].

Various mechanisms were suggested to be involved in ARID1A tumor suppression activity. One study demonstrated that ARID1A expression negatively regulates gene and protein expression of the TERT enzyme, as well as an increase in the telomerase activity of the enzyme. ARID1A overexpression was associated with recruitment of ARID1A and the transcriptional repressor SIN3A as well as an increase of H3K9me3 markers to the promoter region (-1.7Kb to TSS) of the TERT gene. This repression complex inhibits TERT activation. Moreover, ARID1A KO and KD reactivated TERT gene transcription and activity [177].

Neuroblastoma (NB) is characterized by poor cell differentiation. A study illustrated that retinoic acid (RA) enhances cell differentiation by decreasing the expression of the TERT gene through ARID1A activity. Based on their findings, the suggested mechanism states that upon RA treatment, ARID1A and SIN3A, a repressor factor, are recruited to the TERT promoter region and suppress its expression in neuroblastoma cells, leading to cell differentiation [178].

Another example, a study has shown that the composite of the SWI/SNF complex could determine the role in transcription regulation. For instance, they found that the expression of cell cycle-related genes such as c-myc, cdc2 and cyclin-E protein expression detection correlates with ARID1A dissociation from their promoter region. Moreover, ARID1A knockdown was associated with an induction of these proteins.

The findings suggest that ARID1A have a suppression effect on the expression of c-myc, cyclin-E and cdc2, associated with anti-proliferative effects. On the other hand, ARID1B knockdown attenuated the induction of the cdc2 and cyclin-E, and the protein expression levels of c-myc were abolished upon ARID1B knockdown, suggesting that ARID1B has proliferation promotion characteristics [179]. The results refer that within the presence of the ARID1A subunit SWI/SNF plays a suppressor role on cell cycle-related genes. In order to activate the expression of the same targets, ARID1B is dominated in the complex.

ARID1A containing SWI/SNF complexes were associated with histone deacetylase (HDAC 1, 2) enzyme forming a repressor complex. Whereas, histone acetyltransferase (HAT) was detected with ARID1B containing complexes associated with gene expression activation. As c-myc is one of the main regulators of the cell cycle, they studied its transcription regulation. In proliferating cells, ARID1B containing SWI/SNF complex was detected on c-myc promoter in association with transcription activators such as E2F1 and STAT3 forming an activation complex, which was abolished upon ARID1BKO. The results refer that ARID1B regulates and activates c-myc transcription in proliferating cells [179].

## 2.6 Hypothesis and Aim of the study:

Bexarotene and carvedilol (Bex+Carv) combination treatment at low doses was associated with anti-proliferative effects in normal immortalized breast epithelial cells. We are investigating the molecular mechanism behind the detected effects. RPPA proteomic results (Reverse Phase Protein Array) showed increased protein levels of ARID1A upon Bex+Carv treatment. The tumor suppressor ARID1A, frequently mutated in different types of cancers, is a subunit in the chromatin remodeling complex SWI/SNF that participates in transcription regulation. We hypothesise that upon Bex+Carv treatment ARID1A alters chromatin accessibility through its recruitment to regulatory elements assigned to genes involved in cancer development and modulates their expression to decrease tumor growth and proliferation. To test the hypothesis we set our specific aims to identify:

1. *ARID1A genomic binding events upon Bex+Carv treatment in normal and transformed cells*
2. *Pathways that are affected by the change in ARID1A enrichment upon Bex+Carv treatment*
3. *The effect of ARID1A enrichment to its target regions on the expression of putative target genes upon Bex+Carv treatment*
4. *The impact of ARID1A knockdown on the detected effect of Bex+Carv treatment on target genes' regulation*
5. *The effect of Bex+Carv treatment on ARID1A targets' downstream signaling*

### 3. Materials

#### 3.1 Equipment

Table 3-1: List of equipment:

<b>Equipment</b>	<b>The company, Reference number</b>
Acrylamide gel cassette	VWR, E2 110-NG-2VWR
Autoclave	Tuttnauer
Balance	Precisa, XB2200C
Biological Safety Cabinet	BIOAIR®, Safemate 1.2
Cassette (Blotting equipment)	SCIE-PLAS, V20-SDB, 30052496
Centrifuge 4°C	HERMLE, Z326k
Centrifuge/Vacuum machine	Eppendorf Concentrated Plus
Cryo Freezing Container	NALGENE, Cat.No: 5100-0001
Electrode Chamber and Electrophoresis Tank	VWR, 170522007
Freezer -20°C	Electrolux
Freezer -60°C	SANYO, AURO-Science
Gel comb	Thermo Fisher
Glass bottles	VWR, BOROSILICATE, 3.3
Haemocytometer Counting chamber (Neubauer), 0.0025mm <sup>2</sup>	Burker Optik Labor
Ice-machine	ALS ANGEL ANTONI LIFE SCIENCE
Imaging system	Odyssey® CLx, (LI-COR)
Incubator (cell culture)	Memmert
Inverted Fluorescent Microscope	LEICA DMI8
Magnetic Separation Rack (12 tubes)	New England Biolabs®, Inc. S1509S
Magnetic Separation Rack (4 tubes)	Invitrogen, Flow Tube, DYNAL®
magnetic stirrer	VELP® ScientificA
Multi-channel pipette	Eppendorf Researchplus
Nanodrop, Spectrophotometer	Thermo Scientific NANODROP 1000
Optical microscopy	OLYMPUS, CKX41
Orbital shaker	Stuart ® miniorbital shaker, SSM1
PCR Thermal Cycler	Applied BioSystem, GeneAmp®, PCR System 2700
pH-meter	Thermo Orion model 420A
Pipet Controller	FALCON ®
Pipettes Series	Eppendorf Researchplus
Plate spectrophotometer	BioTek SYNERGY/LX, multi-mode reader
Power source 250V	VWR™ L:10005811
Programmable rotator mixer	BIOSAN, Multi BioRS-24, PRS-26
Qubit dsDNA HS assay	Invitrogen, Cat. No: Q32857
Real-Time PCR System	Light Cycler® 96 System, Roch Life Science
Real-Time PCR System	Applied biosystem, QuantStudio™ 12KFlex
Refrigerator, 4°C	Electrolux
Repeater	Eppendorf Repeater® plus 4,406,170
Sequencing System	Illumina, NextSeq 500
Sonication device	Bioruptor® Plus Diagenode, Seraing, Belgium

Thermo Mixer	Eppendorf, ThermoMixer® C
Vortex mixer	Advanced IR Vortex Mixer, VELP, SCIENTIFICA
Water bath	Grant, SUB2B

### 3.2 Consumable:

Table 3-2: List of consumables:

Consumable	The company, Reference number
15 mL polystyrene tubes	FALCON® A Corning Brand, Ref: 352095
15mL and 50 mL tubes	CELLSTAR® TUBES, Cat.No: 188271
6- 12- 24 and 96 well cell culture plate	TPP®
96-well Multiplate PCR plate Clear	Applied biosystems® by lifetechnologies, MicroAMP® Fast 96-well Reaction plate (0.1mL) Ref:4346907
96-well Multiplate PCR plate White	Roche, LightCycler® 480 MultiWell Plate 96, 04729692001
96-well PCR plates Sealing film	Platemax® CyclerSeal, AXYGEN®, A Corning Brand
96-well PCR plates Optical adhesive film	Applied biosystems, Thermo fisher scientific, Micro AMP™ optical Adhesive Film
Cell scraper	Greiner bio-one
Cryo Tube™ Vial (1.8 mL)	ABDOS
Gel blotting paper	GEHealth Care, Whatman™ , Life Sciences, Cat.no: 3001-861
Sterile Syringe Filter 0.2µm	VWR, PN: 28145-501
Low-binding microtubes 1.5mL	MAXYUM RECOVERY, Ref: MCT-150-L-C
Microtube 1.5 mL, 2 mL	AXYGEN
PARAFILM	Alpha laboratories, WS5000-10
Pipette filter tips	Biosphere® plus
Pipette tips	AXYGEN, A Corning band
Combitips	Eppendorf Combitips Advanced® Cat.no: 0030089405 (0.1mL)
Pipettes, serological	CellSTAR® greiner bio-one
PVDF membrane	AmerSham™ Hybond™, P0.45 PVDF, Cat.no: 10600023
Tissue	KIMTECH Science 200, Kimberly-Clark professional
tissue culture dish 100×20 mm	TPP®
tissue culture dish 145×20 mm	TPP®

### 3.3 Chemicals and Reagents:

Table 3-3: List of Chemicals:

Chemical	The company, Reference number
Acryl amide	SIGMA A3699-100ML, PCode: 1002994620
Ammonium Chloride	Honeywell, Fluka, 31107-1KG, 017-014-00-8
Ammonium per sulfate	VWR, LIFE SCIENCE, Product. No: 0486-100G
BCA reagent	Thermo Scientific, Ref:23225, pierce™ BCA protein Assay kit

Beta-mercaptoethanol	VWR, BIOH PROLABO®, Electran®, product.No: 436022A
Bovine Serum Albumin	biowest®, ID number: PAO214C032
Butanol	Honeywell, 537993-1L, PCode:101746671
Chloroform	Honeywell Riedel-deHaën®, 34854-1L
Dimethyl sulfoxide (DMSO)	SIGMA-ALDRICH®, D5879-1L
dNTPs	BIOLINE, Lot: DM-516403
Dynabeads™ protein A	Invitrogen, Thermo Scientific, Ref:1002D
Dynabeads™ protein G	Invitrogen, Thermo Scientific, Ref:1004D
Ethanol Absolute	VWR, BDH, CHEMICALS, 20821.330
Ethylenediaminetetraacetic acid (EDTA)	SIGMA-ALDRICH, 34549-100G
Formaldehyde 16% Methanol-free	Thermo Scientific, Ref: 28908
Formalin 8%	SPEKTRUM-3D, PUFFEROLTFORMALIN, 07100510
Glycerol	Honeywell, Riedel-deHaën®, 49770-1L
Glycine	SIGMA, G7126-1KG, PCode:1003023211
Goat serum	biowest®
Goat Serum	biowest® S2000-100
Hydrochloric acid	SIGMA-ALDRICH®, 30721-1L-M
Hydrogen Peroxide solution (H2O2) 30%	SIGMA H1009-100ML
Isopropanol	SIGMA-ALDRICH®, 278475-1L
Lithium Chloride	SIGMA, LIFE SCIENCE, L9650-100G
Magnesium Chloride	VWR, LIFE SCIENCE, Product. No: E525-100ML
Methanol	VWR, BDH, CHEMICALS, 20903.368
Mounting buffer	BIOTIUM, Cat.no: 23002
Nonidet™ P40	SIGMA, LIFE SCIENCE, 74385-1L
PCR Reference Dye	R4526-3ML, Source # SLCK 1389
pH solutions (pH 4.01, 7.01, 10.01)	Honeywell Fluka, 33646-500mL
Protease inhibitor tables	Roche, Ref: 11 836 153 001
Protein Marker	SERVA Electrophoresis, Cat.no:39252
Sodium bicarbonate	SIGMA, LIFE SCIENCE, S5761-1KG
Sodium Chloride	VWR, BDH, CHEMICALS, 27800.360
Sodium deoxycholate	SIGMA, LIFE SCIENCE, 30970-100G
Sodium dodecylsulfate (SDS)	VWR, LIFE SCIENCE, Product. No: 022-1KG
Sodium Hydroxide	Honeywell, Fluka™, 06203-1KG
SYBR Green I	Roche, Light Cycler®, 480SYBR®, Ref: 04887352001
TEMED	SIGMA, LIFE SCIENCE, T7024-100ML, PCode: 101637561
Transfection reagent	Dharmacon™, DharmaFECT™1, Cat.No: T-2001-02
Tris-Base	Roche, Diagnostics GmbH, Ref: 10708976001
Tris-Hcl	SIGMA, LIFE SCIENCE, Trizma® hydrochloride, T3253-500G

Triton X-100	Triton® X-100, Molecular Biology Grade, Ref: H5142
Trizol	TRIZOLATE Reagent, GENOMED, Cat.No: URN0102
Trypan blue	SIGMA, LIFE SCIENCE, T8154-100ML
Tween-20	Tween®20, Molecular Biology Grade, Ref: H5151

### 3.4 Drugs:

Table 3-4: List of the used drugs

Drug	Source
Bexarotene (Targretin, LGD1069; Bex)	MedChemExpress
Carvedilol (Carv)	Sigma

### 3.5 Buffers:

Table 3-5: List of the used buffers

Buffer	Composition
NaAc, 3M pH= 5.0	100 ml: 24.609 g up to 100ml MQ H2O
NaHCO <sub>3</sub> , 1M	10ml: 840mg NaHCO <sub>3</sub>
SDS 20%	100ml: 20 g up to 100ml MQ H2O
TBS (10x), pH=7.5	1L: 20mM Tris Base (24.3g), 150 mM NaCl (87.66g), MQ H2O till 1L
TBST (10x), pH= 7.5	1L: 20mM Tris Base (24.3g), 150 mM NaCl (87.66g), 0.1% Tween (10ml), MQ H2O till 1L
0.5M EDTA, pH= 8	100ml: 18.61 g, to dissolve the powder the pH should be around 8, so add ~ 4ml NaOH 6N and check the pH, up to 100ml MQ H2O
Blotting buffer, pH= 9.2	1L: 48mM Tris Base (5.82 g), 39mM Glycin (2.93g), 20% Methanol (200ml), MQ H2O till 1L
ChIP lysis buffer	500ml: 1% Triton x-100 (5ml), 0.1% SDS (2.5ml SDS 20%), 150mM NaCl (4.383 g), 1mM EDTA (1ml; 0.5M EDTA pH=8.0) , and 20mM Tris (10ml; 1M Tris pH= 8.0)
ChIP washing buffer 3	250ml: 0.25M LiCl (2.65 g), 0.5% NP-40 (1.25ml), 1mM EDTA (0.5ml; 0.5M EDTA pH=8.0), 20mM Tris (5ml; 1M Tris pH=8.0), 0.5% NaDOC (25ml; NaDOC 5%)
ChIP washing buffer 1	250ml: 1% Triton x-100 (2.5ml), 0.1% SDS (1.25ml; SDS 20%), 150mM NaCl (2.1915 g), 1mM EDTA (0.5ml; 0.5M EDTA pH=8.0), 20mM Tris (5.0ml; 1M Tris pH=8.0), 0.1% Sodium deoxycholate (5ml; NaDOC 5%)

ChIP washing buffer 2	250ml: 1% Triton x-100 (2.5ml), 0.1% SDS (1.25ml, SDS 20%), 500mM NaCl (7.305 g), 1mM EDTA (0.5ml; 0.5M EDTA pH=8.0), 20mM Tris (5ml; 1M Tris pH=8.0), 0.1% NaDOC (5ml; NaDOC 5%)
ChIP washing buffer 4 (TE buffer)	250ml: 10mM EDTA (0.5ml; 0.5M EDTA pH=8.0), 200mM Tris (5ml; 1M Tris pH= 8.0)
Elution buffer	10ml: 0.1M NaHCO <sub>3</sub> (1050ul; 1M NaHCO <sub>3</sub> ), 1% SDS ( 525ul; 20% SDS), 8925ul MQ H <sub>2</sub> O
ICC blocking buffer	10ml: 0.1% PBST (9ml), 1% BSA (0.1g), 10% normal goat serum (1ml), 0.3M Glycine (0.225g)
Mild Stripping buffer, pH= 2.2	500ml: Glycin (7.5 g), SDS (0.5g), Tween-20 (5 ml), MQ H <sub>2</sub> O till 500ml
NaDOC 5%	100ml: 5 g up to 100ml MQ H <sub>2</sub> O
PBST	1L: 100ml 10x PBS + 1ml Tween (100:1) + 900 ml H <sub>2</sub> O
permeabilization solution	0.5% triton x-100 (0.5ml) in PBS (100ml)
Phosphate buffered saline (10x )	1L: 1.37 M NaCl (80g), 27 mM KCl (2g), 100 mM Na <sub>2</sub> HPO <sub>4</sub> (17.8 g), and 18 mM KH <sub>2</sub> PO <sub>4</sub> (2.4g)
RIPA buffer	150 mM sodium chloride, 1.0% NP-40, 0.5% sodium deoxycholate, 0.1% SDS, 50mM Tris pH8.0
Running buffer (10x Tris/Glycin/SDS)	1L: 25mM Tris Base (30 g), 190mM Glycine (144 g), 0.1% SDS (10g), MQ H <sub>2</sub> O till 1L
Tris 1M pH=8	250ml: 30.285 g Trizma base
Tris-HCL 0.5M, pH= 6.8	100ml: 6 g Tris Base, 80 ml MQ H <sub>2</sub> O, adjust pH to 8.8 using 6N HCl
Tris-HCL 1.5M, pH= 8.8	100ml: 18.15g Tris Base, 80ml MQ H <sub>2</sub> O, adjust pH to 8.8 using 6N HCl

### 3.6 Kits:

Table 3-6: List of used kits:

The kit	The company, Reference number
ARID1A siRNAs kit	Tri FECTa® RNAi Kit, INTEGRATED DNA TECHNOLOGIES
DNA purification kit (ChIP-Seq)	Qiagen, MinElute ® PCR purification kit (50) Ref: 28004
DNA purification kit (ChIP-qPCR)	Roche, High Pure PCR Template Preparation Kit, Ref:11796828001
Plasmid isolation kit	Thermo Scientific Gene JETPlasmid, Miniprep kit, Ref:K0502
RNA isolation kit	MACHEREY-NAGEL, Nucleospin ® RNA Ref: 740955.50

### 3.7 Enzymes:

Table 3-7: List of used Enzymes:

The enzyme	The company, Reference number
Proteinase K	Thermo Scientific, Ref:E00491
Ribo nuclease A	SIGMA, LIFE SCIENCE, R5503-100MG
RevertAid Reverse Transcriptase 10000 U	Thermo Scientific, Ref: EP0441
Taq DNA polymerase	Thermo Scientific, Ref: EP0702

### 3.8 Oligonucleotides:

Table 3-8: List of primers used for RT-qPCR:

Gene Name or Symbol	Primers 5' $\longrightarrow$ 3'		
	Forward	Reverse	Probes
ARID1A	GCCAGTCGGACAGCA TCAT	CTCTGCATATAACCTCG ATCTTGG	FAM- CCTTCCATGAACCAATCAAGC ATTGCC-BHQ
$\beta$ -actin	CCCTGGCACCCAGCA C	GCCGATCCACACGGAGT AC	FAM- ATCAAGATCATTGCTCCTCCT GAGCGC-BHQ
BMP6	AGAATGCTCCTTCCC ACTCAAC	AAGGTGAACCAAGGTCT GCACA	FAM- CACACATGAATGCAACCAAC CACGC-BHQ
E-cadherin	AACGATGGCATTG AAAACAG	ACCACATTCGTCACTGC TACGT	FAM- AAGGGCTTGGATTTGAGGCCA AGC-BHQ
Fibronectin	AGAGAGTCAGCCTCT GGTTCAGAC	TGGAATCGACATCCACA TCAGT	ATGCCAGTCCTTTAGGGCGAT CAATGTT
FOXQ1	TTTCCGCGGCAGCTA CAC	CACCTTGACGAAGCAGT CGTT	FAM- CGAAAGGTTGTGGCGCACGG AG -BHQ
KLF4	GCTTGCGGCGGTAGC A	TCAGCGAATTGGAGAG AATAAAGTC	SYBR Green
N-Cadherin	ATCCTGCTTATCCTTG TGCTGATG	TTGTTTGGCCTGGCGTT CT	FAM- TGGTATGGATGAAACGCCGG GA-BHQ

FAM, 5-carboxyfluorescein; BHQ, black hole quencher.

TGFBR2	CATGAAGGACAACGT GTTGAGA	CCTGGTGGTTGAGCCAG AAG	FAM- ATCGAGGGCGACCAGAAATT CCCA-BHQ
--------	----------------------------	--------------------------	--

Table3-9: List of primers used for ChIP-qPCR during ChIP optimization step:

Gene Name or Symbol	Primers 5' $\longrightarrow$		Genomic Loci
	Forward	Reverse	
KRT8/18_-4Kb to TSS	GCCTTCCAATCCTCC CTAAT	TGATGGCTCTGGGGAA ACTA	chr12:53,339,301- 53,339,360
MAL2_-900bp to TSS	AATGGTGGGGGAAA GATGG	GAAGTGAGAAGGTGC AAAGG	chr8:120,221,490- 120,221,558
PPARG_-60Kb to TSS	CAAGTGAGTCAGCTG CAACG	TTTGCAGTTGTTCTCTG CTCA	chr3:12,271,479- 12,271,564
PTEN_+98Kb to TSS	GAGGGGGCTAAATG ACTGG	CCAAATGACTGAGTTC CCATC	chr10:89,721,127- 89,721,199

Table3-10: List of primers used for ChIP-qPCR, against the selected regions for the study:

Gene Name or Symbol	Primers 5' $\longrightarrow$		Genomic Loci
	Forward	Reverse	
BMP6_-27Kb to TSS	TTCATGCCAACATGG ATCAC	TCTTTAAACTCTTTGA ATTCTTGCTTC	chr6:7,698,428- 7,698,499
FOXQ1_+13Kb to TSS	TGTTTGCCTCACCGA TCC	AACAGAATGACTCAA AGGGTGAT	chr6:1,326,070- 1,326,148
IGF-1R_+6Kb to TSS	GATGTGATGTGGCTT TAAGTGG	TGCTTCCCAAATGTCA ACAG	chr15:99,198,179- 99,198,267
IGF-1R_+100Kb to TSS	CCATATTTTGCCTAA GAGATTCG	CATGCTGTCACCTGCC TAAG	chr15:99,292,948- 99,293,012
IGF-1R_+131Kb to TSS	TCAAGACTACAGTGA GCCACATTT	CTTTATTTTGAAACAG GGTCTCG	chr15:99,324,281- 99,324,361
IGF-1R_+211Kb to TSS	TCTTAGTAGATTTTG AACTCCGTGAA	TGAGCATATTGGAGAG ACTTGC	chr15:99,403,574- 99,403,645

IRS1_+643Kb to TSS	AATATTTTTCAATAG CTAGGGACCAC	TCACAGTCTGTTTACA ATGCTCAG	chr2:227,020,310- 227,020,390
IRS1_+676Kb to TSS	GGTGGCTAAGGAAA GAGTTTCA	AACGTTTTTATCCACT TATTTGTCG	chr2:226,984,163- 226,984,254
IRS1_+684Kb to TSS	GGGGTTACTCACCAT GCCTA	CCAAATATGCCAAAAG AATGC	chr2:226,980,054- 226,980,130
KLF4_-14Kb to TSS	CACTGGGCAGTGTTT GAGT	TGGGGCAAACCTGGTGG TA	chr9:110,266,666- 110,266,728
TGFBR2_-9Kb to TSS	AATAACCAATGAGTC TATTGTCAGGTT	TTTTACCTTCAGGCAT TTCAAAG	chr3:30,638,800- 30,638,867
TGFBR2_+52Kb to TSS	ACTGCTGGTGCTGTA GCAAG	CGCAGTGGGAGAGAC CTG	chr3:30,701,216- 30,701,279

### 3.9 Primary and Secondary Antibodies:

Table 3-11: List of used primary antibodies:

Antibody	Catalog no. Company	Concentration/assay
Acetyl-Histone H3 (K27) rabbit monoclonal antibody	Cell Signaling, 8173s, Lot # 6	4 µl/IP/ChIP-Seq 2 µl/IP/ChIP-qPCR
ARID1A rabbit monoclonal antibody	Abcam, ab182560, Lot # GR3240244-2	4 µg/IP/ChIP-qPCR 8 µg/IP/ChIP-Seq 1:500 / WB 1:1000/ ICC
ARID1A mouse monoclonal antibody	Santa Cruz Biotechnology, PSG3X, sc-32761x, Lot# C0116	8 µg/IP/ChIP-Seq
β-actin mouse monoclonal antibody	NOVUS, NBP1-47423, Lot # C-5	1:1000 /WB
BRG1 rabbit monoclonal antibody	Abcam, ab110641, Lot # GR3208604-17	2.5 µg/IP/ChIP-qPCR
E-cadherin rat monoclonal antibody	Invitrogen, 14-3249-82, Lot # 2340002	1:100/IC
Fibronectin rabbit polyclonal antibody	Invitrogen, PA5-29578, Lot # WI3371694C	1:50/ICC

FOXQ1 antibody	mouse	monoclonal	Invitrogen, MA5-26943, Lot # VL3143634	1:250/ WB
IGF-1R antibody	mouse	monoclonal	R&D SYSTEMS, MAB391	1:200/ WB 1:50/ICC
IRS1 antibody	rabbit	monoclonal	Cell Signaling Technology, #3407	1:500/ WB 1:200/ICC
N-cadherin antibody	mouse	monoclonal	Invitrogen, MA1-159, Lot # VH312184	1:50/ICC
Negative control for Ab-1	Rabbit IgG		NeoMarkers, NC-100-P1, Lot # 100P18118	4 µg/IP/ChIP-qPCR
Normal mouse IgG1			Santa Cruz, sc-3877, Lot# K0127	4 µg/IP/ChIP-qPCR
SMAD4 antibody	rabbit	monoclonal	Thermo Scientific, 701682, (10H10L15)	1:250/ ICC

Table 3-12: List of used conjugated secondary antibodies:

Antibody	Catalog no. Company	Concentration/assay
Anti-rabbit IgG	Dy Light™ 800, 51515, Cell signaling Technology	1:30000/WB
Anti-mouse IgG	Dy Light™ 680, 5470, Cell signaling Technology	1:30000/WB
Anti-rabbit IgG	Alexa fluor™ 546 Alexa fluor™ 488 invitrogen, Thermo Scientific	1:1000/ICC 1:1000/ICC
Anti-mouse IgG	Alexa fluor™ 546 invitrogen, Thermo Scientific	1:1000/ICC
Anti-Rat IgG	Alexa fluor™ invitrogen, Thermo Scientific	1:1000/ICC

### 3.10 Human cell lines:

Table 3-13: List of used cell lines:

Cell Line	Organism	Tissue	Cell type	Disease	Source
HEK293	Human	Kidney	Embryonic cells	Normal, immortalized	Uray Iván, University of Debrecen
HME-hTert	Human	Breast, Mammary gland	epithelial cells	Normal, immortalized	Uray Iván, University of Debrecen
MCF-7	Human	Breast, Mammary gland	epithelial cells	adenocarcinoma	Powel H. Brown, UT MD Anderson Cancer Center, Houston, TX
MDA-MB231	Human	Breast, Mammary gland	epithelial cells	adenocarcinoma	Uray Iván, University of Debrecen
T47-D	Human	Breast, Mammary gland	epithelial cells	ductal carcinoma	Uray Iván, University of Debrecen

### 3.11 Cell culture media and Supplements:

Table 3-14: List of used culture media and supplements:

Trypsin-EDTA (0.05%)	bioSera ID.no: MSOOC4101F
DMEM medium	CORNING, Ref:17-207-CVR
Fetal bovine serum (FBS)	BioSERA
MEBM medium	Lonza Clonetics®, MEGM®, Single Quots®, Cat.No: CC-4136
Penicillin/Streptomycine/ L-Glutamine, 100X	CORNING, Ref: 30-009Cl
Phenol-red free medium	gibco, Ref:A14430-01
Serum-low medium (Optimum)	gibco/ OPTI-MEM®I (1X) Ref: 31985-062
Trypsin	Lonza Clonetics® Cat.no: CC-5012
Trypsin Neutralizing solution	Lonza Clonetics® Cat.no: CC-5002

### 3.12 Software:

Table 3-15: List of used software:

Software	Purpose
CellProfiler 4.1	Cell-by-cell images analyses
GraphPad Prism 6.1	Numerical data analysis and visualization
ImageJ	<ul style="list-style-type: none"> <li>Image analysis and cell counting based on nuclear segmentation of their DAPI signal</li> <li>Western-blotting bands analysis</li> </ul>
LasX	Cell imaging using fluorescent microscope
Microsoft Excel, Word, PowerPoint	Sorting and analyzing data, writing scripts, data presentation
Primer Express 3.0.1	Primer design

### 3.13 Tools and software used for ChIP-Seq data analysis and visualization:

Table 3-16: List of tools used for ChIP-Seq using Linux server:

Tool	Function
Bedtools with intersectBed command	Regions overlap
BurrowsWheeler Aligner (BWA)	Fastq files (Raw data) alignment to the hg19 human reference genome, output: BAM
HMCAn	Peak calling, output: BED
Homer	<ul style="list-style-type: none"> <li>Motif enrichment analyses with findMotifsGenome.pl command</li> <li>Tag density values with annotatePeaks.pl command</li> <li>Annotation with annotatePeaks.pl command</li> </ul>

Table 3-17: List of tools used for ChIP-Seq using Galaxy server: (Order based on the sequence in the analysis pipeline)

Tool	Function	Version
FastQC	Read Quality reports	Galaxy Version 0.72+galaxy1
Tim Galore	Quality and adapter trimmer of reads	Galaxy Version 0.4.3.1

Bowtie2	Map reads against a reference genome	Galaxy Version 2.3.4.3+galaxy0
multiBamSummary	Calculates average read coverages for a list of two or more BAM/CRAM files	Galaxy Version 3.0.2.0
plotCorrelation	Create a heatmap or scatter plot of correlation scores between different samples	Galaxy Version 3.0.2.0
plotFingerprint	Plots profiles of BAM files; useful for assessing ChIP signal strength	Galaxy Version 3.0.2.0
bedtools Intersect intervals	Find overlapping intervals in various ways	Galaxy Version 2.27.1
bamCoverage	Generates a coverage bigWig file from a given BAM or CRAM file	Galaxy Version 3.0.2.0
bamCompare	Normalizes and compares two BAM or CRAM files to obtain the ration, log2ratio or difference between them	Galaxy Version 3.0.2.0
MACS2 callpeak	Call peaks from alignment results	Galaxy Version 2.11.20160309.6
Sort	Sort data in ascending or descending order	Galaxy Version 1.1.1)
Select last	Select last lines from a dataset (tail)	Galaxy Version 1.1.0)
Get flanks	Returns flanking region/s for every gene	Galaxy Version 1.0.0
Remove beginning	Remove beginning of a file	Galaxy Version 1.0.0
Advanced Cut	Cut columns from a table (cut)	Galaxy Version 1.1.0
Concatenate datasets	Concatenate datasets (cat)	Galaxy Version 0.1.0
bedtools SortBED	Order a feature file by chromosome or other criteria	Galaxy Version 2.29.0
bedtools MergeBED	Combine overlapping/nearby intervals into a single interval	Galaxy Version 2.29.0
computeMatrix	Prepares data for plotting a heatmap or profile of given regions	Galaxy Version 3.0.2.0
plotHeatmap	Creates a heatmap for score distributions across genomic regions, for example ChIP enrichment values around the TSS of genes	Galaxy Version 3.0.2.0
Extract Genomic DNA	Extract genomic DNA using coordinates from assembled/unassembled genomes	Galaxy Version 3.0.3

Table 3-18: List of software used for ChIP-Seq analysis and visualization:

<b>Software</b>	<b>Purpose</b>
Galaxy	ChIP-Seq and RNA-Seq data analysis
Genomic Regions Enrichment of Annotations Tool (GREAT)	Gene ontology analysis (ChIP-Seq)
Integrative Genomics Viewer (IGV)	Bigwig files Visualizing (ChIP-Seq binding events)
Java TreeView	Heatmaps for ChIP-Seq data

### 3.14 Accession numbers of available ChIP-Seq datasets generated in this study:

Table 3-19: List of publicly available datasets:

<b>Sample name</b>	<b>BioProject</b>	<b>BioSample</b>	<b>SRA Study</b>	<b>SRA Run</b>	<b>SRA Experiment</b>
hs_MCF-7_Bex-Carv_H3K27ac_ChIP-Seq	PRJNA799783	SAMN25209215	SRP357002	SRR17779475	SRX13941920
hs_MCF-7_Bex-Carv_ARID1A_ChIP-Seq	PRJNA799783	SAMN25209214	SRP357002	SRR17779476	SRX13941919
hs_MCF-7_Bex-Carv_Input_ChIP-Seq	PRJNA799783	SAMN25209213	SRP357002	SRR17779477	SRX13941918
hs_MCF-7_Veh_H3K27ac_ChIP-Seq	PRJNA799783	SAMN25209212	SRP357002	SRR17779478	SRX13941917
hs_MCF-7_Veh_ARID1A_ChIP-Seq	PRJNA799783	SAMN25209211	SRP357002	SRR17779479	SRX13941916
hs_MCF-7_Veh_Input_ChIP-Seq	PRJNA799783	SAMN25209210	SRP357002	SRR17779480	SRX13941915
hs_HMEC-hTert_Veh_Input_ChIP-Seq	PRJNA810076	SAMN26234275	SRP361403	SRR18136229	SRX14284262
ARID1A_Abcam_ChIP-	PRJNA810076	SAMN26234276	SRP361403	SRR18136228	SRX14284263

hs_HMEC-hTert_Veh_ARID1A_SantaCruz_ChIP-Seq	PRJNA810076	SAMN26234277	SRP361403	SRR18136227	SRX14284264
hs_HMEC-hTert_Veh_H3K27ac_ChIP-Seq	PRJNA810076	SAMN26234278	SRP361403	SRR18136226	SRX14284265
hs_HMEC-hTert_Bex-Carv_Input_ChIP-Seq	PRJNA810076	SAMN26234279	SRP361403	SRR18136225	SRX14284266
hs_HMEC-hTert_Bex-Carv_ARID1A_Abcam_ChIP-Seq	PRJNA810076	SAMN26234280	SRP361403	SRR18136224	SRX14284267
hs_HMEC-hTert_Bex-Carv_ARID1A_SantaCruz_ChIP-Seq	PRJNA810076	SAMN26234281	SRP361403	SRR18136223	SRX1428428
hs_HMEC-hTert_Bex-Carv_H3K27ac_ChIP-Seq	PRJNA810076	SAMN26234282	SRP361403	SRR18136222	SRX14284269

Table 3-20: List of tools used for RNA-Seq using Galaxy server:

<b>Tool</b>	<b>Function</b>	<b>Version</b>
FastQC	Read Quality reports	Galaxy Version 0.72
Trimmomatic	Flexible read trimming tool for Illumina NGS data	Galaxy Version 0.36.5
MultiQC	Aggregate results from bioinformatics analyses into a single report	Galaxy Version 1.7.1
HISAT2	A fast and sensitive alignment program	Galaxy Version 2.1.0
featureCounts	Measure gene expression in RNA-Seq experiments from SAM or BAM files	Galaxy Version 1.6.4
Column join	Join columns on multiple datasets	Galaxy Version 0.0.3
annotateMyIDs	Annotate a generic set of identifiers	Galaxy Version 3.7.0
Advanced Cut	Cut columns from a table (cut)	Galaxy Version 1.1.0
limma	Perform differential expression with limma-voom or limma-trend	Galaxy Version 3.38.3
Filter	Filter data on any column using simple expressions	Galaxy Version 1.1.1

## 4. Methods

### 4.1 Cell cultivation system

#### 4.1.1. Cell culture and treatment:

Immortalized primary human mammary epithelial cells (HME-hTert) were cultured in MEBM medium (Mammary Epithelial Cell Growth Basal Medium) supplemented with 50 µg/ml bovine pituitary extract, 5 µg/ml insulin, 10 ng/ml human recombinant epidermal growth factor, 0.5 µg/ml hydrocortisone, 30 µg/ml gentamicin, and 15 ng/ml amphotericin-B.

MCF-7 breast cancer cells with confirmed identity were kindly provided by Powel H. Brown, UT MD Anderson Cancer Center, Houston, TX. MCF-7 breast cancer cells were cultured in Dulbecco's modified Eagle's medium (DMEM, bioSera, MS00ER1003), supplemented with 10% fetal bovine serum (FBS, Biosera, S00402000M) and 100% streptomycin/ampicillin/glutamine (CORNING, 30-0090CI). To reduce estrogen-like effects, 24 hours before treatment with agents of interest, the medium was changed to phenol-red free DMEM (Gibco™, A14430-01) supplemented with 10% fetal bovine serum (FBS, Biosera, S00402000M) and 100% streptomycin/ampicillin/glutamine (CORNING, 30-0090CI). HEK293 and MB-MDA231 cells were maintained in Roswell Park Memorial Institute (RPMI, bioSera, MS00OQ1008) medium supplemented with 10% fetal bovine serum and 100% streptomycin/ampicillin/glutamine (CORNING, 30-0090CI).

Cells were tested to be mycoplasma free and maintained in a humidified atmosphere with 5% CO<sub>2</sub> at 37 °C, and were passaged every 3-4 days. Cells were frozen in a culture medium containing 20% FBS and 20% DMSO and were stored in liquid nitrogen at -180°C.

Bexarotene (Targretin, LGD1069; Bex) and carvedilol (Carv) were purchased from MedChemExpress and Sigma, respectively. The drugs were dissolved in DMSO/ethanol (50/50) solution. , DMSO/ethanol alone was used as a control treatment (Vehicle). Cells were treated at 30-40% confluence in triplicate. The agents were diluted in cell culture media before adding to cells, with DMSO final concentration not to exceed 0.01%. HME-hTert cells at 40% confluence were treated with TGF-Beta (Biotec, Lot#5180305401) at 5ng/ml final concentration, diluted in the culture medium. Cells were plated in different cell culture containers based on the experimental purpose; cells were seeded in 96-well optical plates for proliferation assessment. 24-well plates were used for generating RNA samples, 6 or 12-well plates for protein samples, on coverslips placed in 24-well plate for immunostaining, in culture inserts placed in 24-well plate for scratch assay, and in 20cm<sup>2</sup> plates for chromatin immunoprecipitation.

#### 4.1.2. siRNA transfection:

HME-hTert cells or MCF-7 cells were seeded in 24-well plates. Transfection was conducted at 30-40% confluence for 2 or 3 days, using a pool of three ARID1A-specific siRNAs (TriFECTa® RNAi Kit, Integrated DNA Technologies) and Dharmafect I transfection reagent (DharmaCon™, cat#T-2001-02). Transfection conditions were optimized to reach 70- 90% knockdown level using 20 nM or 10nM final concentration

of siARID1A in the case of HME-hTert or MCF-7 cells respectively, (Table 4-1). As a negative control, we transfected cells with siRNA against Luciferase transcript, not expressed in mammalian cells. The mixture of siRNA and the transfection reagent was incubated at RT for 15 min before the addition to the cultured cells. During the first 12-24 hours of transfection, cells were maintained in an antibiotic-free reduced serum medium (OPTI-MEM, REF 31985-062) to reduce the possibility of the antibiotics being taken up by the cells. ARID1A transcript was assessed using RT-qPCR and protein levels were measured in the transfected cells through Western blotting or immunostaining.

Table 4-1: siRNA transfection protocol in HME-hTert and MCF-7 breast cells:

\*Optimem: antibiotic-free reduced serum medium

	<b>si Luciferase, stock concentration: 20uM</b>		<b>Volume</b>	<b>Medium</b>	<b>Final siRNA concentration</b>
<b>HME-hTert</b>	Mixture 1: siRNA diluted in Optimem	0.2ul siRNA+ 19.8ul Optimem	20ul		
	Mixture 2: DharmaFECT diluted in Optimem	0.4ul DharmaFECT+ 19.6ul Optimem	20ul		
	1+2		40ul	160ul	20nM
	<b>siARID1A, stock concentration: 10uM</b>		<b>Volume</b>	<b>Medium</b>	<b>Final siRNA concentration</b>
	Mixture 1: siRNA diluted in Optimem	0.4ul siRNA+ 19.6ul Optimem	20ul		
	Mixture 2: DharmaFECT diluted in Optimem	0.4ul DharmaFECT+ 19.6ul Optimem	20ul		
	1+2		40ul	160ul	20nM
<b>MCF-7</b>	<b>si Luciferase, stock concentration: 20uM</b>		<b>Volume</b>	<b>Medium</b>	<b>Final siRNA concentration</b>
	Mixture 1: siRNA diluted in Optimem	0.1ul siRNA+ 19.9ul Optimem	20ul		
	Mixture 2: DharmaFECT diluted in Optimem	0.4ul DharmaFECT+ 19.6ul Optimem	20ul		
	1+2		40ul	160ul	10nM
	<b>siARID1A, stock concentration: 10uM</b>		<b>Volume</b>	<b>Medium</b>	<b>Final siRNA concentration</b>
	Mixture 1: siRNA diluted in Optimem	0.2ul siRNA+ 19.8ul Optimem	20ul		
	Mixture 2: DharmaFECT diluted in Optimem	0.4ul DharmaFECT+ 19.6ul Optimem	20ul		

	1+2		40ul	160ul	10nM
--	-----	--	------	-------	------

#### 4.1.3. Escherichia. Coli transformation with ARID1A cDNA plasmid and further plasmid extraction procedure from the bacterial stock:

ARID1A cDNA plasmid was a kind gift from Dr Guang Peng, MD Anderson Cancer Center, Houston, TX. Plasmid DNA was incubated with E.coli DH5 alpha competent cells (1:10), mixed and incubated on ice for 30 min. The mixture was placed to a 42°C water bath for 60 sec to introduce a heat shock. Then the bacteria-DNA mixture was incubated on ice for 2 min. LB medium was added to the mixture to let the bacteria grow at 37°C for 45 min with agitation. 50 µl of the grown bacteria was plated in LB agar plates containing ampicillin and incubated in inverted position at 37°C overnight. One bacterial clone was taken and amplified in LB culture medium and ampicillin. The bacterial stocks were generated and stored at -70°C.

Plasmid bacterial stock was stored in -70°C degree. For plasmid preparation, bacteria were cultured in Lysogeny Broth (LB) medium (sterilized) with Ampicillin antibiotic (AM) added to it at 50µg/ml final concentration. Ampicillin stock concentration is 100µg/µl, kept at 4°C. A 15ml bacterial tube containing 500µl LB+AM was prepared. Bacterial plasmid stocks were kept on ice during the procedure (be sure not to let them thaw completely), using 20 ul tip, a scratch from the stock was taken and mixed in the LB medium. The bacterial culture was incubated at 37°C, with agitation at highest speed, for about 4-6h. Bacterial growth was checked through considering the cloudiness as a marker. Next, bacterial colonies in the cultured media were transferred into 50ml tube (5ml LB+AM) or an Erlenmeyer flask (sterilized) (50ml LB+AM), and incubated at 37°C, with agitation at highest speed, overnight. Plasmids were isolated the next day using GeneJET Plasmid Miniprep kit (K0502, K0503) according to the manufacturer's instructions.

#### 4.1.4. Transfecting human cell lines with cDNA plasmids:

HEK293 cells were plated in 6-well plate and cultured in 2.5ml RPMI medium. A day before transfection the medium was changed to 1 ml fresh RPMI. The next day cells were transfected at 40% confluence with a mixture of Opti-MEM I Reduced-Serum medium, 1 µg Plasmid DNA, and TransIT-BrCa Reagent (MirusBio, ML058-Rev.D 0117) (Table 4-2). The mixture was incubated for 20 min at RT, and then added to the cells gently. Transfection efficiency was checked after 24 hours under a fluorescent microscope through detecting m-Cherry fluorescent signal, as a transfection positive control. Cells were harvested after 2 days of transfection and protein samples were generated and prepared for gel electrophoresis.

Table 4-2: Transfecting HEK293 cells with cDNA plasmid using TransIT-BrCa reagent:

Warm the TransIT-BrCa Reagent to room temperature and vortex gently			
Prepare the mixture to be added to 1ml medium	<b>ARID1A Transfected sample</b>	<b>mCherry Transfected sample (transfection positive control)</b>	<b>Transfection negative control sample</b>
<b>Opti-MEM I Reduced-Serum medium</b>	100µl	100µl	100µl
<b>Plasmid DNA</b>	10µl (0.1 µg/µl)	2µl (0.5µg/µl)	-
<b>TransIT-BrCa Reagent</b>	2µl	2µl	2µl

#### 4.1.5. Proliferation assay:

MCF-7 cells were seeded in 96-well optical plate and treated at 20% confluence with agents of interest. Treatment was repeated every second day. After 5 days of treatment, cells were fixed with 4% formaldehyde in PBS for 30 min at RT. Cells were washed with cold PBS for 3x5 minutes then incubated with permeabilization solution (0.5% Triton X-100 in PBS) for 40 min at RT, followed by washing steps. Cell nuclei were stained with DAPI (1 mg/ml) for 15 minutes at RT, washed with PBS and imaged using a fluorescent microscope (LEICA DMi8). Cell counting based on nuclear segmentation of DAPI signal was performed using ImageJ software.

#### 4.1.6. Colony formation assay:

1 ml agarose (1%) was added to 1 ml 2x full DMEM medium, and then 1.5ml mixture was added to each well/6-well plate to form the bottom layer and left for 30 min at RT for solidification. To generate the top layer 1 ml agarose (0.6%) was mixed with 1 ml 2x full DMEM medium and about  $15 \times 10^3$  MCF-7 cells, then the mixture was poured on the top of the bottom layer and left for 30-40 min to solidify. 1 ml of media containing treatment was added to the cells. The cells were kept at 37 °C and 5 % CO<sub>2</sub> for 4 weeks, Figure 4-1. Treatment containing medium was replaced every third day. Pictures for the colonies were taken using phase contrast mode within LEICA DMi8 microscope using the LasX software. Colonies larger than 300 µm in diameter were counted using ImageJ software. The experiment was performed in three biological replicates.

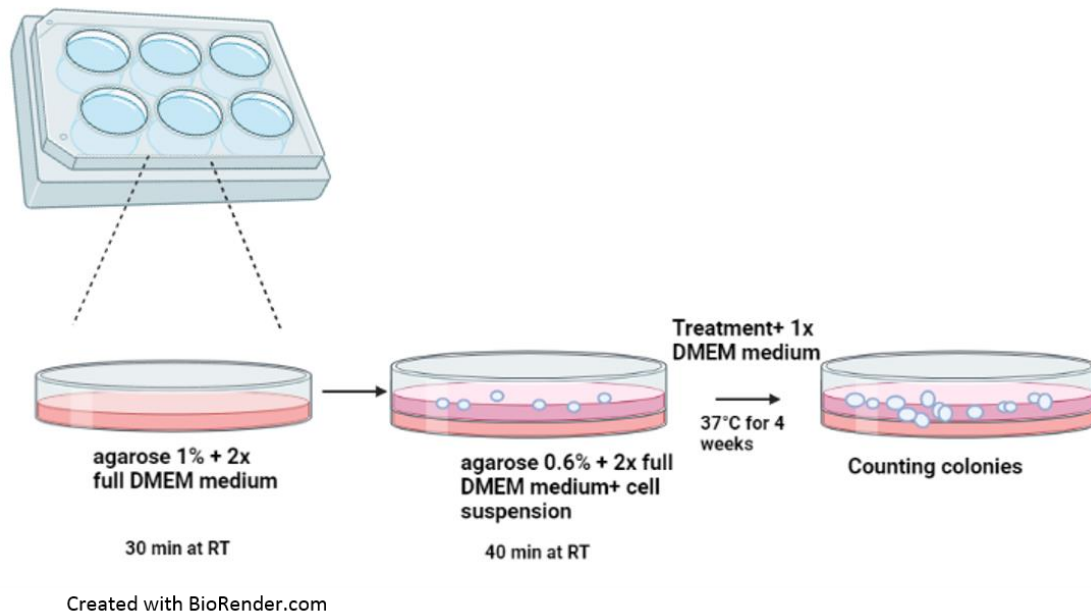


**Figure 4-1:** Steps of the colony formation assay

#### 4.1.7. Wound healing assay:

Culture inserts were placed in each well of a 24-well plate,  $35 \times 10^3$  cells in 70ul phenol red-free and serum-free medium were seeded on each side of the culture insert. Within 24 hrs cells reached 100% confluence, we removed the insert carefully, washed the cells and applied fresh medium containing the treatment (Veh, or Bex100+Carv300 nm) Figure 4-2. At zero time point, we took pictures of the wound. We checked the cells consistently and repeated the treatment every second day. On day 5 we noticed a change between the different studied groups, which was considered the end time point of the experiment. Pictures of the healed wounds were taken through a phase contrast mode using a microscope (LEICA DFC7000 T) and Las X software.

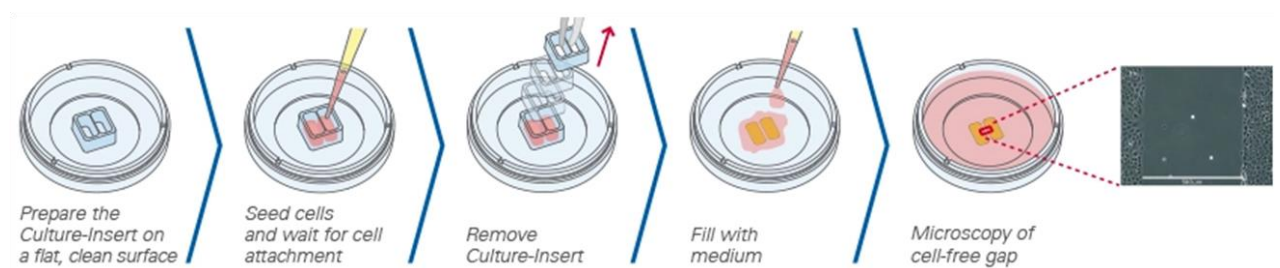


**Figure 4-2:** wound healing assay using culture insert (<https://ibidi.com/culture-inserts/24-culture-insert-2-well.html>)

#### 4.1.8. Studying the effect of IGF-1R neutralization on MCF-7 cell proliferation:

MCF-7 Cells were seeded in 96-well optical plate and maintained in a normal DMEM or phenol-red free DMEM medium. Cells were treated for 3 days with  $11 \mu\text{g/ml}$  IgG antibody against IGF-1R (R&D SYSTEMS, MAB391). After that cells were fixed with 4% formaldehyde in PBS1X for 30 min at RT. Cells were washed with PBS (3x5) and

then incubated with permeabilization solution (0.5% Triton X-100 in PBS) for 40 min at RT, followed by washing steps. Cell nuclei were stained with DAPI (1 mg/ml) for 15 minutes at RT. After which, all cells were counted by automated fluorescent microscopy (LEICA DMI8) using the LasX software based on the DAPI signal, which represents cell nuclei. Image analysis was performed using ImageJ software.

## 4.2 Protein Biochemical technologies

### 4.2.1. Protein extraction and protein concentration measurement:

Cells were seeded in 6 or 12-well plate, and treated in triplicates at ~40% confluence. Treatment duration varied based on the experimental purpose. Cells were washed twice with ice-cold PBS1X then lysed and incubated for 5 min in RIPA lysis buffer (150 mM sodium chloride, 1.0% NP-40, 0.5% sodium deoxycholate, 0.1% SDS, 50mM Tris pH8.0) with protease and phosphatase inhibitor cocktail added to it. The cell lysate was collected and transferred to 1.5ml tubes. To decrease the viscosity caused by the genomic material, the cell lysate was sonicated for 5min in total (5 cycles, 30 sec on, 30 sec off) (Bioruptor® Plus, diagenode) followed by 20 min centrifugation at 12000xg at 4°C. The supernatant was collected, and total protein concentration was measured using a BCA assay, based on colorimetric detection. The principle of the BCA method is that in the presence of protein the copper  $\text{Cu}^{++}$  is reduced to  $\text{Cu}^{+}$  which chelates with a BCA reagent (bicinchoninic acid) to form a purple-colored product that absorbs light at 560nm with increased intensity based on protein concentration. A standard series was generated using 0.125, 0.25, 0.5, 0.75, 1, 1.5  $\mu\text{g}/\mu\text{l}$  of BSA (Bovine Serum Albumin) solutions. 200 $\mu\text{l}$  of a mixture of Reagent A and B (50:1) was added to each protein sample (10 $\mu\text{l}$ ) and incubated at 37 °C for 30 min. The absorbance of the purple-colored products was detected using a plate spectrophotometer (BioTek SYNERGY/LX) at 562nm. The concentration of the tested protein sample was detected based on a standard curve calculation. 25 $\mu\text{g}$  -35 $\mu\text{g}$  total protein was used for sample preparation for gel electrophoresis. Proteins were denatured by the addition of denaturation buffer (375 mM Tris/HCl, 10% SDS, 30% glycerol, 0.02% bromophenol blue, 9.3% DTT) and heated at 95 °C for 5 min.

### 4.2.2. Western-blotting:

25-50  $\mu\text{g}$  of total protein from each sample was loaded into a 6% SDS-polyacrylamide gel. During gel preparation we prepared two types the bottom one is 6% separating gel and the top one is 10% stacking gel where the purpose of it to line up protein samples to enter the separating gel at the same time. Proteins are separated based on their molecular weight. The Electrophoresis step consists of two steps, 30 min at 90 volts followed by 45 min at 120 volts. Proteins were transferred from the gel to a polyvinylidene fluoride membrane (PVDF) for 25 min to transfer small proteins (40-90KDa) and for 3 hrs for large proteins (180-300KDa) at 0.12 Ampere. Blots were then blocked with 5% low-fat milk in tris-buffered saline (TBS) buffer for 1 hr at room temperature (RT). Blots were probed with primary antibodies overnight at 4°C (Table 3.11), followed by washing steps with tris-buffered saline, and 0.1% tween (TBST) buffer for 5 times 5 min each. Then we probed the membranes with fluorescent

conjugated secondary antibodies with 30,000 x dilution for 1h at RT (Table 3.12), followed by (5x5) washing steps. Signal detection was performed using Odyssey® CLx imaging system (LI-COR). Image J software was used to quantify the signal intensity of the detected bands. The relative abundance of a protein of interest was calculated after normalization to the protein levels of the  $\beta$ -actin housekeeping gene.

#### 4.2.3. Protein samples preparation for sequencing:

30  $\mu$ g total proteins, generated from HEK293 cells transfected with ARID1A cDNA plasmid were separated in 10% SDS-PAGE gel. After 3 hours of electrophoresis separation, the gel was stained with Coomassie Blue stain for 1 hour at RT. The gel was washed with MQ water for 5 min 4 times and then incubated for overnight in MQ water at RT. The next procedures were all done in the proteomic core facility. The work was done in a clean environment (to avoid any contamination with skin or surface keratins), to a clean and sterilized glass the gel was transferred. The bands at the molecular weight 120-140, 250, or 270-300KDa were cut. Every band was handled separately and cut into very tiny pieces and then transferred to a 1.5ml tube containing 1ml MQ water. To de-stain the gel pieces, the MQ water was removed using loading tips. 50-250 $\mu$ l 25mM Ammonium Bicarbonate in 50% ACN was added till covering all gel pieces and mixed for 20 min. This step was repeated until the gel pieces become clear. After the last wash, gel pieces were dried with the speed-vacuum, for 1 hour or less. 50-250 $\mu$ l of 20mM DTT in 100mM ammonium bicarbonate buffer (enough to cover the gel pieces) was added. Vortex, spin and then incubate the tubes for 60 min at 56°C. To remove the DTT solution, centrifuge the tubes and remove it. Within the alkylation next step 100-200 $\mu$ l of IAA solution (55mM iodoacetamide in 100mM ammonium bicarbonate buffer) was added, vortex, spin, and incubated in dark at RT for 45min. IAA solution was removed and 100-200 $\mu$ l of 25mM ammonium bicarbonate in 50% ACN (enough to cover the gel pieces) was added to the gel pieces and vortex for 10 min. the last step was repeated twice. Trypsin (0.5 $\mu$ g/ $\mu$ l) was used to digest the proteins. 50mM ammonium Bicarbonate was used to dilute Trypsin stocks (198 $\mu$ l: 2 $\mu$ l). 40 $\mu$ l from the diluted trypsin was added to the gel pieces. Gel pieces were rehydrated on ice for 15-45mins, then covered with 200 $\mu$ l of 50mM ammonium bicarbonate, and incubated at 37°C overnight. Trypsin reaction was stopped using formic acid; 1 $\mu$ l of 100% bFA solution, vortex for a few seconds. After removing the solution from the previous step, we started the extraction step; 100 $\mu$ l 5% ACN/0.1% TFA was added to the gel pieces, vortex for 40min at RT, this step was repeated twice. Then 100 $\mu$ l of 50% ACN/0.1% TFA solution were added to the gel pieces, vortex for 40min. After a short spin, the solvents were transferred into new tubes. Speed vacuum the sample will produce a pellet. In case of using the samples immediately for protein sequencing, then 50  $\mu$ l 1% FA was added (in case samples will be frozen and later sequenced, don't add FA). After dissolving the pellet in 50 $\mu$ l FA1%, 10 $\mu$ l was taken and placed in a vial for HPLC-MS analysis which was performed by the proteomic core facility members, University of Debrecen.

#### 4.2.4. Immunocytochemistry/Immunofluorescence:

Cells were seeded on sterilized coverslips placed in a 24-well plate, treated at 30- 40% confluence, and then fixed with 4% formaldehyde in PBS1x for 30 min at RT. Cells were washed with PBS 3 times and then incubated with permeabilization solution (0.5% Triton-x 100 in PBS) for 40 min at RT. In order to prevent non-specific bindings cells

were incubated with blocking buffer (1% BSA/ 10% normal goat serum/ 0.3M glycine in 0.1% PBS-Tween) for 1 hour at RT, followed by washing steps with PBST 3 times. Primary antibody was added and incubated with the cells overnight at 4°C (see table 10 for Primary Antibody information), followed by washing steps with PBST 3 times. Secondary Ab (Alexa fluor conjugated antibodies 1:1000) (Table 3.12) was added to the cells and incubated for 1 hour at RT. The complex; protein-primary Ab- secondary Ab was then cross-linked by incubating the cells with 4% formaldehyde in PBST for 10 min, followed by quenching the formaldehyde effect using Ammonium chloride at 100mM final concentration (1M Ammonium chloride diluted 1:10 in PBS) for 10 min at RT. Cell nuclei were stained with DAPI (1mg/ml, 1:1000) for 15 minutes at RT, followed by washing steps with PBST 3 times. The fluorescent signal was detected using an inverted fluorescent microscope (LEICA DMi8) through LasX software. Data analysis was performed using the CellProfiler 4.2.1 cell image analysis software based on cell by cell analysis.

### 4.3 Genomics and Analysis of nucleic acids

#### 4.3.1. RNA isolation:

Cells were plated, seeded, in a 24-well plate, and treated in triplicates for different time points depending on the experimental purpose. RNA was isolated using either a NucleoSpin RNA isolation kit (MACHEREY-NAGEL, Ref: 740955.50) according to the manufacturer's instructions or using a Trizol reagent as described below. After removing the medium, 200ul Trizol (TRIZOLATE Reagent, GENOMED, Cat.No: URN0102) was added to each well. Cells were incubated in Trizol at RT for 5 min, and then cell lysate was harvested and transferred into 1.5ml labeled tubes. Cell lysate in Trizol was shaken for 5 min at RT. 40ul chloroform was added to each sample, and mixed for 5 min at RT. Samples were centrifuged at 12000 xg for 15 min. Then we got three layers including; the aqueous phase (containing the RNA molecules), the interphase (containing proteins) and the organic phase (containing DNA molecules and other cell components). Carefully the aqueous phase was transferred into 1.5ml tubes. Isopropanol was then added to each sample with an equivalent volume to the aqueous phase. Samples were mixed and centrifuged at 12000 xg for 10 min at 4°C. The supernatant was removed, and RNA pellet was washed with 75% cold ethanol, and then centrifuged at 7500 xg for 5 min. After removing the ethanol and the salts dissolving in it, tubes were left under the hood for 20-30 min until ethanol residues evaporated completely. The RNA pellet was dissolved in 35ul nuclease-free water and kept at -70 °C.

#### 4.3.2. RT-qPCR:

1 ul RNA was used for the reverse transcription reaction, to generate complementary DNA, through the following conditions; 50°C for 30 min followed by an enzyme deactivation step at 72°C for 5 min using reverse primers specific to the target regions. The produced cDNA molecule was amplified through quantitative real-time PCR. Most of the target transcripts were amplified using TaqMan assay with the following conditions: initial denaturation at 95 °C for 2 min followed by 40 cycles of denaturation at 95 °C for 10 seconds then annealing and extension at 60 °C for 30 seconds for each

cycle. For some targets, we used SYBR Green as a fluorescent dye with the following PCR program: initial denaturation at 95 °C for 5 min followed by 40 cycles of denaturation at 95 °C for 15 seconds then annealing and extension at 60 °C for 30 seconds for each cycle. As SYBR Green binds double-strand DNA non-specifically then a melting curve program was added including the following steps: 95 °C for 15 seconds, 60 °C for 60 seconds, and then 95 °C for 15 seconds, the signal is recorded at the last step when the temperature is increasing from 60 to 95 °C, expecting one peak that represents one specific product. We had two types of negative controls, the first one is a No-RT control for each sample; all RT reaction components are added except the reverse transcriptase enzyme. The other type is NTC; no RNA template control to detect any genomic DNA contamination. Absolute quantification method was used for data analysis. Target gene transcript levels were normalized to its corresponding  $\beta$ -actin levels within the same sample. Primers and probes were designed using the Primer Express 3.0.1 program ensuring low primer dimer or hairpin formation. Primers were selected after checking their specificity using the NCBI primer-blast tool. Sequences of the oligos used for RT-qPCR are shown in Table 3.8. Table 4-3, 4-4, 4-5, 4-6 represents the compositions of RT and qPCR reactions using Taqman and SYBR GREEN assays.

Table 4.3: RT reaction for Taq man assay

Reagents	Volumes for 1 reaction $\mu$ l
NFW	1.93/2.68
RT Buffer 5Xdt	1.0
dNTPs 2.5mM/100mM	1.0/0.25
Reverse primer (-) 100uM	0.02
Reverse transcriptase 200U/ul	0.05
RNA template 100ug/ul	1

Table 4-4: qPCR reaction for Taq man assay

Reagents	Volumes for 1 reaction $\mu$ l
NFW	15.425/16.145
PCR Buffer 10x (Mgcl2, 20mM)	2.0
Mgcl2 50mM	1.0
dNTP 2.5mM/100mM	1.2/0.3
Reverse Primer (-) 100uM	0.08
Forward Primer (+) 100uM	0.1
Probe FAM-BHQ (100uM)	0.025
Rox (50x)	0.05
Taq polymerase (5U/ul)	0.1

Table 4-5: RT reaction for SYBR GREEN assay

Reagents	Volumes for 1 reaction $\mu$ l
NFW	1.96/1.16
RT Buffer 5Xdt	0.8
dNTPs 2.5Mm/100mM	1/0.2
Reverse primer (-) 100uM	0.016
Reverse transcriptase 200U/ul	0.04
RNA template 100ug/ul	1

Table 4-6: qPCR reaction for SYBR GREEN assay

Reagents	Volumes for 1 reaction $\mu$ l
NFW	0.4
Reverse and Forward Primer (5 $\mu$ M)	0.5
SYBR GREEN Master	5
Rox (50x)	0.02

#### 4.3.3. Chromatin immunoprecipitation (ChIP):

Cells plated in 20cm<sup>2</sup> plates were treated as the experimental design. After treatment cells were fixed using 1% formaldehyde in PBS for 10 min at RT. Formaldehyde activity was quenched using glycine in PBS at 125mM final concentration for 10 min at RT. Fixed cells were washed twice using ice-cold phosphate-buffered saline. Cells were lysed using lysis buffer (1% Triton X-100, 0.1% SDS, 150mM NaCl, 1mM EDTA pH=8.0, 20mM Tris pH=8.0) plus protease inhibitor tablets (Roche, cOmplete Mini, Cat# 11836153001) (40 ml lysis buffer: 3 protease inhibitor tablets). Cell nuclei pellet was collected by centrifugation at 4 °C for 12,000g for 1min. Cell nuclei were washed three times with the lysis buffer. Chromatin was sheared through the sonication step using the following conditions (3 x 5 min long cycles with 30 sec on and 30 sec off) using the Diagenode Bioruptor® Plus sonicator. After centrifugation, the supernatant was collected and transferred into 1.5ml low binding tubes. The input sample was set aside as 10% of the sheared chromatin from each IP. The sheared chromatin was diluted (1:9) using the lysis buffer. A clearing step was added to the procedure to reduce the background generated from nonspecific interactions, including incubation of the diluted chromatin with a mixture of protein A and protein G (1:1) (Dynabeads, Invitrogen, Thermo Fisher Scientific, Dynabeads protein A and protein G) beads coated with IgG for overnight at 4°C. In parallel beads (blocked by 0.5% filter BSA in PBS) were incubated with antibodies against target proteins overnight at 4°C in a lysis buffer solution. The immunoprecipitation step was performed through the incubation of sheared and cleared chromatin with beads coated with antibodies against the protein of interest overnight at 4°C. The precipitated beads-antibody-protein-DNA complex was washed using 4 different washing buffers (Table 3-5). At the last washing step (using TE buffer) the beads-antibody-protein-DNA complex in TE buffer was transferred into fresh 1.5ml low binding tubes. From this step, we included the input samples. DNA-protein complex was eluted through incubation with elution buffer (0.1M NaHCO<sub>3</sub>, 1%SDS) for 15 min at 1,000 rpm at RT. DNA-protein interactions were de-cross-linked by incubating the samples with 0.2M NaCl overnight at 65°C. DNA was purified by the addition of 10  $\mu$ g RNase A (10 $\mu$ g/ $\mu$ l), 20  $\mu$ g proteinase K (20 $\mu$ g/ $\mu$ l), 0.04M Tris-HCl pH=7.0, 0.02M EDTA pH=8.0, the mixture was incubated for 2 hours at 45°C on a thermomixer at 1,000 rpm. The last purification step was performed using Qiagen MinElute PCR purification kit (REF 28004) for ChIP samples to be sequenced or with High Pure PCR Template Preparation Roche Kit in case of ChIP-qPCR (Table 3.6). Finally, we measured DNA concentration by the Qubit dsDNA HS assay. Library preparations and sequencing of ChIP samples were performed by the Genomic core facility (University of Debrecen, Debrecen, Hungary), using 10 ng of DNA and Illuminas TruSeq ChIP Sample Preparation. Sequencing was performed using

Illumina's NextSeq 500 instrumental mode. Enrichment of specific target regions in DNA samples was tested in qPCR reactions. Figure 4-3.

#### 4.3.4. ChIP-qPCR:

IP and input samples were diluted 3 times with nuclease-free water after DNA purification. Input samples were used as a control; the amount of DNA of a target region in each IP sample was normalized to the DNA copy number in the corresponding input sample. 1 µl DNA from each sample was used in a qPCR reaction using SYBR Green I Master (Roche Diagnostics GmbH) as a fluorescence reporter dye, with the following PCR conditions: initial denaturation at 95 °C for 5 min followed by 40 cycles of denaturation at 95 °C for 15 seconds then annealing and extension at 60 °C for 60 s. To test assay specificity for the studied target, 1 cycle of a melting curve program was added for 15sec at 95°C followed by 1 min at 60°C, then 10 sec at 95°C. The signal was recorded during the transition from 60 to 95°C. We designed primers for ARID1A binding regions using the online universal probe library. Figure 4-3. Primer sequences used for ChIP-qPCR are indicated in Table 3-9, and Table 3-10.

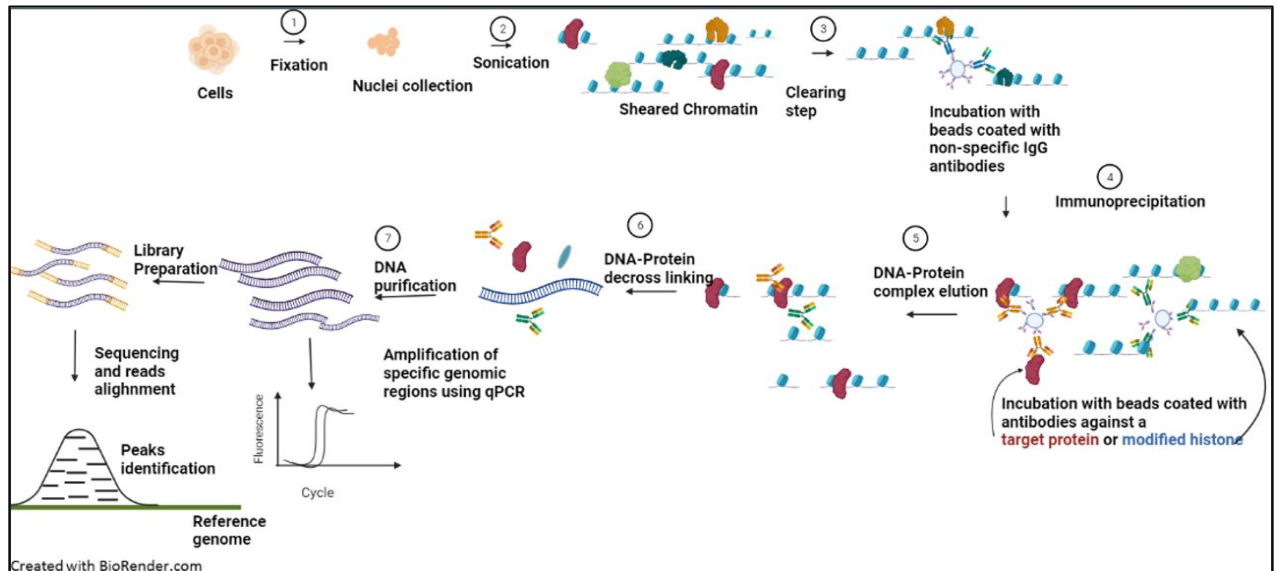


**Figure 4-3:** Chromatin immunoprecipitation steps.

## 4.4 Data analysis and Bioinformatics

### 4.4.1. Fluorescent image analysis:

The fluorescence intensity of target proteins was measured based on cell-by-cell analysis using CellProfiler 4.2.1 software. Images related to one group of samples were uploaded to the program. Primary objects were selected based on a reference dye; in the case of nuclear proteins DAPI stain, and in the case of cytoplasmic proteins, Tubulin-Beta was used. Then the integrated intensity for the target protein was calculated in the selected objects. To measure the nuclear translocation of a certain target, we used two reference dyes; one for the nucleus (primary object) and the other for the cytoplasm (secondary object). We measured the nuclear translocation by dividing the target protein's nuclear-integrated intensity by the cytoplasmic integrated

intensity and generated a ratio. My colleague Máté Lengyel has helped in image analysis using Cell profiler software.

#### 4.4.2. ChIP-Seq data processing:

Fastq files (75 bp Single-end reads) were obtained from the Genomic core facility, University of Debrecen. ChIP-Seq data were analyzed using two different platforms. The functions and tools used for analysis using the Galaxy platform are mentioned in table 16. Briefly, the quality of sequencing was detected using FASTQC. Using Trim Galore we removed the low-quality reads. The trimmed fastq reads were mapped to the hg19 version of the human genome using Bowtie software (v 2.3.43) to produce BAM files. Peaks were called using MACS2 software and BED files were generated. The FDR q value to call peaks was set at  $\leq 0.05$ . To generate representative heatmaps and to identify ARID1A genomic distribution analysis was performed using Homer software by a published computational pipeline [59]. Raw data were aligned to an hg19 reference dataset using Burrows-Wheeler Aligner (BWA). Peaks were called using HMCAN [60]. Artifact peak list was downloaded from the Encyclopedia of DNA Elements (ENCODE) and was removed from our peak sets. Overlap regions were determined using Bedtools with the intersectBed command. Reads were normalized to sequencing depth through the bam-coverage function and bigwig files were generated to visualize the binding events with the Integrative Genomics Viewer (IGV).

Motif enrichment analyses were performed using Homer software with the findMotifsGenome.pl command. The size parameter was 100 bp. Tag density values were calculated based on summits of peaks flanking with  $\pm 1000$  base pair region for ARID1A and with  $\pm 2000$  for H3K27ac using Homer software with annotatePeaks.pl command options. Annotation was performed using Homer software with annotatePeaks.pl command. Heatmaps for ChIP-Seq data were created using the Java TreeView software. Plots were created using GraphPad Prism 6 software. ChIP-Seq raw data availability accession numbers are illustrated in Table 3-19. ChIP-Seq analysis using the Linux server including identifying ARID1A genomic distribution, heatmaps and histograms production, and motif enrichment analysis was performed by Dr Edina Erdős.

#### 4.4.3. Statistical analysis:

Three independent biological replicates were performed for each experiment. Statistical values are expressed as the mean  $\pm$  SD. Comparisons between two groups were performed using the unpaired two-tailed student's t-test. Comparisons between more than two groups were performed using a one-way ANOVA test followed by the Tukey post-hoc test. P-value  $<0.05$  represents a statistically significant difference between the studied groups.

## 5. Results

### 5.1 Bexarotene and carvedilol (Bex+Carv) combination treatment decreased normal and transformed breast cell proliferation:

The combination treatment of Bex+Carv was associated with a significant decrease in the proliferation of normal immortalized breast epithelial cells HME-hTert, which represents a good model to detect the in-vitro cancer-preventive effects of the combined treatment. The detected effect upon the combined treatment was superior to the one identified upon the individual treatments (**Figure 5-1 A**). This data was generated by Dr Iván Uray. Moreover, the combination treatment of Bex+Carv in different concentrations showed antiproliferative effects on MCF-7 breast cancer cells (**Figure 5-1 B**). On the other hand, the combination treatment showed no significant effect on MCF-7 cell invasion (**Figure 5-1 C, D**) or transformation ability (**Figure 5-1 E**).

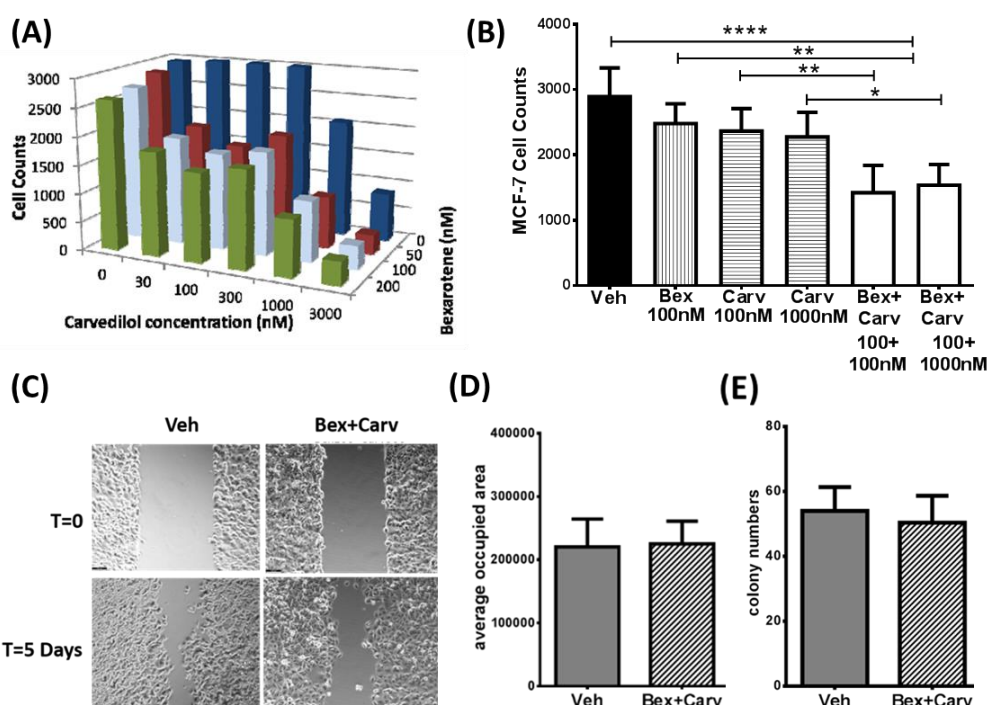


**Figure 5-1: Bex+Carv treatment is associated with antiproliferative effects in HME-hTert cells and MCF-7 cells.** (A) Dose-response relationship of the non-selective adrenergic inhibitor carvedilol and the rexinoid bexarotene on HME-hTert cells' proliferation upon the individual or combined treatment for 4 days. (B) MCF-7 cell counts evaluated by microscopy after 5 days of Bex and/or Carv treatment (Veh; Vehicle, Bex + Carv; bexarotene+carvedilol. DAPI stained nuclei imaged at 5x). (C, D) Wound healing assay was performed in MCF-7 cells treated with Bex and/or Carv treatment. Pictures were taken at zero time point and repeatedly every day until day 5. Representative images are shown (n = 12), scale bar = 100 μm. (E) Colony formation assay on MCF-7 cells upon Bex+Carv or Vehicle treatment; average colony counts from 3 replicates are shown. The results are expressed as mean ± SD \*P < 0.05, \*\*P < 0.01, \*\*\*\*P < 0.0001 by One-way ANOVA, Tukey post-hock test.

## 5.2 Bexarotene and carvedilol combination treatment induced ARID1A protein levels in HME-hTert cells:

ARID1A protein expression levels were detected to be upregulated in HME-hTert cells upon Bex+Carv treatment using a high-throughput screening method; Reverse phase proteomic array (RPPA) (Figure 5-2 A), the RPPA data were generated by Dr Iván Uray. We validated the RPPA results using Western-blotting (Figure 5-2 B, C) and immunofluorescence (Figure 5-2 D, E) assays, showing an induction in ARID1A protein levels after 48 hours of exposure to Bex+Carv treatment. Furthermore, to study if the change in ARID1A protein levels is transcriptional independent, we measured ARID1A transcript levels through RT-qPCR after different time points. The results showed no change in ARID1A gene expression levels post 6, 12, or 24 hours of Bex+Carv treatment in HME-hTert cells (Figure 5-2 F).

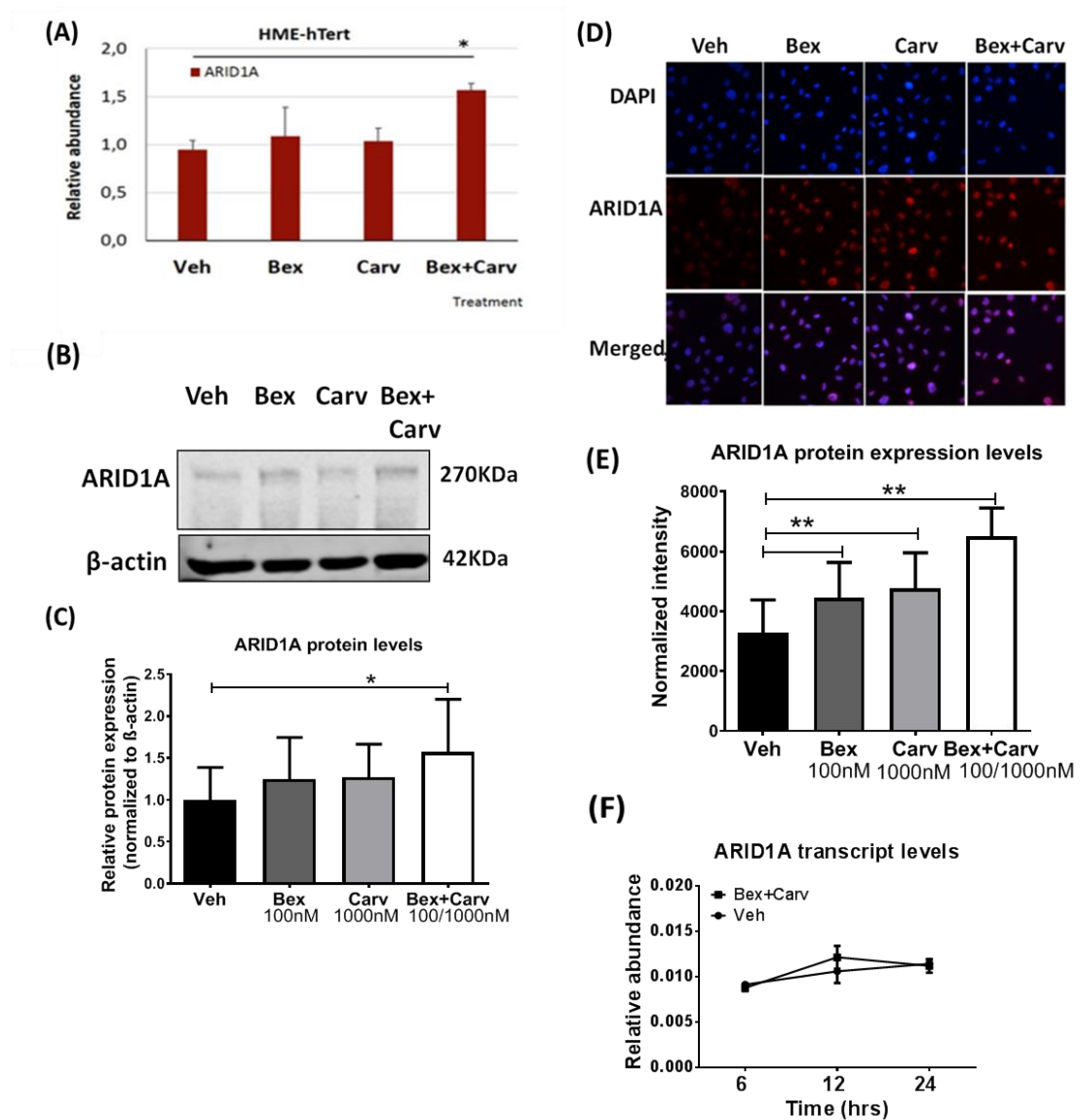


**Figure 5-2: Bexarotene and carvedilol combination treatment induced ARID1A protein but not transcript levels in HME-hTert cells. (A)** Reverse phase proteomic array

results showing ARID1A protein levels upon Bex and/or Carv treatment in HME-hTert cells. **(B)** Western-blotting analysis of ARID1A protein expression levels in extracts from HME-hTert cells treated with the combination of 100nM Bex + 1000nM Carv vs vehicle for 48 hours.  $\beta$ -actin was used for normalization. **(C)** Quantification of ARID1A protein expression, N=3 representing biological replicates. **(D)** Representative images of HME-hTert cells treated with Veh, 100nM Bex, 1000nM Carv or their combination for 48 hours and immunostained with antibody against ARID1A. DAPI nuclear staining was used to stain the nuclei, images were taken at 10 x magnifications. **(E)** Quantification of ARID1A protein expression in HME-hTert cells treated with the combination or the individual treatments. About 200 cells per replicate were analyzed using ImageJ software based on integrated cellular pixel intensities of the immunostaining for ARID1A, normalized to cell numbers based on DAPI nuclear staining. **(F)** Graph line representing RT-qPCR analysis for ARID1A transcript levels in HME-hTert cells treated with the combination of 100nM Bex + 1000nM Carv for 6, 12 or 24 hours. The results are expressed as mean  $\pm$  SD \*P < 0.05, \*\*\*\*<0.0001 by a two-tailed Student's t-test.

### 5.3 Overexpression of ARID1A protein levels:

To confirm that the detected over-expressed bands upon Bex+Carv treatment in Western-blotting represent ARID1A, we transfected the human embryonic kidney cells (HEK293) with ARID1A cDNA plasmid. Transfection efficiency was checked at the cellular level through an m-Cherry fluorescent signal in the control sample which was transfected with m-Cherry cDNA plasmid (**Figure 5-3 A**), as well as at the protein levels through the detection of V5-tag protein, an exogenous protein, in the ARID1A cDNA transfected sample which is not detected in the control sample (**Figure 5-3 B**). ARID1A transcript levels were also assessed upon ARID1A cDNA transfection for 24 hours with a detected increase but did not reach significance (**Figure 5-3 C**). Moreover, the western blotting analysis showed an amplified signal in ARID1A cDNA transfected sample (**Figure 5-3 D, E**) mainly at the molecular weight 270KDa. The bands at molecular weights 150, 250 or ~ 270 KDa were cut from the acrylamide gel and the proteins were processed and sequenced through Mass spectrometry. The results revealed that the extracted proteins from the ~ 270 band contained ARID1A with 100% probability (**Figure 5-3 F**), but not the other bands. Therefore, we considered the 270KDa band representing ARID1A. The results also support that the used antibody (Santa Cruz Biotechnology, PSG3) can recognize ARID1A as it is going to be used for immunoprecipitation.

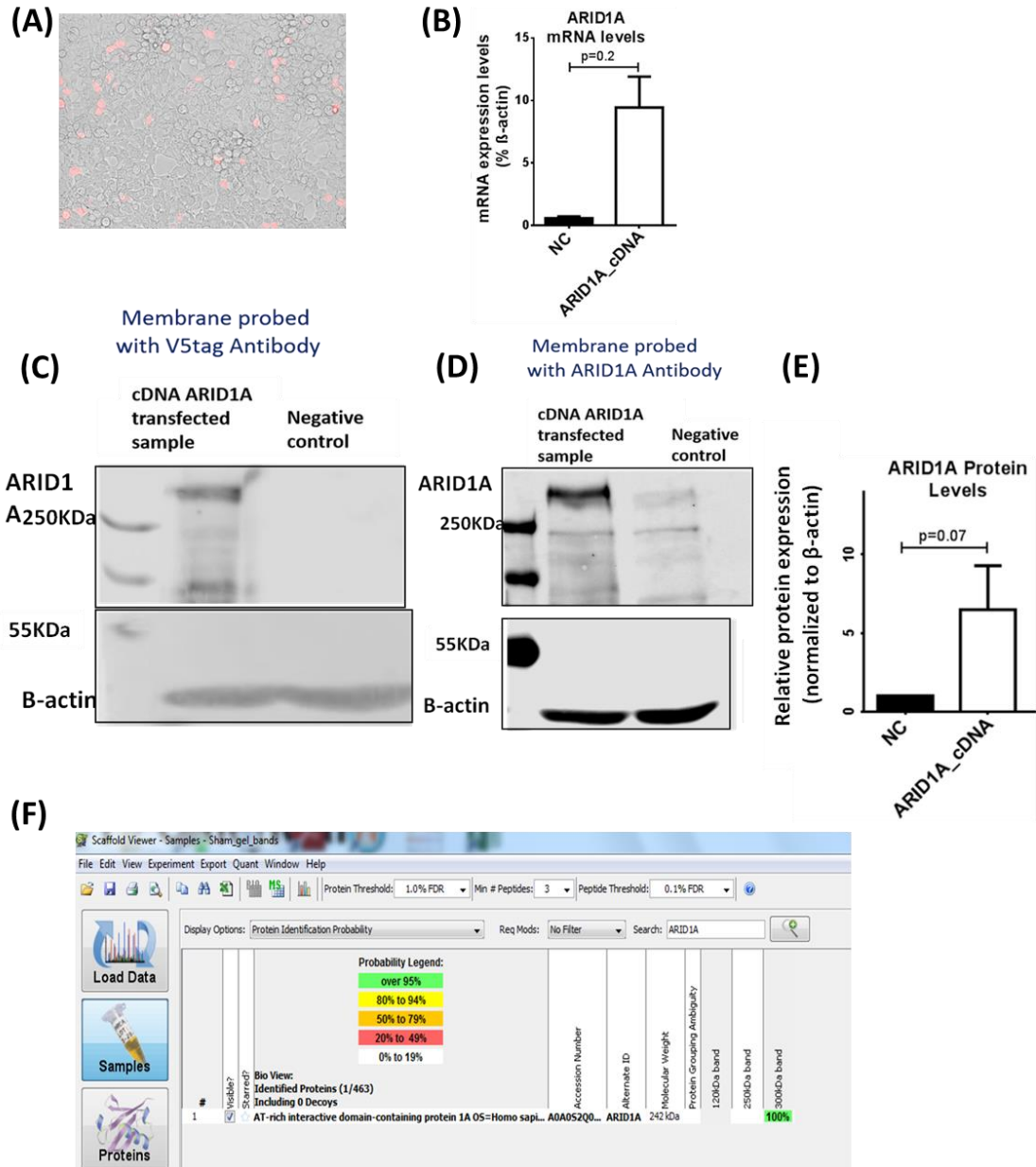
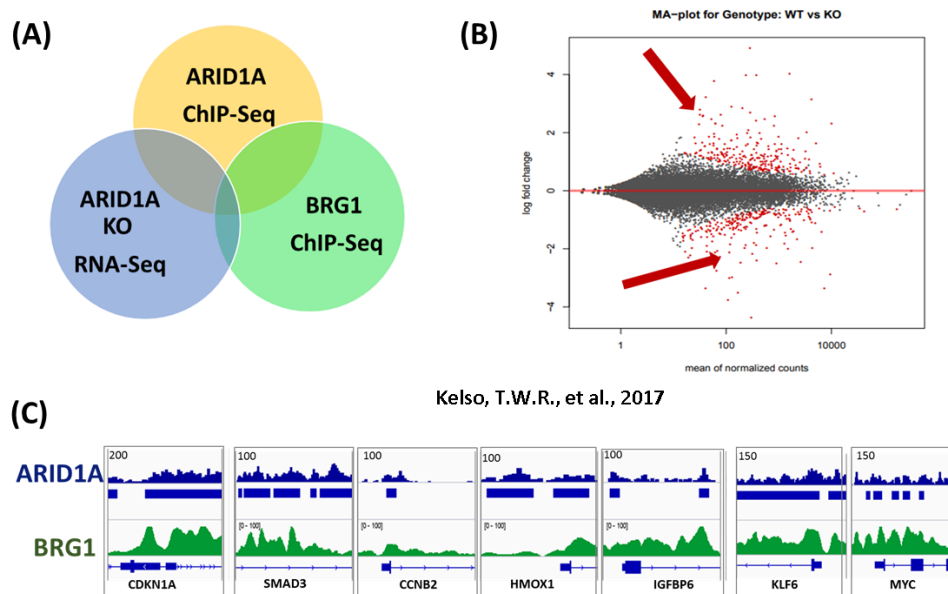


**Figure 5-3: ARID1A overexpression in HEK293 cell line:** (A) microscopic image of HEK293 cell line transfected with m-Cherry plasmid upon 24 hours of transfection. (B) ARID1A transcript levels upon 24 hours of ARID1A cDNA plasmid transfection in HEK293 cell line. (C) Western blotting analysis of V5-tagged ARID1A as an exogenous protein in ARID1A transfected HEK293 cells (first lane) and in the control sample (second lane). (D) ARID1A western blot analysis of HEK293 cells transfected with ARID1A cDNA or m-Cherry cDNA plasmids for 48 hours, blots were probed with ARID1A Ab (Santa Cruz Biotechnology, PSG3). (E) Quantitative analysis of ARID1A protein expression levels upon ARID1A cDNA plasmid transfection in HEK293 cells. The results are expressed as mean  $\pm$  SD. Statistics were done by a two-tailed Student's t-test. (F) A screenshot of the Scaffold Viewer software illustrating that the band at the molecular weight  $\sim$  300KDa contains ARID1A protein with 100% probability.

#### 5.4 Identifying putative ARID1A target genes through in Silico analysis of publicly available ChIP-Seq and RNA-Seq datasets:

To test our hypothesis that ARID1A alters chromatin accessibility to modulate the expression of genes involved in cancer development upon Bex+Carv treatment, we planned to run chromatin immunoprecipitation (ChIP) followed by sequencing to characterize ARID1A binding events across the genome. As a first step, we started optimizing the ChIP protocol based on our conditions. To do so, we first ran ChIP-qPCR to test the efficiency of the antibody to pull down ARID1A out of the other cellular proteins. To test ARID1A occupancy at a specific genomic region, then we need to identify ARID1A targets. Therefore, we reanalyzed publicly available ARID1A and BRG1, chromatin immunoprecipitation in RMG1 [174] and MDAMB231 [180] cell lines, respectively, as well as RNA-Seq datasets upon ARID1A Knock-out in HCT116 colon cancer cell lines [181]. Even though the selected datasets were on different cell lines but the intersection between the different datasets could provide information about ARID1A targets (**Figure 5-4 A**). We could identify several genes differentially expressed upon ARID1A KO (**Figure 5-4 B**). A list of ARID1A and BRG1 target regions were identified and assigned to genes involved in cell cycle regulation based on ChIP-Seq datasets (**Figure 5-4 C**).



Kelso, T.W.R., et al., 2017  
Takaku M., et al., 2016, Trizzino M., et al., 2018

**Figure 5-4: Identifying putative ARID1A target genes through in silico analysis of publicly available ChIP-Seq and RNA-Seq datasets:** (A) Criteria followed to identify ARID1A putative target regions, RNA-Seq upon ARID1A KO in HTC116 colon cancer cell line. ARID1A ChIP-Seq in RMG ovarian clear cell carcinoma cell line. BRG1 ChIP-Seq in MDAMB231 breast cancer cell line. (B) MA-plot representing genes that are differentially expressed in Wild type and ARID1A KO HTC116 cell line. The filter was

performed based on  $P\text{-adj (FDR)} \leq 0.01$ . (C) Interactive Genomics Viewer (IGV) snapshot of ARID1A and BRG1 ChIP-seq tags coverage representing ARID1A and BRG1 binding regions related to regulatory elements assigned to CDKN1A, SMAD3, CCNB2, HMOX1, IGFBP6, KLF6, and MYC genes. ChIP-Seq tracks of ARID1A were generated in RMG1 ovarian carcinoma cell line, and from MDA-MB231 breast cancer cell line in case of BRG1.

## 5.5 Optimization of ARID1A chromatin immunoprecipitation protocol in breast cell lines:

The next step after identifying some of ARID1A putative target regions is to optimize the ChIP protocol in breast cell lines. We changed several elements that were identified to have a high influence on the quality and productivity of the method. We tested the protocol in different breast cell lines including HME-hTert, T47D, MDA-MB231, and MCF-7 cells. Another element which dramatically affects the ChIP output is the starting cell number; as the ChIP procedure comprises of many steps, there is always a chance to lose some of the starting materials, therefore, it is recommended to start with a high number of cells for each IP. We started the protocol with 500 thousand cells /IP and increased gradually to 1 million cells, 2 million, 3 million cells/ IP until we identified 5 million cells /IP is the optimal number for ChIP-qPCR and 20 million cells/IP in case of ChIP followed by sequencing. To test the antibody's ability to IP ARID1A, we run immunoprecipitation followed by Western-blotting in T47D treated with Veh or Bex+Carv (**Figure 5-5 A**). We were able to immunoprecipitate ARID1A in Bex+Carv treated sample however a similar band was detected in the negative control sample. Moreover, as ARID1A was identified to be mutated in the T47D cell line, then we run IP-WB in MCF-7 cells. ARID1A IP, input, negative control IP, and a positive control IP (the latest is to confirm that the IP-WB protocol is working) were run. We used for the positive control CTCF antibody, which is an Ab used successfully in CTCF ChIP in MCF-7 cell line. The positive control band refers that the protocol is working. A band at 250KDa was detected in the flowthrough and input samples. Bands at 120KDa as well as faint bands at 250KDa were detected in ARID1A IP but also IgG IP samples (**Figure 5-5 B**). The results might refer that the antibody is able to pull down ARID1A and the difference in the molecular weight might be because of the cross-linking procedure in the protocol. Moreover, as we detected bands at the same molecular weight in the negative control sample we decided to decrease the background through the addition of a clearing step to the protocol. The clearing step process includes the incubation of the sheared chromatin with beads coated with non-specific IgG overnight, to reduce the signal coming from the non-specific bindings. The amount of antibody/ IP (4 $\mu$ g/IP/ ChIP-qPCR) and the sonication conditions (15 cycles; 30sec on and 30 sec off) to reach 200-1000bp chromatin were also optimized. ARID1A was identified to play a critical role in the regulation of estrogen antagonism response in MCF-7 cells [173]. TFF-1 is a gene regulated by the estrogen receptor. The TFF-1 promoter region was selected to test ARID1A occupancy. ARID1A chromatin

immunoprecipitation followed by quantitative PCR at ARID1A putative target region (TFF-1 promoter) was performed showing a detectable signal at ARID1A ChIP compared to the IgG sample (**Figure 5- 5 C**). Overall the optimal conditions through which we were successfully able to IP ARID1A include; 5 million MCF-7 cells for each IP, a clearing step was added through the incubation of sheared chromatin with beads coated with non-specific antibodies, 4  $\mu$ g ARID1A antibody (Santa Cruz Biotechnology, PSG3) (see ChIP method).

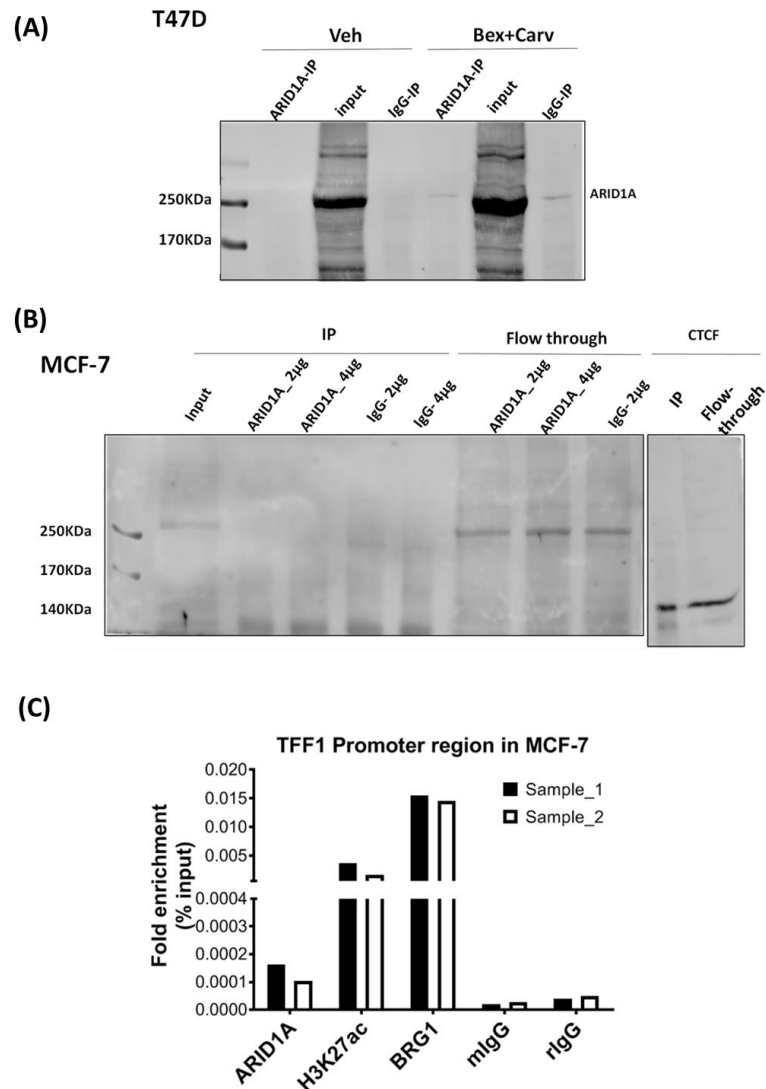


**Figure 5-5: ARID1A ChIP-Seq optimization in breast cancer cell lines:** (A) Western blot analysis of ARID1A in immunoprecipitated samples from T47D cells treated with Veh or Bex100nM + Carv 300nM for 48 hours. (B) Western blot analysis of ARID1A in immunoprecipitated or flow-through samples from MCF-7 cells, 2 different concentrations of antibodies were tested 2 $\mu$ g or 4 $\mu$ g. To the right of the blot CTCF IP and flow-through as a positive control for the IP assay. (C) ChIP-qPCR for ARID1A, H3K27ac, BRG1 and negative control at TFF1 promoter region in MCF-7 cells.

## 5.6 ARID1A genomic characterization in MCF-7 cells upon Bex+Carv combination treatment:

Bex+Carv treatment showed antiproliferative effects in MCF-7 breast cancer cell line. MCF-7 is considered a good model relatively for ChIP experiment. Moreover, based on a study done by Nagarajan and colleagues, SWI/SNF participates in MCF-7 cell response to estrogen modulators, and that ARID1A is recruited to ER target genes in non-estrogenic conditions. These factors encourage us to use MCF-7 ER positive breast cancer cell line as a model to study the effect of Bex+Carv treatment on ARID1A occupancy across the genome in non-estrogenic conditions and its relation to the detected antiproliferative effects of the combined treatment. We performed Chromatin immunoprecipitation followed by sequencing (ChIP-Seq) in MCF-7 cell line upon 100nM Bex +300nM Carv treatment for 48 hours. Alongside ARID1A, we profiled H3K27ac, a marker for transcriptionally active regions. The results showed that ARID1A mainly binds to intronic (~50%) and intergenic (~45%) regions in control and treated samples (**Figure 5-6 A**). Moreover, ARID1A is localized mainly in genomic regions 5-500 Kb either upstream or downstream of the TSSs of the assigned genes with less than 5% of ARID1A sites localized in the promoter region (**Figure 5-6 B**). Around 27 thousand ARID1A binding regions were detected upon Bex+Carv treatment, compared to about 16 thousand regions identified in the Veh sample. The intersection between ARID1A binding regions identified in the two groups indicated that 66% of ARID1A binding sites in the Bex + Carv treated sample were unique and about 34% overlapped with vehicle-treated samples. About  $17 \cdot 10^3$  ARID1A binding events were gained upon Bex+Carv treatment, whereas around  $6 \cdot 10^3$  were lost. On the other hand, about  $10 \cdot 10^3$  ARID1A binding sites were identified in both control and Bex + Carv treated samples. Even though about 66% of ARID1A binding events were gained upon Bex+Carv treatment, only 9% (5660 of the total 62854 of all binding sites) associated with an increase in H3K27ac active marker sites, suggesting that regions bound by ARID1A tend to be suppressed (**Figure 5-6 C, D, E**). ARID1A genomic distribution, heatmaps histograms, and motif enrichment analysis were performed by Dr Edina Erdős.

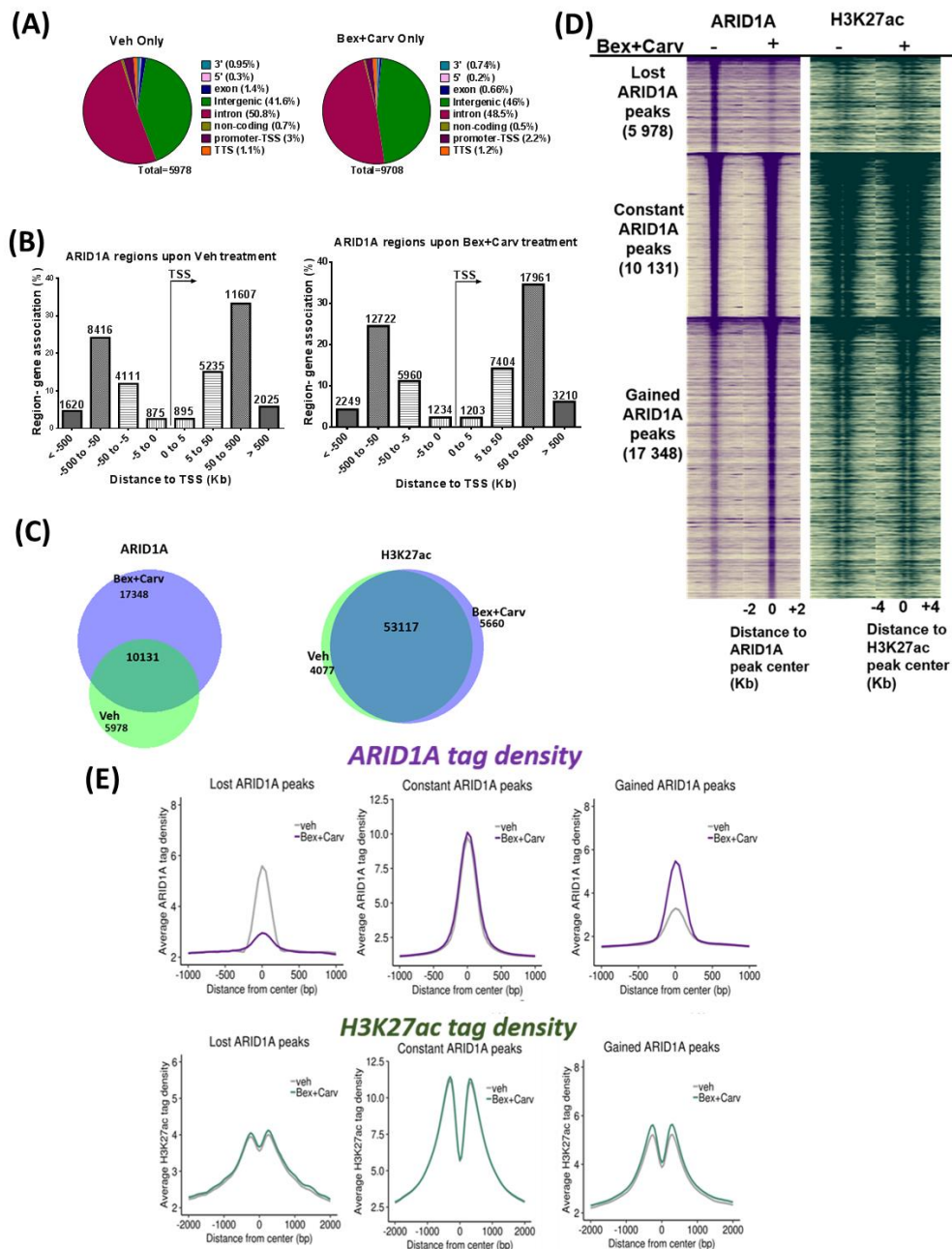


**Figure 5-6. ARID1A genomic occupancy upon Bex+Carv treatment in MCF-7 cells**  
**(A)** Genomic distribution of ARID1A binding sites in control and Bex+Carv-treated samples. **(B)** Region-gene association analysis of ARID1A binding regions in relation to the transcription start sites (TSS) in the vehicle and Bex+Carv treated samples. **(C)** Venn-diagram (upper) depicting overlap among ARID1A peaks identified within ChIP-Seq in MCF-7 cells treated with 100nMBex + 300nMCarv or Vehicle. Venn-diagram (lower) depicting overlap among H3K27ac marks identified within ChIP-Seq in Bex + Carv treated sample and the control sample. **(D)** ChIP-Seq heat maps of ARID1A and H3K27ac binding

events, ordered in descending order of ARID1A occupancy, clustered into ARID1A lost, constant or gained binding events upon Bex + Carv treatment compared to the control sample. (E) Density plots represent the average of ARID1A tags coverage (top row) in the three different identified clusters, or the average of H3K27ac tags coverage (lower row) associated with ARID1A peaks. ARID1A was immunoprecipitated using 8mg ARID1A antibody (Santa-Cruz, PSG3X)/IP.)

To study the correlation between ARID1A genomic occupancy and other transcription regulators, we applied motif enrichment analysis, demonstrating that ARID1A bound sites were enriched at TRE (a motif for AP-1), Forkhead Box M1 (FOXM1) and Grainyhead Like Transcription Factor 2 (GRHL2) motifs (**Figure 5-7 A**).

**(A)**

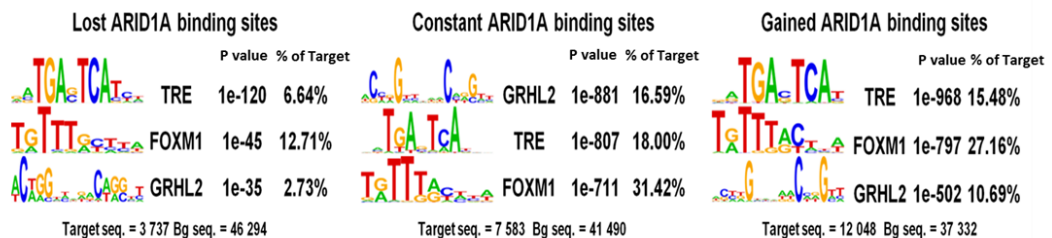


**Figure 5-7.** ARID1A motif enrichment analysis in MCF-7 cells. (A) ARID1A de novo motifs identified in the three clusters of ARID1A-bound regions, lost, constant or gained upon Bex+Carv treatment in MCF-7 cells.

To validate the quality of the ChIP-Seq experiment, we select 3 ARID1A regions (among the highest identified peaks; -4Kb to KRT18 TSS, -98Kb to PTEN TSS, -60Kb to PPARG TSS) and we applied ChIP-qPCR using two different antibodies (Santa Cruz Biotechnology, PSG3X) and (Abcam, ab182560). On the other hand, to confirm that the detected signal represents SWI/SNF complex, we IP BRG1 in parallel with ARID1A and H3K27ac (**Figure 5-8 A, B, C**). The results showed a detectable signal at ARID1A, and BRG1 IP compared to the negative control sample, confirming that the identified peaks derived from ChIP-Seq data represent ARID1A bindings.

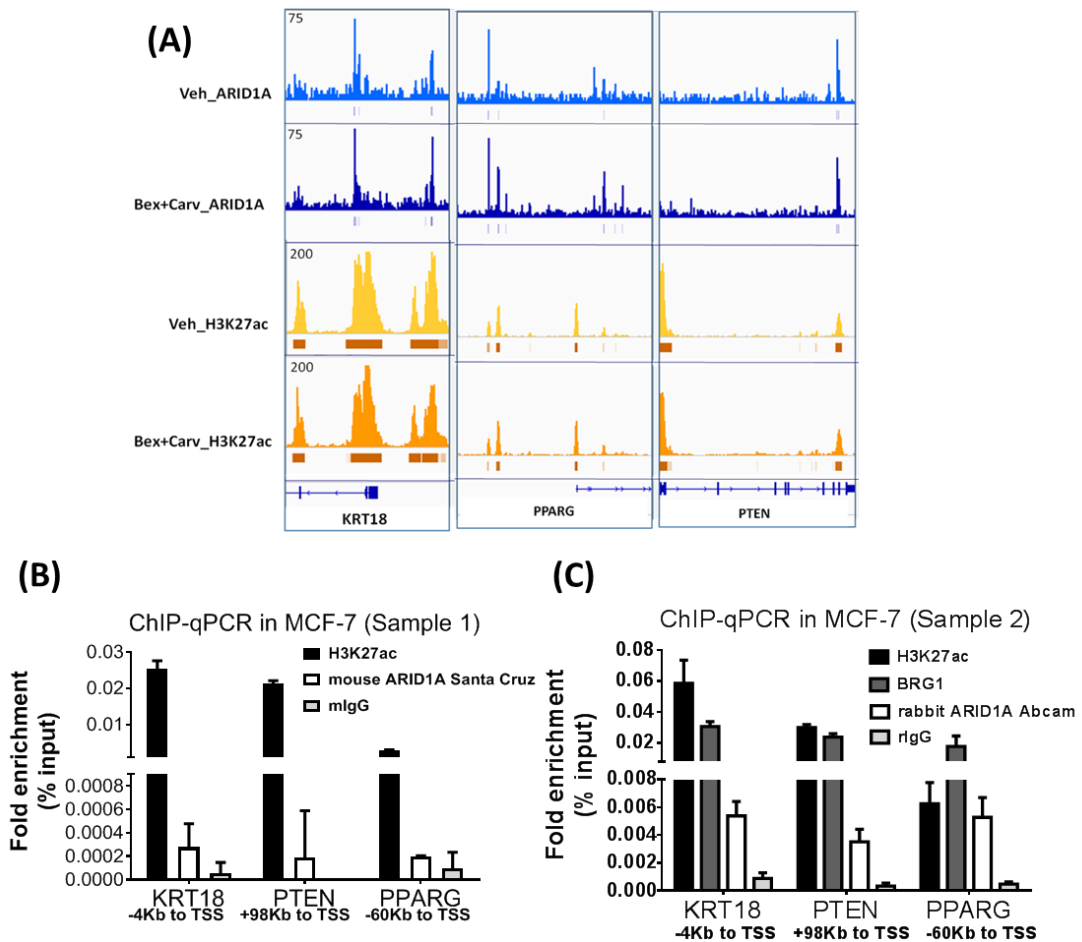


**Figure 5-8:** Validation of ARID1A ChIP-Seq in MCF-7 cells. **(A)** Integrative Genomics Viewer (IGV) snapshot of ARID1A and H3K27ac ChIP-seq tags coverage representing ARID1A binding regions related to PTEN, PPARG and KRT18 genes in Bex+Carv or vehicle-treated MCF-7 cells. **(B)** Validation of ARID1A identified peaks and H3K27ac marks to the target regions of PTEN, PPARG and KRT18 genes by ChIP-qPCR in MCF-7 cells. **(C)** Validation of the identified ARID1A and BRG1 peaks at target regions by ChIP-qPCR in MCF-7 cells using different antibody for ARID1A.

### 5.7 ARID1A is enriched to regulatory elements assigned to genes involved in cell proliferation and IGF1 signaling pathway upon Bex+Carv treatment in MCF-7 cells

To identify the correlation between ARID1A genomic occupancy and pathways that might be modulated upon Bex + Carv treatment, we performed gene ontology analysis for the annotated genes related to ARID1A binding sites gained upon Bex + Carv treatment identified within ChIP-Seq dataset. The results illustrated that regulatory regions assigned to genes involved in differentiation and proliferation and insulin-like growth factor receptor signaling pathway were more occupied by ARID1A upon Bex+Carv treatment compared to the control sample in MCF-7 cells (**Figure 5-9 A**). Two members of the IGF1 signaling pathway were studied including insulin-like growth factor receptor (IGF-1R) and insulin receptor

substrate (IRS1). ARID1A enrichment to 4 regulatory regions across IGF-1R gene (+ 6Kb, +100Kb, +131Kb, and +211Kb to TSS) and to 3 regulatory regions upstream of IRS1 gene (+ 643 Kb, + 676Kb, and +684Kb to TSS) were identified through ChIP-Seq (**Figure 5-9 B,C**) and validated through ChIP-qPCR using ARID1A antibody (Santa-Cruz, sc-32761x).

3 out of the 4 ARID1A binding regions identified across the IGF-1R gene, those located 100kb, 131kb and 211kb downstream from the transcription start site, were confirmed as significantly elevated in ARID1A occupancy by ChIP-qPCR (**Figure 5-9 D**). 2 out of 3 regions in the IRS1 gene indicated a trend of increased ARID1A binding upon Bex+Carv (**Figure 5-9 F**). H3K27ac histone marks flanking each ARID1A peak identified in the respective regions were also assessed. In contrast to ARID1A, acetylated H3K27 at the same genomic loci showed a non-significant, yet consistently lower level of binding compared to the control treatment (**Figure 5-9 E, G**).

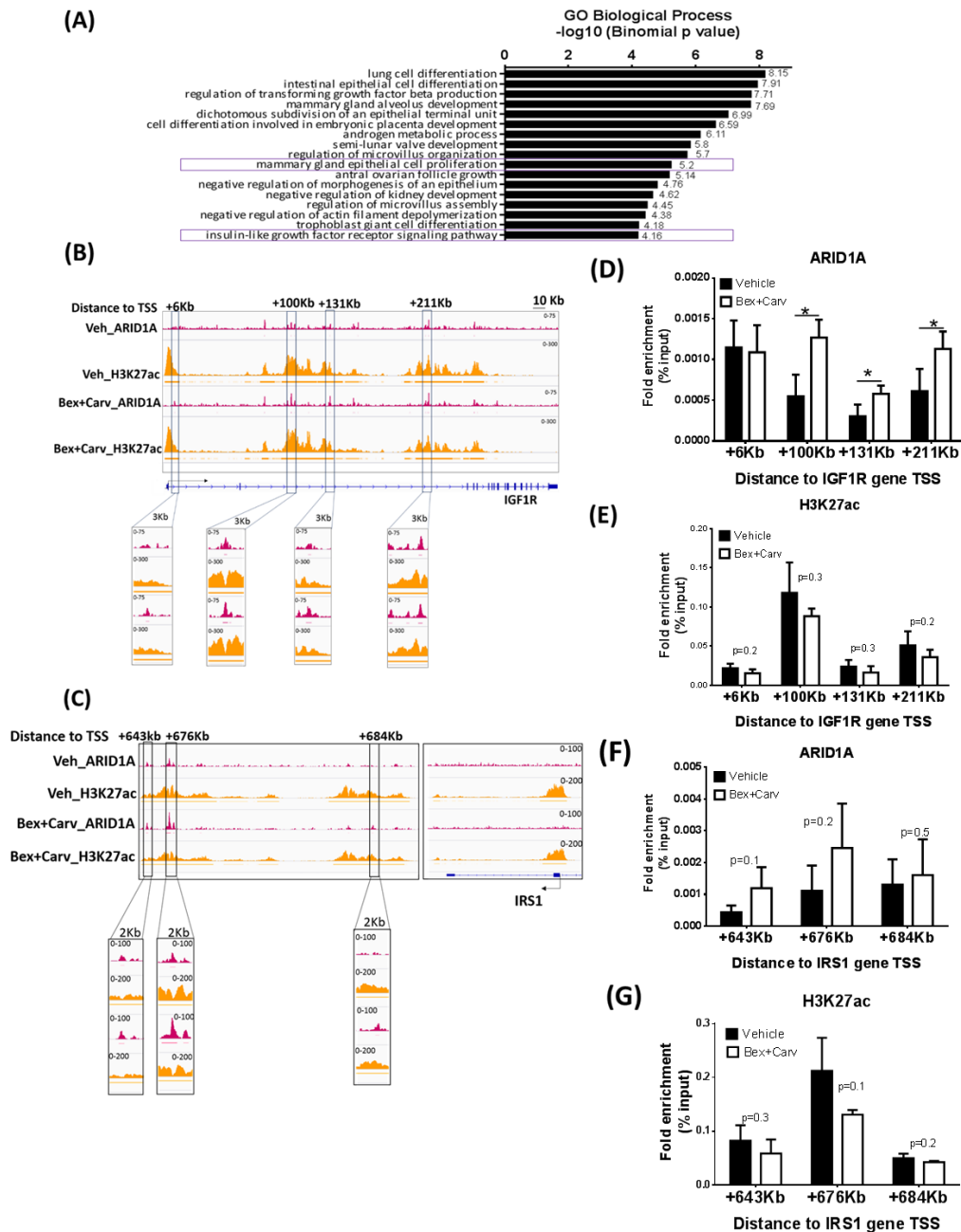


**Figure 5-9. Functional analysis of ARID1A genomic occupancy in MCF-7 cells upon Bex+Carv treatment. ARID1A and H3K27ac enrichment in genomic loci of the IGF pathway.** (A) Gene ontology analysis of the annotated genes related to ARID1A binding events gained upon Bex+Carv treatment in MCF-7 cells. Integrative Genomics Viewer (IGV) snapshot of ARID1A and H3K27ac ChIP-seq tags coverage representing ARID1A binding regions related to IGF-1R and IRS1 genes in Bex+Carv or vehicle-treated MCF-7 cells. ChIP-Seq tracks of ARID1A and H3K27ac in control and Bex+Carv treated MCF-7 cells in the genomic locus of (B) IGF-1R and (C) IRS1 exported from the Integrative Genomics Viewer (IGV) application. (D-G) Validation of ARID1A enrichment to its target regions assigned to (D) IGF-1R and (F) IRS1 genes by ChIP-qPCR in MCF-7 cells.

Validation of H3K27ac marks identified at the target regions of (E) IGF-1R and (G) IRS1 genes by ChIP-qPCR in MCF-7 cells. N=3 representing 3 biological replicates. The results are expressed as mean  $\pm$  SD \*P < 0.05 by a two-tailed Student's t-test.

### 5.8 Insulin like growth factor receptor 1 (IGF-1R) and Insulin receptor substrate (IRS1) protein levels are downregulated upon Bex+Carv treatment:

Next we studied the impact of ARID1A enrichment at putative regulatory regions assigned to IGF-1R and IRS1 genes on their protein expression levels upon Bex+Carv treatment. IGF-1R and IRS1 protein levels were assessed by Western-blotting analysis showing a significant decrease upon 48 hours of Bex+Carv treatment in MCF-7 cells, relative to controls. However, no significant changes in ARID1A protein levels were detected (**Figure 5-10 A, B**).

IGF-1R and IRS1 immunostaining in MCF-7 cells confirmed the membrane localization of the IGF-1R, and a cytoplasmic presence of IRS1. Furthermore, quantitative image analysis based on integrated cellular pixel intensities supported our Western-blotting findings with a significant reduction in IGF-1R and IRS1 protein levels upon Bex+Carv treatment (**Figure 5-10 F, G, upper images**) (**Figure 5-10 H,I left comparison**). However, upon ARID1A knockdown (**Figure 5-10 C, D, E**) the downregulation effects of Bex+Carv treatment on IGF-1R and IRS1 protein expression levels were abolished. (**Figure 5-10 F, G, lower images**) (**Figure 5-10 H, I right comparison**).

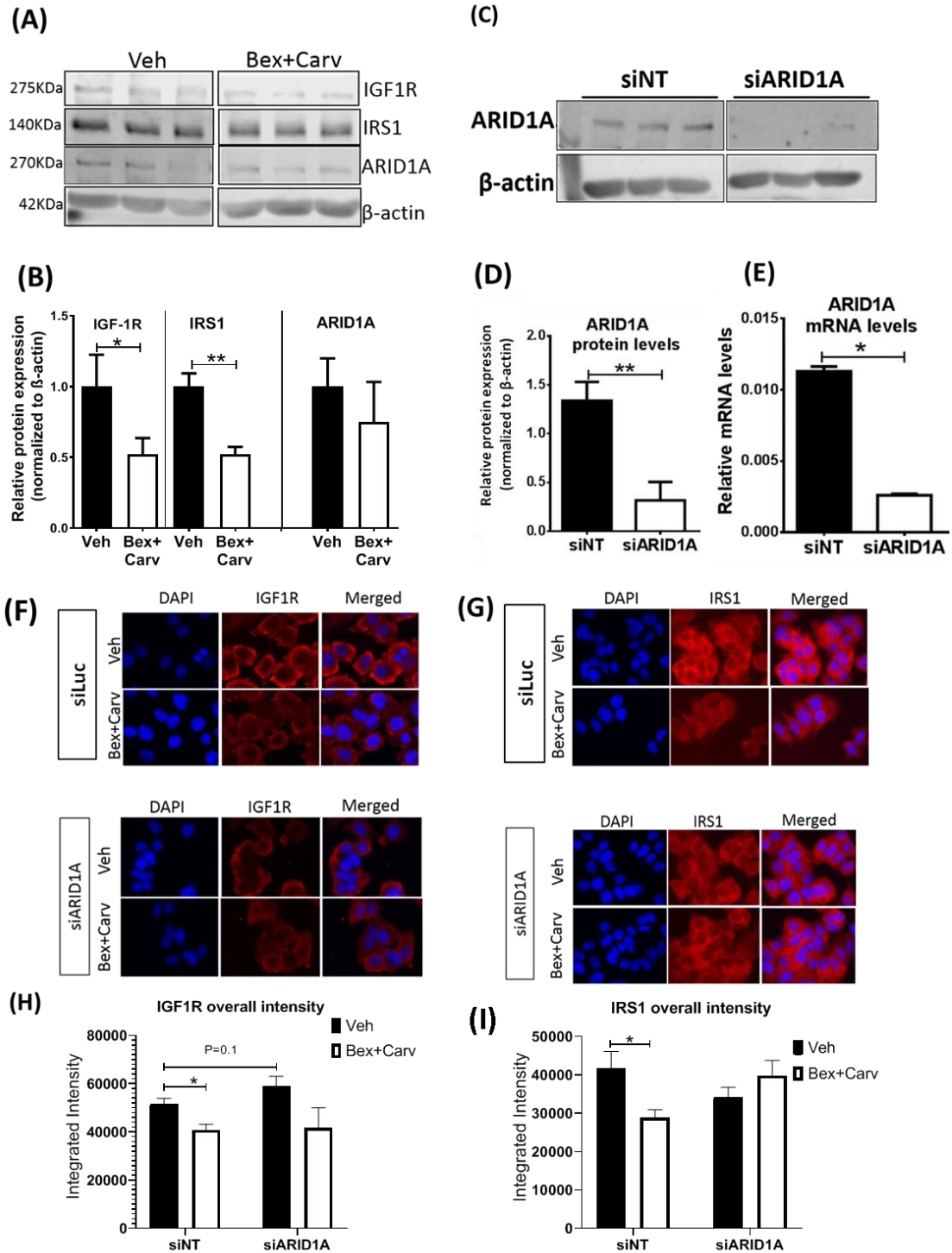


**Figure 5-10: Determination of IGF-1R and IRS1 protein levels upon Bex+Carv treatment and the effect of ARID1A behind it.** **A)** Western-blotting analyses of IGF-1R, IRS1 and ARID1A protein levels in cell extracts from MCF-7 cells treated with vehicle or a combination of bexarotene and carvedilol for 48 hours.  $\beta$ -actin was used as a housekeeping gene. **B)** Quantitation of IGF-1R, IRS1 and ARID1A protein expression upon Bex+Carv treatment in MCF-7 cells. N=3, representing three biological replicates. **F,** **G)** Representative images of MCF-7 cells transfected with either siRNA against luciferase as a control (upper) or with a pool of siRNAs against ARID1A (lower) for overall 3 days

and treated with either Vehicle or Bex+Carv for 2 days and immunostained with antibodies against **F)** IGF-1R or **G)** IRS1 proteins. DAPI nuclear stain was used to identify the nuclei at 20x magnification. **H, I)** Bar graphs represent the results from quantitative image analysis of at least 200 cells per replicate, based on overall integrated cellular pixel intensities of the immunostaining for IGF-1R and IRS1 protein expression. The numerical results are expressed as mean  $\pm$  SD \*P < 0.05. \*\*P < 0.01 by two-tailed Student's t-test.

### 5.9 ARID1A knockdown increased IGF1R protein expression and MCF-7 cell growth:

Based on our findings we identified ARID1A to be enriched at regulatory elements assigned to genes involved in cell proliferation regulation. Based on overall intensity detection of IGF-1R signal we found that its protein expression levels are tend to be upregulated upon ARID1A knockdown. To investigate more about the correlation between ARID1A and IGF-1R expression on the cellular level we reanalyzed the data on cell-by cell bases. The results demonstrated an increase in the protein expression levels of IGF-1R based on cell-by-cell image analysis (**Figure 5-11A**). Moreover, MCF-7 cell proliferation upon ARID1A knockdown over a period of 6 days showed a significant increase in cell number compared to the control group as determined based on the DAPI stain signal by automated microscopy (**Figure 5-11B**).

As IGF signaling plays a significant role in the regulation of cell growth and proliferation, we validated that the growth of MCF-7 cells is driven by this pathway. We neutralized the effects of insulin-like growth receptor using anti-IGF-1R antibodies and assessed cell proliferation using normal DMEM medium or phenol-red free medium to reduce the estrogen like effects. The results demonstrated that the number of MCF-7 cells declines significantly upon neutralizing IGF-1R effects in both of the tested conditions (**Figure 5-11 C**).

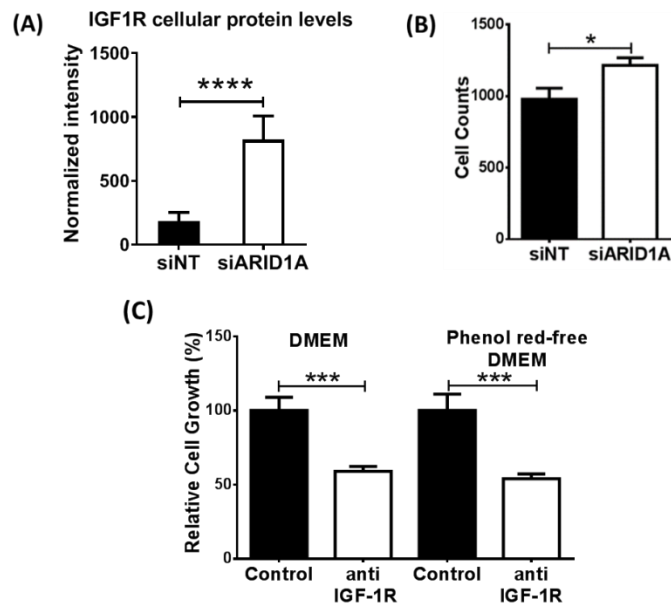


**Figure 5-11. ARID1A knockdown induces IGF-1R protein expression associated with an increase in MCF-7 proliferation:** (A) Quantitation of IGF-1R protein levels in control (siNT) vs ARID1A specific siRNA MCF-7 transfected cells. (B) Microscopy-based proliferation assay on MCF-7 cells showing cell counts upon ARID1A knock-down 6 days post-transfection. 4 replicates per treatment were applied and all cells were counted in each well. (C) Image-based measurement of MCF-7 cell proliferation over 3 days in the presence of neutralizing anti-IGF-1R antibody compared to controls, assessed in regular and non-estrogenic (phenol red-free) cell culture media. Results are expressed as mean  $\pm$  SD \*P < 0.05, \*\*P < 0.01, \*\*\*P < 0.001, \*\*\*\*P < 0.0001 by two-tailed Student's t-test.

### 5.10 ARID1A ChIP optimization in HME-hTert cells:

The other part of the study focuses on HME-hTert normal cells and identifies the role of ARID1A behind the antiproliferative effect of bexarotene and carvedilol combination.

Previously we validated the RPPA data that showed an induction in ARID1A protein levels using two different methods Western-blotting and immunostaining. Later on, to investigate the impact of the combined treatment on ARID1A genomic occupancy in normal cells, we started by optimizing the ChIP protocol on HME-hTert cells, testing Abcam or Santa Cruz antibodies against ARID1A. Several ARID1A targets were selected based on ARID1A ChIP-Seq study in MCF-7 cells. The binding of BRG1, the ATPase subunit within the SWI/SNF complex, and H3K27ac marks, active enhancer marker, were assessed through ChIP-qPCR in parallel with ARID1A. We were able to detect ARID1A signal using both antibodies, whereas, the signal generated using the Abcam antibody was higher (**Figure 5-12A**). Therefore, we used the Abcam antibody for further ChIP analysis in HME-hTert cells.

At first, we immunoprecipitated ARID1A post 48 hours of Bex+Carv treatment, a time point in which we were able to detect an elevation in ARID1A protein levels, however, no marked change was detected in ARID1A enrichment to a number of target regions. On the other hand, taken into consideration that in MCF-7 cells the change in ARID1A genomic occupancy upon Bex+Carv treatment was detected without a detectable change in its protein levels. Therefore, we decided to investigate ARID1A genomic occupancy in normal HME-hTert cells at a shorter time point, 6 hours of Bex+Carv treatment, where no change in ARID1A or BRG1 protein levels was detected (**Figure 5-12 B, C**) suggesting that the combined treatment leads to SWI/SNF complex redistribution regardless of the protein levels of its subunits.

To map ARID1A occupancy across the genome upon Bex+Carv treatment in HME-hTert cells, we performed chromatin immunoprecipitation followed by sequencing using two different antibodies against ARID1A with a few ARID1A regions detected. ARID1A putative target genes were selected based on intersecting the annotated ARID1A regions identified within ChIP-Seq dataset with a list of genes

expressed differentially upon Bex+Carv treatment in HME-hTert cells (**Figure 5-12 F**).

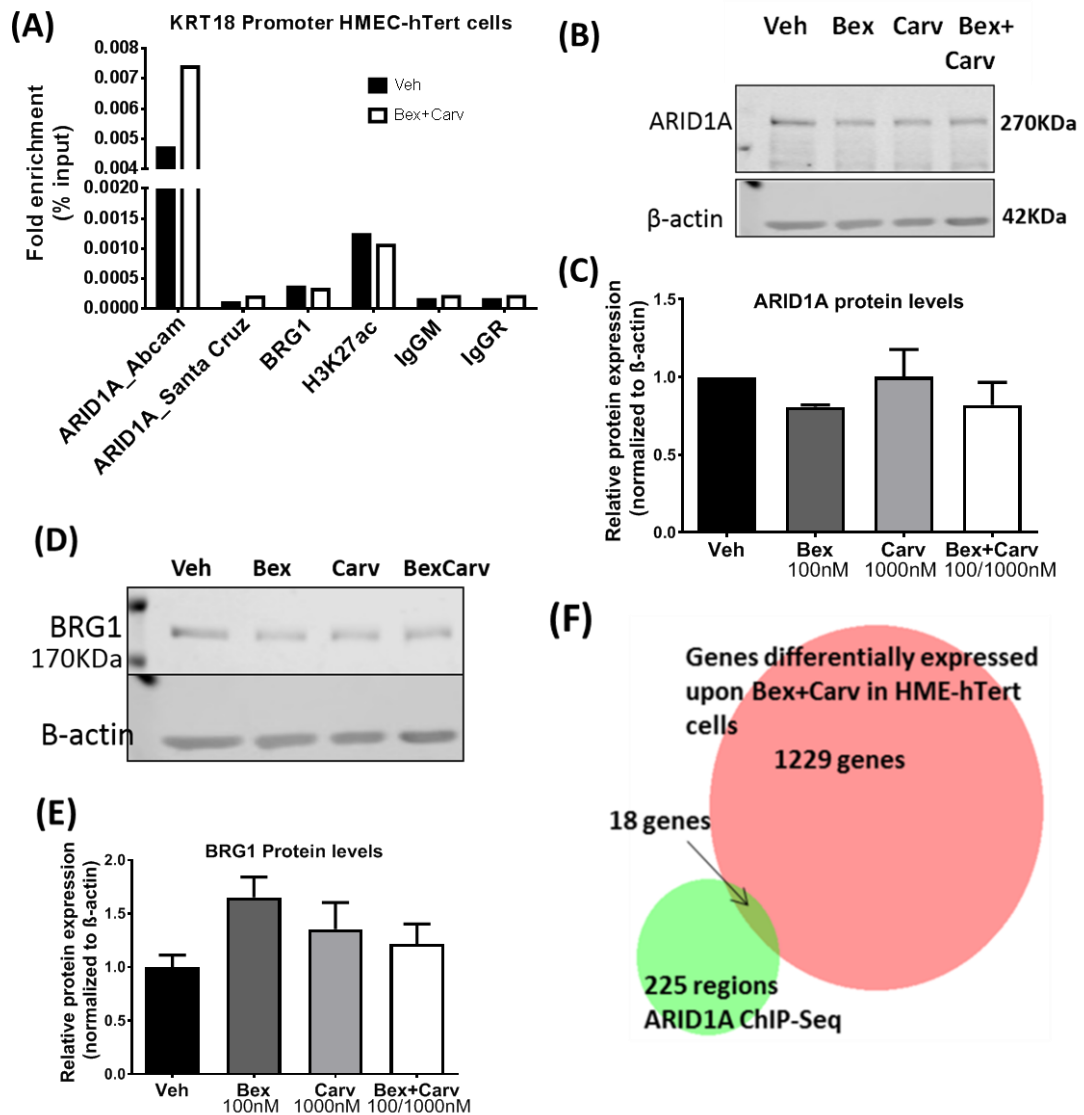


**Figure 5-12: ARID1A ChIP optimization in HME-hTert cells.** **A)** ChIP-qPCR for ARID1A, BRG1, H3K27ac, and negative control at the KRT18 promoter region in HME-hTert cells. **B, C)** Western-blotting analysis of ARID1A (**B**) and BRG1 (**C**) protein expression levels in HME-hTert cell extracts treated with Vehicle, 100nM Bex, 1000nM Carv or their combination for 6 hours.  $\beta$ -actin was used as a housekeeping gene. **D, E)** Quantification of ARID1A or BRG1 protein expression, N=3 representing three biological replicates. **F)** Venn-diagram depicting overlap among ARID1A peaks identified within ChIP-Seq using Abcam antibody in 100nM Bex + 1000nM Carv treated HME-hTert cells and a list of genes differentially expressed upon Bex+Carv treatment in HME-hTert cells.

### 5.11 ARID1A is recruited to regulatory elements assigned to genes involved in transforming growth factor Beta pathway upon bexarotene and carvedilol combination treatment in HME-hTert cells:

Among the list of putative ARID1A targets, a number of genes were identified related to proliferation regulation including; Kruppel like Factor 4 (KLF4) and Forkhead Box Q1 (FOXQ1), as well as genes involved in the transforming growth factor beta pathway, including Bone Morphogenetic Protein 6 (BMP6) and Transforming Growth Factor Beta Receptor (TGFBR2). ChIP-qPCR analysis showed an enrichment of ARID1A and BRG1 to regulatory elements assigned to FOXQ1 (+13Kb to TSS), KLF4 (-14Kb to TSS), BMP6 (-27Kb to TSS), and TGFBR2 at two identified regions (-9Kb, and +52Kb to TSS) post 6 hours exposure to Bex+Carv treatment compared to the control sample (**Figure 5-13 A, B**). H3K27ac marks showed higher but not significant levels at ARID1A genomic loci assigned to FOXQ1 and BMP6 genes, in Bex+Carv treated sample compared to the control sample. On the other hand, ARID1A and BRG1 enrichment at target regions assigned to KLF4 (-14Kb to TSS) and TGFBR2 (+52Kb to TSS) were associated with a significant decrease in the acetylated histone 3 marks at K27 (**Figure 5-13 C**).

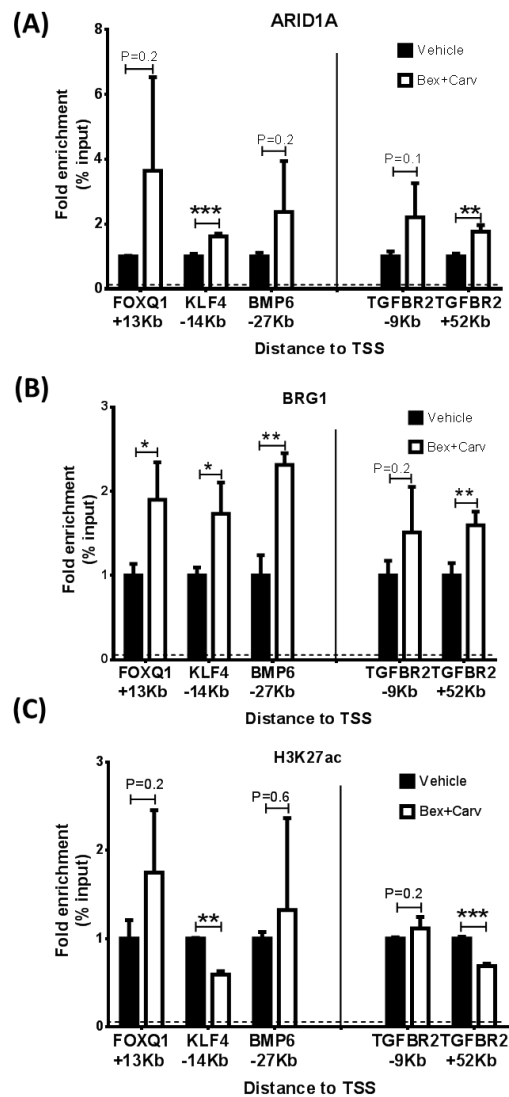


**Figure 5-13: ARID1A is recruited to regulatory elements assigned to genes involved in TGF- $\beta$  signaling pathway and proliferation regulation upon Bex+Carv combination treatment in HME-hTert cells. A, B) ARID1A and BRG1 enrichment to the putative regulatory elements assigned to FOXQ1, KLF4, BMP6 and TGFBR2 genes upon Veh or 100nM Bex + 1000nM Carv treatment for 6 hours in HME-hTert cells. C) H3K27ac marks along ARID1A target regions assigned to the mentioned genes in HME-hTert cells upon Veh or 100nM Bex + 1000nM Carv treatment. N=3 representing 3 biological replicates. The dashed line represents the signal coming from the negative control sample. The results are expressed as mean  $\pm$  SD \*P < 0.05, \*\*P < 0.01, \*\*\*P < 0.001, by two-tailed Student's t-test.**

5.12 ARID1A enrichment to its target regions upon Bex+Carv treatment is associated with a change in the expression of the corresponding genes in HME-hTert cells:

To study the effect of ARID1A and BRG1 enrichment to their target regions, on the expression of the corresponding genes, we measured transcript levels of FOXQ1, KLF4, TGFBR2, and BMP6 upon 100nM Bex+1000nM Carv treatment. The results showed a decrease in FOXQ1 transcript and protein levels post 24 or 48 hours of the combined treatment, respectively (**Figure 5-14 A, B**). TGFBR2 gene expression was downregulated post 24 hours of Bex+Carv exposure (**Figure 5-14 C**). While the change in FOXQ1 and TGFBR2 gene expression levels was discovered within 24 hours of Bex+Carv treatment, the effect of the combined treatment on KLF4 and BMP6 transcript levels was detected at a shorter time point (6 hours). KLF4 gene expression levels declined, whereas, BMP6 elevated post 6 hours of Bex+Carv treatment in HME-hTert cells (**Figure 5-14 D**).

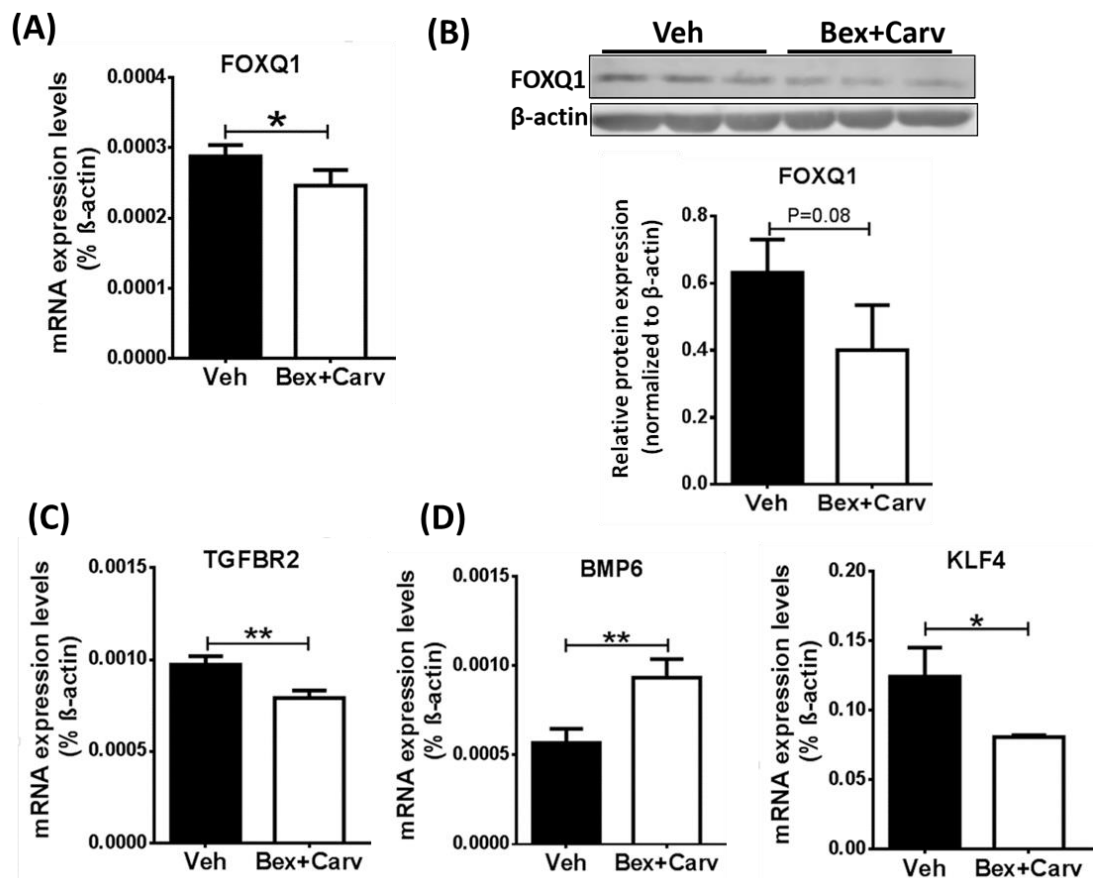


**Figure 5-14: ARID1A target's gene expression is changing upon Bex+Carv treatment in HME-hTert cells.** (A) RT-qPCR analysis of FOXQ1 transcript levels upon Bex+Carv treatment in HME-hTert cells after 24 hours, N=3 representing biological replicates. (B) Western blotting analysis for FOXQ1 protein levels in HME-hTert cells extracts upon Vehicle vs 100nM Bex + 1000nM Carv treatment for 48 hours. β-actin was used as a house keeping gene. N=3 representing 3 biological replicates. (lower) quantification of FOXQ1 protein expression levels (C) RT-qPCR analysis of TGFBR2 transcript levels in HME-

hTert cells upon Vehicle vs 100nM Bex + 1000nM Carv treatment for 24 hours. **(D)** RT-qPCR analysis of BMP6 and KLF4 transcript levels in HME-hTert cells upon Vehicle vs 100nM Bex + 1000nM Carv treatment for 6 hours. The results are presented as a percentage relative to the control sample (siNT). N=3 representing 3 biological replicates. The results are expressed as mean  $\pm$  SD \*P < 0.05, \*\*P < 0.01 by two-tailed Student's test.

### 5.13 ARID1A knockdown affects its target gene expression in HME-hTert cells:

To confirm that the identified genes are ARID1A targets we assessed the impact of ARID1A knockdown on their expression. We transfected HME-hTert cells with siRNA against luciferase (siNT) or a pool of three ARID1A-specific siRNAs at 20 nM final concentration and measured the transcript levels of FOXQ1, KLF4, TGFBR2, and BMP6. The results revealed that 90% knockdown in ARID1A transcript levels, is associated with a significant increase in FOXQ1 gene expression levels but a decrease in BMP6 transcript levels post two days of transfection. KLF4 mRNA levels tend to be induced upon ARID1A knockdown. On the other hand, the reduction in TGFBR2 transcript levels was detected post three days of siRNA transfection (**Figure 5-15 A**).

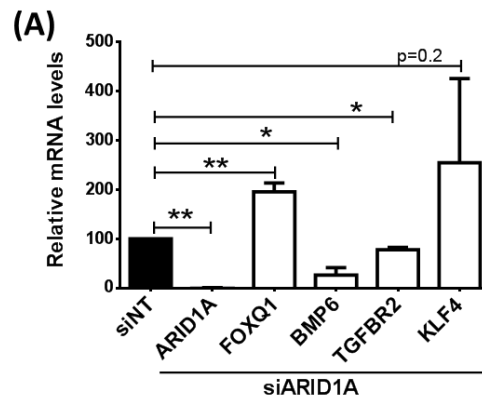


**Figure 5-15: ARID1A KD affects the expression of its putative target genes: A)** RT-qPCR analysis of ARID1A, FOXQ1, BMP6 and KLF4 gene expression upon 20nM siRNA transfection for 2 days with more than 90% knock-down, and TGFBR2 gene expression upon 3 days of 20nM siRNA transfection. The results in are presented as a percentage relatively to the control sample (siNT). N=3 representing 3 biological replicates. The results are expressed as mean  $\pm$  SD \*P < 0.05, \*\*P < 0.01 by two-tailed Student's test.

### 5.14 ARID1A controls SMAD4 nuclear translocation upon Bex+Carv treatment:

As we identified ARID1A to be recruited to regulatory elements assigned to TGF- $\beta$  pathway upon Bex+Carv treatment in HME-hTert cells, which was associated with a reduction in TGFBR2 gene expression, we next studied the effect of the combined treatment on TGF- $\beta$  signaling activation. The activity of TGF- $\beta$  signaling can be evaluated through the elevation of SMAD4 protein expression and nuclear

translocation (**Figure 5-16 A, B**). Post 24 hours of Bex+Carv treatment SMAD4 protein expression and nuclear translocation were significantly reduced in HME-hTert cells. These effects were reversed upon 3 days of transfection with 20nM siRNA against ARID1A, with a marked elevation in SMAD4 protein expression and nuclear translocation. On the other hand, the knockdown of ARID1A (without Bex+Carv treatment) caused a significant decline in SMAD4 protein expression and nuclear translocation (**Figure 5-16 C-F**), suggesting that ARID1A behaves differently upon Bex+Carv treatment.

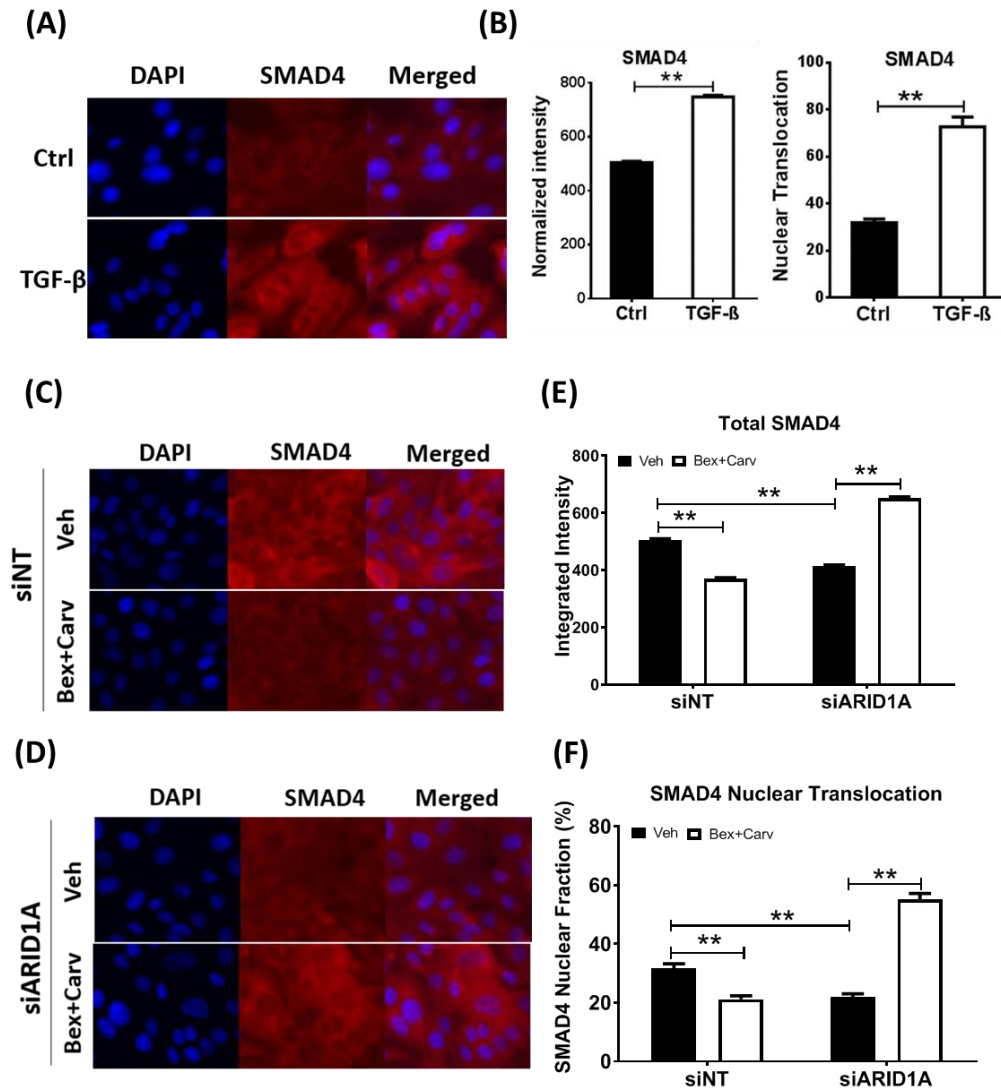


**Figure 5-16: Bexarotene and carvedilol combination affects TGF-β signaling pathway activation, mediated by ARID1A.** (A) Representative images of HME-hTert cells treated with TGF-β for 5 days. Cells are immunostained with antibodies against SMAD4. DAPI nuclear staining was used to stain the nuclei. (B) Quantification of SMAD4 protein expression and the ratio of its nuclear translocation in HME-hTert cells upon TGF-β treatment for 5 days. (C, D). Representative images of HME-hTert transfected with 20 nM siRNA against Luciferase (C) or ARID1A (D) for 3 days and treated with Veh vs 100nM Bex+ 1000nM Carv for 24 hours and immunostained with antibody against SMAD4. DAPI nuclear staining was used to stain the nuclei. (E, F) Quantification of SMAD4 protein

expression (**E**) and the ratio of its nuclear translocation (**F**) in HME-hTert cells transfected with 20 nM siRNA against Luciferase (siNT) or ARID1A (siARID1A) for 3 days and treated with Veh vs 100nM Bex+ 1000nM Carv for 24hours. The signal was derived from about 500 cells per image with 16 images per sample. The data was analyzed cell by cell using CellProfiler software based on SMAD4 integrated intensity in the nucleus and the cytoplasm, images were taken at 20 x magnifications. The results are expressed as mean  $\pm$  SEM \*P < 0.05, \*\*P < 0.01, \*\*\*P < 0.001 by two-tailed Student's test.

### 5.15 ARID1A mediates the suppression effects of Bex+Carv on gene and protein expression of the mesenchymal markers:

TGF- $\beta$  is a well-known inducer of the epithelial to mesenchymal transition (EMT) process [182]. FOXQ1 was also identified to enhance and promote the expression of the EMT markers [183]. Therefore, to assess the impact of Bex+Carv treatment on the EMT process, we measured gene and protein expression of the mesenchymal markers Fibronectin-1 and N-cadherin, and gene expression of the epithelial marker E-cadherin. The results illustrated no detectable transcript levels of E-cadherin in the control sample; however, its levels were markedly induced post 24 hours of the combined treatment. On the other hand, Fibronectin-1 and N-cadherin gene expression levels were downregulated upon 24 or 6 hours of treatment, respectively (**Figure 5-17 A**). To study the protein expression of Fibronectin and N-cadherin upon the combined treatment at the cellular level, HME-hTert cells were immunostained with antibodies against Fibronectin or N-cadherin (**Figure 5-17 B-E**). Cell-by-cell analysis of protein expression levels showed a significant decline upon Bex+Carv treatment for 24 hours. These effects were reversed upon ARID1A knock-down (**Figure 5-17 F, G**).

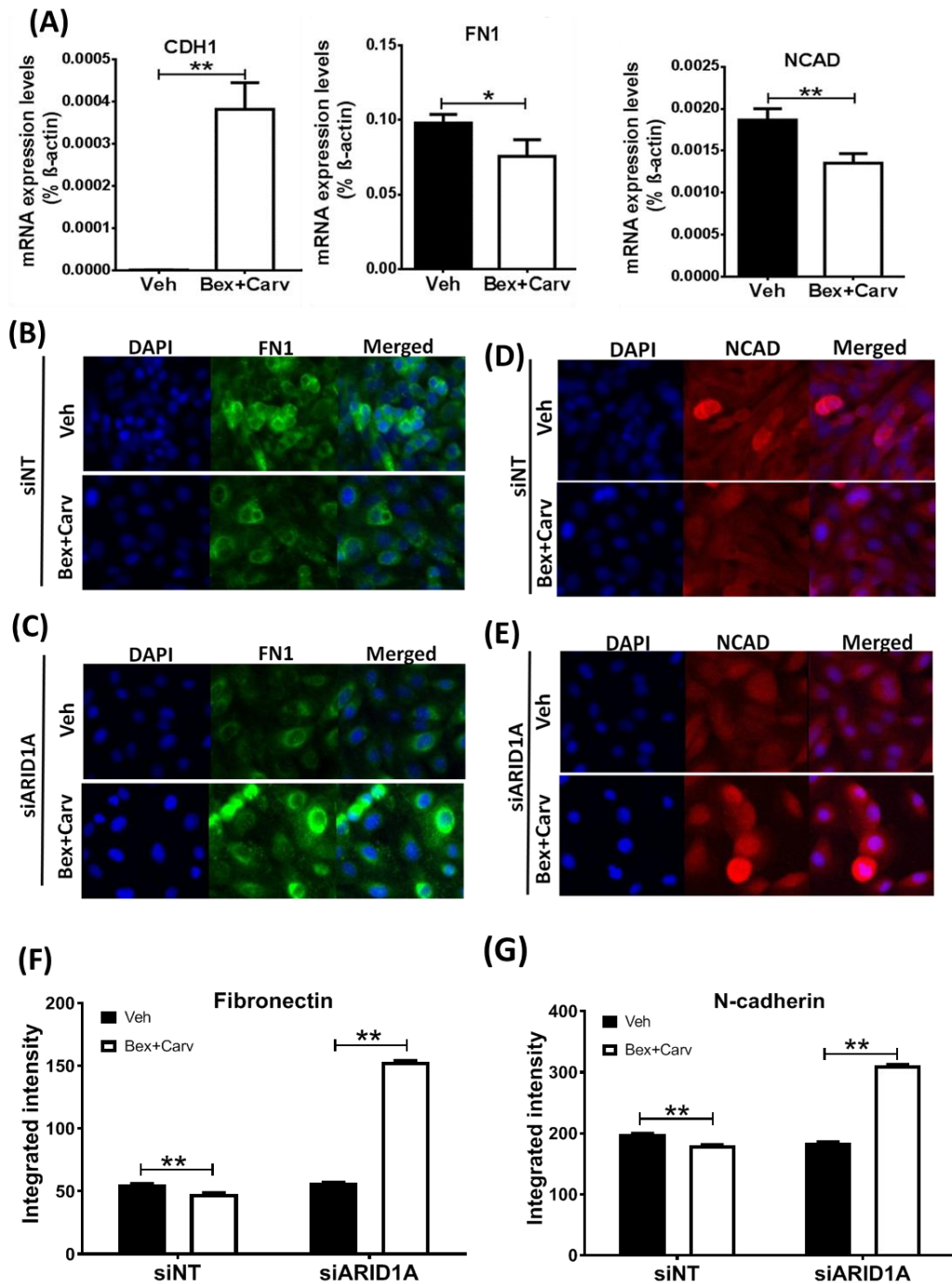


**Figure 5-17: Bexarotene and carvedilol combination treatment affects the downstream signaling of ARID1A target genes.** (A) RT-qPCR analysis for E-cadherin and Fibronectin transcript levels after 24 hours and N-cadherin after 6 hours of Bex+Carv combination treatment in HME-hTert cells. (B-E) Representative images of HME-hTert cells transfected with 20nM siRNA against luciferase as a control (B, D) or ARID1A (C, E) for 3 days and treated with Veh or 100nM Bex+1000nM Carv for 24hrs and immunostained with antibody against Fibronectin (B, C) or N-cadherin (D, E). DAPI nuclear staining was used to stain the nuclei. (F, G) Quantification of Fibronectin (F) and N-cadherin (G) protein expression levels in HME-hTert cells upon 20nM siRNA transfection for 3 days and 24 hrs Bex+Carv treatment. The signal was derived from about

500 cells per image with 100 images per sample. The data was analyzed cell by cell using CellProfiler software based on fibronectin or N-cadherin integrated intensity in total cell and cytoplasm. Images were taken at 20 x magnifications. The results are expressed as mean  $\pm$  SEM \*P < 0.05, \*\*P < 0.01 by two-tailed Student's test.

## 6. Discussion

Breast cancer is the most frequently occurring cancer among women and a life-threatening medical condition facing humanity worldwide [184]. Targeting the main growth regulators implicated in the development of breast cancer, including estrogen receptor (ER) or human epidermal growth factor receptor (Her-2), has shown successful results in improving patients' overall survival [185, 186]. Even though ER modulators and Her-2 targeting agents have shown effectiveness in treating breast cancer, cancerous cells are developing mechanisms to avoid treatment by relying on other signaling pathways in their growth regulation leading to the development of resistance against the therapeutic agents during the course of treatment [187, 188].

Moreover, clinical trials have demonstrated the feasibility of preventing breast cancer in patients with a high risk to develop the disease. Tamoxifen, a selective estrogen receptor modulator, has been used successfully for the prevention of ER-positive breast cancer in people at high risk to develop the disease [189]. However, more than 25% of breast cancer cases are ER-negative [190], which do not respond to ER modulators. Therefore, identifying agents that could prevent and/or treat breast cancer in an ER-independent status is at the forefront of interest.

Rexinoids are synthetic retinoids that bind selectively to retinoid X receptors (RXR) and trigger the expression of genes involved in the regulation of cell proliferation and apoptosis [191]. Bexarotene is an RXR selective agonist that got FDA approval to be used for the treatment of cutaneous T-cell lymphoma [192]. On the other hand, in vivo studies showed promising results regarding the usage of bexarotene in preventing the development of breast cancer [93], however, when it comes to clinical usage even minor toxicity should be taken into consideration. Therefore, identifying agents that show synergistic anti-tumor effects gives a chance to reduce the dosage and thereby the associated side effects.

Carvedilol, non-selective beta blocker, showed anti-tumor effects and its usage was associated with a reduction in mortality among breast cancer patients [138]. The combination treatment of bexarotene and carvedilol (referred to in the study as Bex+Carv) was associated with anti-proliferative effects in normal immortalized breast epithelial cells and MCF-7 breast cancer cells. In this study, we investigated the molecular mechanisms underlying these effects.

We studied the proteomic profile through reverse phase proteomic array (RPPA) upon Bex+Carv treatment. RPPA results revealed that the protein levels of the tumor suppressor ARID1A, AT-rich interactive domain 1A, increased significantly upon the combination treatment in normal epithelial HME-hTERT cells. ARID1A is a subunit of the chromatin remodeling complex SWI/SNF that participates in the regulation of biological processes including transcription activation or suppression, DNA damage repair and DNA replication. We hypothesized that upon Bex+Carv treatment ARID1A alters chromatin accessibility to modulate expression of genes involved in cancer development. To test the hypothesis we optimized chromatin immunoprecipitation

(ChIP) protocol to characterize ARID1A binding events across the genome upon the combined treatment.

ChIP results revealed that ARID1A was enriched to regulatory elements assigned to genes involved in insulin-like growth factor (IGF-1) signaling pathway upon Bex+Carv treatment in MCF-7 breast cancer cell line. ARID1A enrichment to the regulatory elements assigned to insulin-like growth factor receptor (IGF-1R) and insulin receptor substrate (IRS1) genes were associated with a downregulation in their protein levels upon Bex+Carv treatment, and antiproliferative effects in MCF-7 cells. These effects were abolished after ARID1A knockdown. The findings suggest that ARID1A mediates the suppressive effects of Bex+Carv treatment on IGF-1 pathway-related members, as a mechanism for the antiproliferative effects of the combination in MCF-7 breast cancer cells.

Further investigations in normal breast epithelial cells demonstrated that ARID1A occupied regions assigned to genes involved in proliferation regulation and transforming growth factor Beta (TGF- $\beta$ ) signaling pathway with an increased enrichment upon Bex+Carv treatment in HME-hTert cells. The recruitment of ARID1A as well as BRG1, ATPase subunit of the SWI/SNF complex, to the identified regulatory elements was associated with a change in target genes expression levels. Forkhead box Q1 (FOXQ1), a transcription factor that is associated with promoting cell proliferation in different tumors [183, 193], was found to be down-regulated upon Bex+Carv treatment in HME-hTert cells on the transcript and protein levels.

Further analysis illustrated that ARID1A targets in HME-hTert cells are involved in the regulation of the epithelial to mesenchymal transition process. EMT markers Fibronectin and N-cadherin gene and protein expression levels were downregulated whereas; E-cadherin expression levels were upregulated upon Bex+Carv treatment. These effects were abolished upon ARID1A silencing in HME-hTert cells.

Overall, our study revealed a new mechanism behind ARID1A tumor suppression activity through the regulation of IGF1 signaling pathway. The recruitment of ARID1A to its target regions was enriched upon Bex+Carv treatment in breast cancer cells MCF-7, associated with antiproliferative effects. In normal cells Bex+Carv treatment prevents the EMT process through the actions of ARID1A, which was identified to be enriched to regulatory regions assigned to genes involved in TGF- $\beta$  pathway participating in the regulation of EMT markers' expression. The study provides new insights about novel targets of ARID1A that are regulated through rexinoid-based combination in breast epithelial cells.

## 6.1 Bex+Carv treatment induced ARID1A protein expression levels in a transcriptional independent manner

The combined treatment was associated with an increase in ARID1A protein levels in normal breast epithelial cells (HME-hTert) with no change detected on its transcript levels. The results suggest a posttranscriptional regulation of ARID1A protein

expression upon the combined treatment which might be mediated by small non-coding RNA regulation. Based on literature ARID1A is targeted by several miRNA molecules. In head and neck squamous cell carcinoma miR-31 targets ARID1A mRNA and degrades it participating in the pathology of the disease [194]. Another study showed that ARID1A is a target for miR-185 in Colon Adenocarcinoma [195]. Targeting ARID1A in gastric cancer through miR-223-3p plays a role in promoting proliferation [196]. MiR-221 and miR-222 stimulate proliferation by regulating ARID1A expression in cervical cancer [197]. Moreover, retinoids were found to regulate the expression of several miRNA molecules [198]. Therefore, we suggest that the combined treatment could suppress the expression of miRNAs that negatively regulate the expression of ARID1A.

## 6.2 Bex+Carv treatment affects ARID1A genomic occupancy in MCF-7 cells to be more enriched to regulatory elements assigned to genes involved in epithelial cell proliferation

ARID1A is mutated in ~50% of ovarian clear cell carcinoma cases. ARID1A genomic behavior was characterized in ovarian clear cell carcinoma (RMG1) through ARID1A ChIP-Seq to identify ARID1A binding events, and ATAC-Seq upon ARID1A knockdown to study the effect of ARID1A on chromatin accessibility. The study revealed that ARID1A binds active promoter and enhancer regions, with a high correlation between ARID1A occupancy and the active enhancer regions mark (H3K27ac).

On the other hand, a study showed that ARID1A and SWI/SNF complex are recruited to enhancer regions assigned to ER target genes even before ligand activation, meaning in an ER-independent manner in MCF-7 cells [173].

Our study revealed ARID1A genomic distribution to be enriched to intronic and intergenic regions (40-50%), mainly enhancer regions in estrogen deprivation conditions. On the other hand, the occupancy in the promoter region was around 5% which does not match with another study showing that ARID1A recruitment to the TSS-promoter region is around 25% [174]. We interpret the results mainly because we cultured the cells in non-estrogenic conditions, which is a condition that was not applied in the other study. Suggesting that estrogenic activity might affect ARID1A to occupy promoter regions whereas, ARID1A was enriched to enhancer regions in non-estrogenic conditions.

ARID1A genomic occupancy increased in MCF-7 cells; with 66% of ARID1A binding regions identified upon Bex+Carv treatment were unique compared to the control group. However, no marked change was detected in the level of H3K27ac marks upon the combination treatment, suggesting that there might be another modified histone reflected the epigenetic change in target genes and/or that ARID1A binding events tend to have suppressive effects on target genes expression. Motif enrichment analysis reveals the genomic motifs occupied by a studied target, in our case ARID1A, under

different conditions. Motif analysis illustrates the potential cooperation between transcription factors. One study showed that ARID1A was enriched to AP1 motifs [199]. Another study revealed that ARID1A genomic binding regions overlap with Hnf4a and Foxa2 motifs in liver cells [168]. Our findings showed that ARID1A is enriched to FOXM1, AP-1, and GRHL2 motifs. FOXM1 is a transcription factor that is implicated in the initiation and progression of tumor as well as in regulating the expression of genes involved in cell cycle transition [200, 201]. Activating protein 1 family is a family of transcription factors that consists of members involved in the suppression or activation of transcription of genes involved in the regulation of cell proliferation and differentiation [202, 203]. The transcription factor grainyhead-like 2 (GRHL2) regulates the expression of E-cadherin and claudin 4 (Cldn4) genes involved in epithelial cells differentiation. The results refer to the cooperation between the SWI/SNF complex and these transcription factors in the regulation of proliferation and differentiation of breast epithelial cells.

### 6.3 ARID1A is recruited to regulatory elements assigned to genes involved in IGF-1 signaling pathway upon Bex+Carv treatment in MCF-7 cells:

ARID1A was identified to participate in controlling the expression of genes involved in cell cycle regulation including CDKN1A and SMAD3 in a direct or indirect manner [204, 205]. Investigating ARID1A's role in proliferation regulation a study showed that upon ARID1A knockout the acetylated histone marks on the promoter region of the proliferation marker Ki67 were reduced markedly [168]. Here we found that ARID1A was enriched to regulatory elements assigned to genes involved in IGF signaling pathway, and mammary epithelial cell proliferation upon Bex+Carv treatment in MCF-7 cells, associated with a suppression of IGF-1R and IRS1 protein expression levels. Bexarotene is a ligand for a nuclear receptor that participates through the ligand-receptor axis in the regulation of expression of genes involved in cell cycle arrest and proliferation regulation including Cyclin D1, and IGFBP6. The activity of the IGF1 pathway is regulated by the level of IGFBP proteins [206]. Previously it was shown that bexarotene induced the expression of IGFBP6 protein, participating in the downregulation of the IGF1 signaling pathway, as the former competes with IGF-1R in order to bind to the ligand and inhibits pathway activation [207].

On the other hand, retinoids have also extra nuclear activity including the regulation of AKT/MAPK signaling pathways [208].

IGF-1R is normally expressed in normal tissues participating in growth, development, and differentiation regulation [209]. On the other hand, IGF-1R is overexpressed in cancer and was shown to be implicated in tumor development [210, 211]. IRS1

phosphorylation was found to affect the interaction between epithelial cadherin and beta-catenin participating in invasiveness and metastasis regulation [212]. In this study, we found out that Bex+Carv combination treatment decreased the protein expression of the IGF-1R tyrosine kinase receptor and IRS1 substrate in MCF7 cell line.

IGF-1R expression is regulated by different factors including Estrogen, insulin, PDGF [213-215], and transcription factors; SP1, FOXO3, E2F1, and KLF6 which all bind to its promoter region [216, 217]. IGF can induce Bcl2 activation and BAD phosphorylation leading to apoptosis inhibition. Moreover, the central anti-apoptotic effects of IGF are mediated through AKT activation [114].

Studies have shown that ARID1A knockdown enhanced cell proliferation [218, 219]. Moreover, a study showed that ARID1A silencing is associated with an increase in AKT phosphorylation and promotes proliferation [220]. Here we also identified ARID1A silencing to promote MCF-7 breast cancer cell proliferation through increasing the expression of IGF-1R protein expression levels. Our study showed that the bexarotene and carvedilol combination treatment has antiprolifartive effects in MCF-7 cells mediated by the suppression of the IGF1 signaling pathway, **Figure 6-1**.

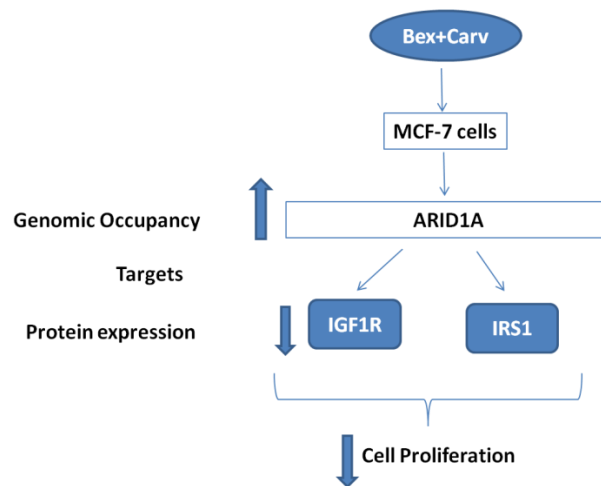


**Figure 6-1:** Schematic diagram showing a summary of the detected effects of Bex+Carv treatment on MCF-7 transformed cells mediated by ARID1A actions.

#### 6.4 ARID1A enrichment to regulatory elements assigned to genes involved in transforming growth factor Beta pathway is associated with a change in the expression of target genes upon Bex and Carv combination treatment in HME-hTert cells

TGF- $\beta$ -related genes (BMP4, ID4, DUSP4, TGF-B, TGF-B I TGF-B R2, and THBS1) were identified to be direct targets for ARID1A in human endometrial epithelial cells. ARID1A inactivation impaired TGF- $\beta$  signaling activity thereby SMAD3 phosphorylation that affects PTEN gene expression which is a direct target of SMAD3 [221]. Retinoids were found to suppress the activity of TGF- $\beta$  [222]. Here we introduced a correlation between rexinoids-based combination and ARID1A in the

regulation of TGF- $\beta$  signaling pathway activity in HME-hTert normal immortalized breast cells.

In this study, we found that upon Bex+Carv combined treatment ARID1A was enriched to regulatory elements assigned to genes involved in TGF- $\beta$  signaling pathway regulation including transforming growth factor beta receptor 2 (TGFBR2), Forkhead box Q1 (FOXQ1), Krüppel-like Factor 4 (KLF4), and Bone morphogenetic protein 6 (BMP6) in HME-hTert cells.

FOXQ1 is a transcription factor that belongs to the Forkhead box family. Its upregulation was correlated with tumor progression in different kinds of cancers including colorectal, breast, and small cell lung cancer [193, 223, 224]. On the other hand, low FOXQ1 transcript levels were associated with poor prognosis in breast cancer patients [223]. FOXQ1 promotes the EMT process (epithelial-mesenchymal transition) through negatively regulating the expression of the E-cadherin gene and positively regulating  $\beta$ -catenin and vimentin [183, 224, 225]. In hepatocellular carcinoma cells, FOXQ1 activates the expression of ZEB2 and Versican V1 genes [226]. In colorectal cancer cells, FOXQ1 is overexpressed and regulates p21 and TWIST1 genes leading to promoting tumor growth and metastasis respectively [227]. In this study, we found that Bex+Carv treatment is associated with downregulation of FOXQ1 on transcript and protein levels regulated by ARID1A recruitment to its regulatory element. TGF- $\beta$  signaling regulates the expression of the FOXQ1 gene in epithelial cells. Whereas, FOXQ1 knockdown blocks the TGF- $\beta$ -induced EMT process [183].

TGF-  $\beta$ /TGFR activation leads to the phosphorylation and activation of Smad2/Smad3 (R-Smad) complex that interacts with Smad4 (Co-Smad) [228]. Smad4 was found to bind to the promoter region of the MYC gene associated with its activation independently of TGF-  $\beta$  signaling [229]. Here we found that Bex+Carv treatment decreased Smad4 protein expression and nuclear translocation, these effects were reversed upon ARID1A knockdown in HME-hTert cells.

Moreover, an increased level of Smad4, was associated with a decrease in  $\beta$ -catenin mRNA levels [230]. FOXQ1 prevents the nuclear translocation of  $\beta$ -catenin, causing suppression in the Wnt signaling pathway [231].

Upon TGF- $\beta$  signaling, PTEN becomes phosphorylated through p38 kinase, leading to its dissociation from KLF4. KLF4 can then be phosphorylated through Smad proteins. The phosphorylated KLF is the active form, that binds to p300 and the complex accumulates to TGF-B target genes and enhances histone 3 acetylation and gene transcription activation [232]. KLF4 is a zinc finger transcription factor. It plays an important role in cell differentiation. It is a tumor suppressor for lung cancer [233].

A study showed that KLF4 plays a tumor inhibition function in MDA-MB-231 triple-negative breast cancer cells. However, the expression of KLF4 $\alpha$  antagonized its effect. The mechanism suggested is that KLF4 $\alpha$  is localized in the cytoplasm and might interact with KLF4 and prevent it from nuclear translocation [234]. It is worth

mentioning that KLF4 is considered a stem cell marker in breast cancer [235], and its high expression levels have been detected in aggressive breast cancer [236]. On the other hand downregulation of KLF4 in certain cancers including colon or gastric cancer might be involved in tumor development [237, 238]. Based on our findings KLF4 is one of ARID1A targets. ARID1A and BRG1 were detected at the KLF4 regulatory region which was associated with a decrease in the levels of H3K27ac, an active region marker, suggesting a suppressive activity for SWI/SNF complex which was confirmed with a reduction in KLF4 gene expression levels upon Bex+Carv treatment.

Another identified target of ARID1A is BMP6, which belongs to the Bone morphogenetic proteins family. BMPs are essential during embryogenesis and adult homeostasis, participating in regulating cell growth, proliferation and apoptosis. BMP6 is a tumor suppressor and its reduced expression is associated with tumorigenesis and poor breast cancer prognosis [239]. BMP6 inhibits MDA-MB-231 cell proliferation and reduced the number of cells in the S phase through the induction of miR-192 expression, a p53 activator leading to cell cycle arrest. Moreover, in vivo study showed that BMP6 suppresses tumorigenesis in MDA-MB-231-derived xenografts. BMP6 induces miR-192 expression through the p38 pathway. BMP6 expression was associated with an induction of ID1 and a reduction of CCNA1 cell cycle markers [240]. BMP6 and BMP7 inhibit breast cancer cell proliferation mediated by p38 MAPK activation [241]. In this study, we identified ARID1A enrichment to BMP6 putative regulatory element which was associated with an induction in its gene expression levels in HME-hTert cells.

### 6.5 ARID1A mediates the suppression effects of Bex+Carv on gene and protein expression of the mesenchymal markers:

Epithelial to mesenchymal transition is a process in which epithelial cells lost their polarity and their interactions with their neighbors and acquire mesenchymal characteristics and stem cell-like features giving them the ability to proliferate and migrate toward other organs [242]. TGF- $\beta$  signal leads to epithelial to mesenchymal transition through a contribution of Smad dependent and independent pathways [243]. TGF- $\beta$  induced activation is Smad independent, a cooperation with Smad pathway is needed To regulate cellular processes such as apoptosis and EMT process [56, 244].

FOXQ1 has a role in promoting epithelial-to-mesenchymal- transition through direct regulation of E-cadherin (CDH1) expression, where FOXQ1 was identified to bind to the CDH1 promoter region and suppress its expression [183]. On the other hand, FOXQ1 positively regulates the expression of N-cadherin, IL-1a, IL-8, fibronectin-1 [245]. Moreover, KLF4 and BMP6 regulate the expression of E-cadherin, and N-cadherin genes. Our results showed that upon Bex+Carv treatment ARID1A is regulating the expression of EMT process regulators, including FOXQ1, KLF4 and BMP6. The identified factors have in common to be involved in TGF- $\beta$  signaling pathway. Bex+Carv treatment decreased SMAD4 nuclear translocation which was associated with a decline in the expression of mesenchymal markers; fibronectin-1 and N-cadherin but an induction of the expression levels of the epithelial marker E-

cadherin. The detected effects were mediated by the action of the chromatin remodeler ARID1A **Figure 6-2**.

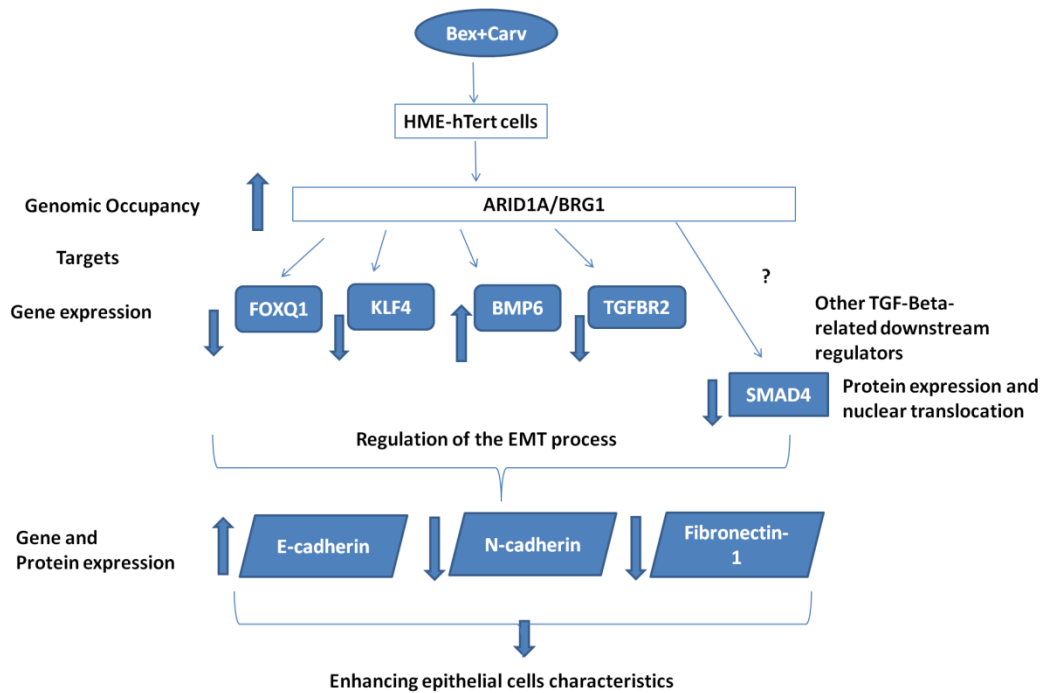


**Figure 6-2:** Schematic diagram showing a summary of the detected effects of Bex+Carv treatment on HME-hTert normal cells mediated by ARID1A and BRG1 actions

## 7. Summary:

Various strategies aiming of targeting breast cancer have been used successfully in controlling its progression, including modulators of the estrogen receptor or human epidermal growth factor receptor. However, at least 20% of breast cancers are not driven by these two growth regulators. On the other hand, targeting a single pathway increased the probability for cancer cells to develop resistance through relying on other signaling pathways in their development. Moreover, clinical trials have demonstrated the feasibility of preventing estrogen-responsive breast cancers. However, new approaches are needed to prevent breast cancer development in hormonal independent status. Retinoids, synthetic retinoids, are agents that bind selectively to the RXR nuclear hormone receptor participating in the regulation of

genes involved in cell differentiation and apoptosis signaling. Retinoids have shown effectiveness in cancer prevention in Her-2 induced mice models in an ER-independent manner. However, when it comes to clinical usage even minor side effects should be taken into consideration. On the other hand, the combination of validated cancer preventive agents may result in appropriate efficacy even at sub-therapeutic doses, while diminishing the chance of adverse effects. Previously we showed that carvedilol (Carv), an adrenergic non-selective beta blocker, synergistically enhanced the anti-proliferative effects of the retinoid, bexarotene (Bex), at sub-therapeutic doses in normal epithelial breast cancer HME-hTert cells. In addition, the combination acts synergistically to suppress breast cancer development in vivo. The combination treatment also suppressed the proliferation of the breast cancer cells MCF-7. To investigate the molecular mechanisms behind these effects, a reverse phase proteomic array (RPPA) was performed to study proteins that are selectively changed after the combination treatment. RPPA results revealed that ARID1A protein levels increased significantly upon the combination treatment in HME-hTert cells. ARID1A, AT-rich interactive domain 1 A, is a tumor suppressor frequently mutated in different types of cancers. ARID1A is a subunit of the SWItch/Sucrose Non-Fermentable ATP- dependent chromatin remodeling complex, which utilizes energy from ATP hydrolysis to modulate nucleosome organization, participating in the regulation of a number of biological processes including DNA damage repair, DNA replication, and transcription regulation. Therefore, we hypothesized that upon Bex+Carv treatment ARID1A alters nucleosome organization to modulate chromatin accessibility to regulate the expression of genes related to cancer development. To test this hypothesis, we performed ARID1A chromatin immunoprecipitation followed by deep sequencing (ChIP-Seq) in order to identify ARID1A binding events across the genome upon Bex+Carv treatment in MCF-7 and HME-hTert cells.

ARID1A ChIP results showed an increase in ARID1A genomic binding events upon Bex+Carv treatment compared to the control sample in MCF-7 cells. ARID1A occupied mainly intronic and intergenic regions. Even though a marked increase in ARID1A binding events was identified upon Bex+Carv treatment, it was associated with a slight change in H3K27ac marks, active enhancer marker, between the two groups, suggesting a suppression effect of ARID1A occupancy upon Bex+Carv. Gene ontology analysis demonstrated that ARID1A is recruited to regulatory regions assigned to genes involved in epithelial cell proliferation and insulin-like growth factor signaling pathway. Further analysis, showed that ARID1A is enriched to regulatory elements assigned to IGF-1R and IRS1 genes in MCF-7 cells, which was associated with a decrease in these targets' protein expression upon Bex+Carv treatment. ARID1A knockdown abolished the suppressing effect of Bex+Carv on IGF-1R and IRS-1 protein expression. In addition, ARID1A silencing was associated with an elevation in IGF-1R protein expression and MCF-7 cells' proliferation. Our findings suggest a mechanism behind the antiproliferative effects of Bex+Carv treatment in MCF-7 cells through

the downregulation of IGF-1R and IRS1 protein expression levels mediated by the regulatory effect of ARID1A **Figure 7-1**.

On the other hand, our study shows that upon Bex+Carv combination treatment, ARID1A is enriched to regulatory regions assigned to genes involved in the TGF- $\beta$  signaling pathway including TGFBR2, BMP2, and BMP6, in addition to genes that showed a connection to the TGF- $\beta$  pathway including FOXQ1, and KLF4 in HME-hTert cells. Further analysis showed that ARID1A enrichment to the regulatory elements of its potential target genes was associated with a change in their gene expression. Bex+Carv treatment caused a decrease in SMAD4 protein expression and nuclear translocation in HME-hTert cells upon the combination treatment which was abolished upon ARID1A knockdown. Furthermore, ARID1A enrichment to FOXQ1 potential regulatory regions was correlated with a downregulation of FOXQ1 transcript and protein levels in HME-hTert cells. Further analysis of TGF-Beta downstream signaling upon Bex+Carv treatment, showed a decrease in the gene and protein levels of EMT markers including fibronectine-1, and N-cadherin but an elevation in the expression levels of the epithelial cells marker; E-cadherin. Overall, the study suggests that one of the mechanisms behind the Bex+Carv effects is mediated through ARID1A actions leading to the downregulation of the EMT process markers referring that the combination treatment stimulating the mechanisms preserving epithelial cells characteristics **Figure 7-2**.

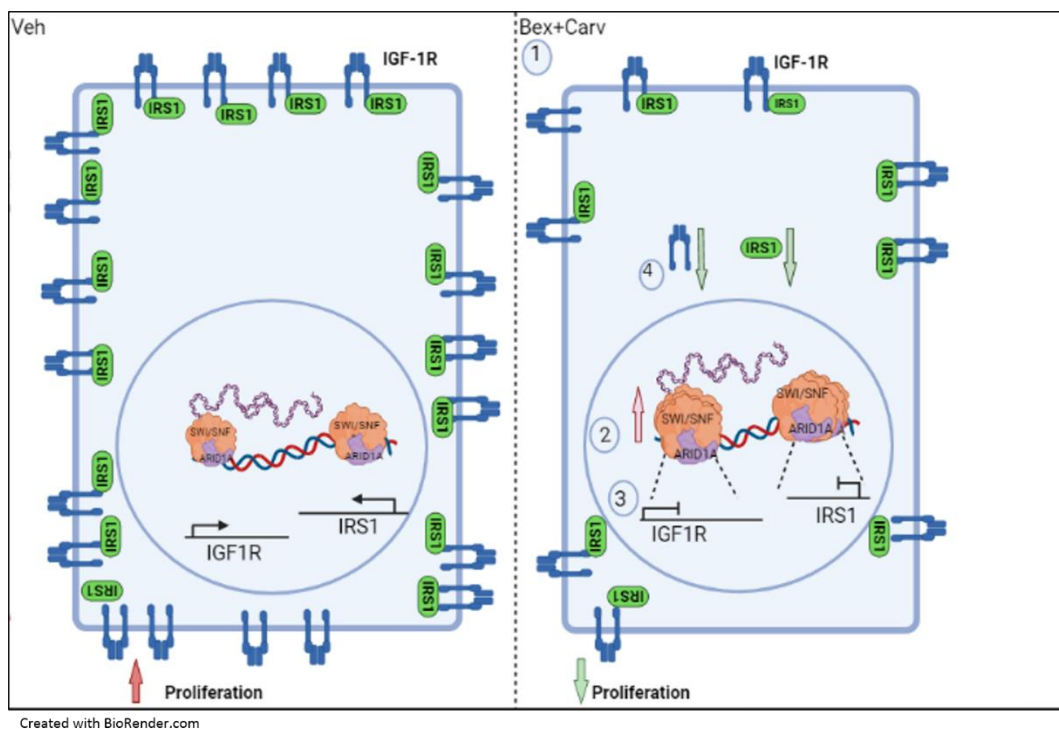


**Figure 7-1: Schematic diagram representing the effects of Bex+Carv treatment on MCF-7 cells (right) compared to Veh-treated cells (left) in modulating IGF-1R**

**signaling pathway through ARID1A activity.** Upon Bex+Carv treatment (1), ARID1A is enriched to the regulatory regions assigned to IGF-1R and IRS1 genes (2). The enrichment of ARID1A is associated with a downregulation of IGF-1R and IRS1 on the protein levels (3, 4). The overall outcome is a decrease in the distribution of IGF-1R and IRS1 on the membrane and inhibition in cell proliferation.

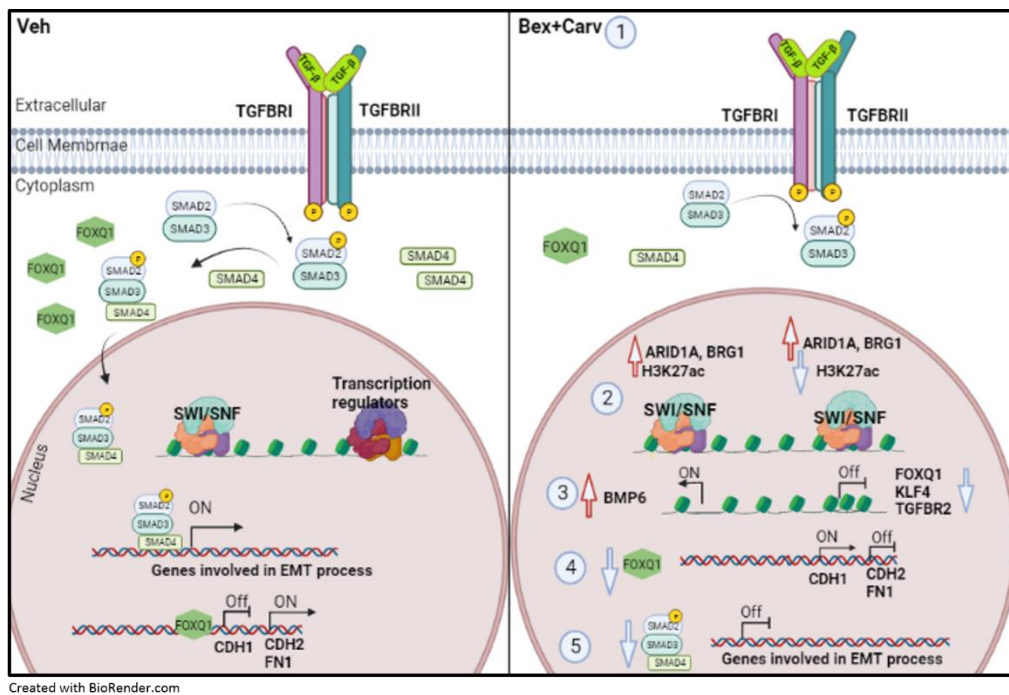


**Figure 7-2: Schematic diagram representing the effects of Bex+Carv treatment on HME-hTert cells (right) compared to Veh-treated cells (left) in modulating TGF-Beta pathway through ARID1A activity.** Upon Bex+Carv treatment (1) ARID1A and BRG1 are enriched to regulatory elements assigned to genes involved to TGF-Beta signaling pathway which are associated with an increase or a decrease in H3K27ac marks (2). The enrichment of SWI/SNF to its target regions alters the expression of target genes; an increase in case of Bmp6, or a decrease in KLF4, FOXQ1, and TGFBR2 transcript levels (3). A decrease in FOXQ1 protein expression levels is associated with a change in its putative target genes' expression (4). SMAD4, a downstream player in TGF-Beta pathway, protein's expression levels and nuclear translocation are downregulated affecting its downstream target genes (5) in HME-hTert cells.

## **8. List of Main New Scientific results:**

1. ARID1A distribution across the genome was characterized upon rexinoids-based combination to occupy mainly intronic and intergenic regions in MCF-7 breast cancer cells under nonestrogenic conditions.
2. We identified ARID1A de novo motifs that match TRE, FOXM1, and GRHL2 transcription factors' motifs.
3. We discovered novel ARID1A target genes, including IGF-1R and IRS1 in MCF-7 cells, and FOXQ1, TGFBR2, BMP6 and KLF4 in HME-hTert cells.
4. ARID1A knockdown induced the protein expression of the insulin-like growth factor receptor, which was associated with an increase in MCF-7 cells' proliferation
5. The study revealed one of the molecular mechanisms behind the antiproliferative effects of Bex+Carv in MCF-7 cells through suppressing the protein expression of IGF-1 pathway-related genes mediated by ARID1A actions
6. ARID1A knockdown was associated with an induction in the expression levels of the tumor-promoting gene FOXQ1 in normal immortalized breast epithelial cells, HME-hTert
7. Bex+Carv treatment caused a decrease in FOXQ1 gene expression levels, which was associated with an elevation in the expression levels of the epithelial marker E-cadherin in HME-hTert cells
8. We found that the protein and nuclear translocation of SMAD4, a canonical regulator in TGF- $\beta$  pathway, are downregulated upon Bex+Carv treatment in HME-hTert cells
9. Bex+Carv combination treatment participates in the inhibition of normal cell transformation by suppressing the expression of mesenchymal markers on gene and protein levels in normal HME-hTert cells through the actions of ARID1A.

## 9. Reference:

1. Visvader, J.E., *Cells of origin in cancer*. Nature, 2011. **469**(7330): p. 314-322.
2. Dagogo-Jack, I. and A.T. Shaw, *Tumour heterogeneity and resistance to cancer therapies*. Nature Reviews Clinical Oncology, 2018. **15**(2): p. 81-94.
3. Davies, M.A. and Y. Samuels, *Analysis of the genome to personalize therapy for melanoma*. Oncogene, 2010. **29**(41): p. 5545-55.
4. Yuan, T.L. and L.C. Cantley, *PI3K pathway alterations in cancer: variations on a theme*. Oncogene, 2008. **27**(41): p. 5497-510.
5. Elmore, S., *Apoptosis: a review of programmed cell death*. Toxicol Pathol, 2007. **35**(4): p. 495-516.
6. Blasco, M.A., *Telomeres and human disease: ageing, cancer and beyond*. Nat Rev Genet, 2005. **6**(8): p. 611-22.
7. Trybek, T., et al., *Telomeres and telomerase in oncogenesis (Review)*. Oncol Lett, 2020. **20**(2): p. 1015-1027.
8. Nishida, N., et al., *Angiogenesis in cancer*. Vasc Health Risk Manag, 2006. **2**(3): p. 213-9.
9. Bergers, G. and S.-M. Fendt, *The metabolism of cancer cells during metastasis*. Nature Reviews Cancer, 2021. **21**(3): p. 162-180.
10. Fares, J., et al., *Molecular principles of metastasis: a hallmark of cancer revisited*. Signal Transduction and Targeted Therapy, 2020. **5**(1): p. 28.
11. Nwabo Kamdje, A.H., et al., *Developmental pathways associated with cancer metastasis: Notch, Wnt, and Hedgehog*. Cancer Biol Med, 2017. **14**(2): p. 109-120.
12. Ames, B.N., M.K. Shigenaga, and T.M. Hagen, *Oxidants, antioxidants, and the degenerative diseases of aging*. Proceedings of the National Academy of Sciences of the United States of America, 1993. **90**(17): p. 7915-7922.
13. Yao, Y. and W. Dai, *Genomic Instability and Cancer*. Journal of carcinogenesis & mutagenesis, 2014. **5**: p. 1000165.
14. Ciccia, A. and S.J. Elledge, *The DNA damage response: making it safe to play with knives*. Mol Cell, 2010. **40**(2): p. 179-204.
15. Friedberg, E.C., et al., *DNA repair: from molecular mechanism to human disease*. DNA Repair, 2006. **5**(8): p. 986-96.
16. Lee, E.Y. and W.J. Muller, *Oncogenes and tumor suppressor genes*. Cold Spring Harb Perspect Biol, 2010. **2**(10): p. 18.
17. KONTOMANOLIS, E.N., et al., *Role of Oncogenes and Tumor-suppressor Genes in Carcinogenesis: A Review*. Anticancer Research, 2020. **40**(11): p. 6009-6015.
18. Osborne, C., P. Wilson, and D. Tripathy, *Oncogenes and tumor suppressor genes in breast cancer: potential diagnostic and therapeutic applications*. Oncologist, 2004. **9**(4): p. 361-77.
19. Williams, A.B. and B. Schumacher, *p53 in the DNA-Damage-Repair Process*. Cold Spring Harb Perspect Med, 2016. **6**(5).
20. Zhu, G., et al., *Mutant p53 in Cancer Progression and Targeted Therapies*. Frontiers in Oncology, 2020. **10**(2418).
21. Baumjohann, D. and P. Brossart, *T follicular helper cells: linking cancer immunotherapy and immune-related adverse events*. J Immunother Cancer, 2021. **9**(6): p. 2021-002588.
22. Tay, R.E., E.K. Richardson, and H.C. Toh, *Revisiting the role of CD4+ T cells in cancer immunotherapy—new insights into old paradigms*. Cancer Gene Therapy, 2021. **28**(1): p. 5-17.

23. Lin, Y., J. Xu, and H. Lan, *Tumor-associated macrophages in tumor metastasis: biological roles and clinical therapeutic applications*. Journal of Hematology & Oncology, 2019. **12**(1): p. 76.
24. Vander Heiden, M.G., L.C. Cantley, and C.B. Thompson, *Understanding the Warburg effect: the metabolic requirements of cell proliferation*. Science, 2009. **324**(5930): p. 1029-33.
25. Hanahan, D. and R.A. Weinberg, *Hallmarks of cancer: the next generation*. Cell, 2011. **144**(5): p. 646-74.
26. Sung, H., et al., *Global cancer statistics 2020: GLOBOCAN estimates of incidence and mortality worldwide for 36 cancers in 185 countries*. CA: A Cancer Journal for Clinicians, 2020. **n/a**(n/a).
27. WHO. *Breast Cancer*. 2021 26 March]; Available from: <https://www.who.int/news-room/fact-sheets/detail/breast-cancer>.
28. Jemal, A., et al., *Global cancer statistics*. CA Cancer J Clin, 2011. **61**(2): p. 69-90.
29. Sheikh, A., et al., *The spectrum of genetic mutations in breast cancer*. Asian Pac J Cancer Prev, 2015. **16**(6): p. 2177-85.
30. Bray, F., P. McCarron, and D.M. Parkin, *The changing global patterns of female breast cancer incidence and mortality*. Breast Cancer Research, 2004. **6**(6): p. 229.
31. Buerger, H., et al., *Different genetic pathways in the evolution of invasive breast cancer are associated with distinct morphological subtypes*. J Pathol, 1999. **189**(4): p. 521-6.
32. Strehl, J.D., et al., *Invasive Breast Cancer: Recognition of Molecular Subtypes*. Breast care (Basel, Switzerland), 2011. **6**(4): p. 258-264.
33. Weigelt, B. and J.S. Reis-Filho, *Histological and molecular types of breast cancer: is there a unifying taxonomy?* Nature Reviews Clinical Oncology, 2009. **6**(12): p. 718-730.
34. Dai, X., et al., *Breast cancer intrinsic subtype classification, clinical use and future trends*. American journal of cancer research, 2015. **5**(10): p. 2929-2943.
35. Eliyatkin, N., et al., *Molecular Classification of Breast Carcinoma: From Traditional, Old-Fashioned Way to A New Age, and A New Way*. J Breast Health, 2015. **11**(2): p. 59-66.
36. Sinn, H.P., B. Helmchen, and C.H. Wittekind, *[TNM classification of breast cancer: changes and comments on the 7th edition]*. Pathologe, 2010. **31**(5): p. 361-6.
37. Feng, Y., et al., *Breast cancer development and progression: Risk factors, cancer stem cells, signaling pathways, genomics, and molecular pathogenesis*. Genes Dis, 2018. **5**(2): p. 77-106.
38. Saha Roy, S. and R.K. Vadlamudi, *Role of Estrogen Receptor Signaling in Breast Cancer Metastasis*. International Journal of Breast Cancer, 2012. **2012**: p. 654698.
39. Wang, Z., et al., *Clinical implications of  $\beta$ -catenin protein expression in breast cancer*. Int J Clin Exp Pathol, 2015. **8**(11): p. 14989-94.
40. Farabaugh, S.M., D.N. Boone, and A.V. Lee, *Role of IGF1R in Breast Cancer Subtypes, Stemness, and Lineage Differentiation*. Front Endocrinol, 2015. **6**(59).
41. Kretzschmar, M., *Transforming growth factor-beta and breast cancer: Transforming growth factor-beta/SMAD signaling defects and cancer*. Breast Cancer Res, 2000. **2**(2): p. 107-15.
42. Sundaresan, S., E. Penuel, and M.X. Sliwkowski, *The biology of human epidermal growth factor receptor 2*. Curr Oncol Rep, 1999. **1**(1): p. 16-22.
43. Pai, S.G., et al., *Wnt/beta-catenin pathway: modulating anticancer immune response*. Journal of Hematology & Oncology, 2017. **10**(1): p. 101.
44. Brennan, K.R. and A.M. Brown, *Wnt proteins in mammary development and cancer*. J Mammary Gland Biol Neoplasia, 2004. **9**(2): p. 119-31.

45. Nagahata, T., et al., *Amplification, up-regulation and over-expression of DVL-1, the human counterpart of the Drosophila disheveled gene, in primary breast cancers*. *Cancer Sci*, 2003. **94**(6): p. 515-8.
46. Ugolini, F., et al., *Differential expression assay of chromosome arm 8p genes identifies Frizzled-related (FRP1/FRZB) and Fibroblast Growth Factor Receptor 1 (FGFR1) as candidate breast cancer genes*. *Oncogene*, 1999. **18**(10): p. 1903-10.
47. Koren, S., et al., *PIK3CA(H1047R) induces multipotency and multi-lineage mammary tumours*. *Nature*, 2015. **525**(7567): p. 114-8.
48. Shi, X., et al., *Research progress on the PI3K/AKT signaling pathway in gynecological cancer (Review)*. *Mol Med Rep*, 2019. **19**(6): p. 4529-4535.
49. Bhutani, J., A. Sheikh, and A. Niazi, *Akt inhibitors: Mechanism of action and implications for anticancer therapeutics*. *Infectious agents and cancer*, 2013. **8**: p. 49.
50. Pérez-Tenorio, G. and O. Stål, *Activation of AKT/PKB in breast cancer predicts a worse outcome among endocrine treated patients*. *Br J Cancer*, 2002. **86**(4): p. 540-5.
51. Dhillon, A.S., et al., *MAP kinase signalling pathways in cancer*. *Oncogene*, 2007. **26**(22): p. 3279-3290.
52. Santarpia, L., S.M. Lippman, and A.K. El-Naggar, *Targeting the MAPK-RAS-RAF signaling pathway in cancer therapy*. *Expert Opin Ther Targets*, 2012. **16**(1): p. 103-19.
53. Yuan, J., et al., *Function of insulin-like growth factor 1 receptor in cancer resistance to chemotherapy (Review)*. *Oncol Lett*, 2018. **15**(1): p. 41-47.
54. Liu, S., S. Chen, and J. Zeng, *TGF- $\beta$  signaling: A complex role in tumorigenesis (Review)*. *Mol Med Rep*, 2018. **17**(1): p. 699-704.
55. Nowrin, K., et al., *Epithelial-mesenchymal transition as a fundamental underlying pathogenic process in COPD airways: fibrosis, remodeling and cancer*. *Expert Rev Respir Med*, 2014. **8**(5): p. 547-59.
56. Zhang, Y.E., *Non-Smad pathways in TGF-beta signaling*. *Cell Res*, 2009. **19**(1): p. 128-39.
57. Gennari, A., et al., *ESMO Clinical Practice Guideline for the diagnosis, staging and treatment of patients with metastatic breast cancer*: *Ann Oncol*. 2021 Dec;32(12):1475-1495. doi: 10.1016/j.annonc.2021.09.019. Epub 2021 Oct 19.
58. Salvatori, L., et al., *Oestrogens and selective oestrogen receptor (ER) modulators regulate EGF receptor gene expression through human ER  $\alpha$  and  $\beta$  subtypes via an Sp1 site*. *Oncogene*, 2003. **22**(31): p. 4875-4881.
59. Morales, J., et al., *Review of poly (ADP-ribose) polymerase (PARP) mechanisms of action and rationale for targeting in cancer and other diseases*. *Crit Rev Eukaryot Gene Expr*, 2014. **24**(1): p. 15-28.
60. Hawsawi, Y.M., et al., *The role of BRCA1/2 in hereditary and familial breast and ovarian cancers*. *Mol Genet Genomic Med*, 2019. **7**(9): p. 17.
61. Topatana, W., et al., *Advances in synthetic lethality for cancer therapy: cellular mechanism and clinical translation*. *Journal of Hematology & Oncology*, 2020. **13**(1): p. 118.
62. Sporn, M.B., *Approaches to prevention of epithelial cancer during the preneoplastic period*. *Cancer Res*, 1976. **36**(7 PT 2): p. 2699-702.
63. Jack Cuzick, I.S., Simon Cawthorn, Hisham Hamed, Prof Kaija Holli, Prof Anthony Howell, *Tamoxifen for prevention of breast cancer: extended long-term follow-up of the IBIS-I breast cancer prevention trial*. 2015. **16**( 1): p. P67-75.
64. Wu, K., et al., *The retinoid X receptor-selective retinoid, LGD1069, prevents the development of estrogen receptor-negative mammary tumors in transgenic mice*. *Cancer Res*, 2002. **62**(22): p. 6376-80.

65. Liby, K., et al., *The Combination of the Retinoid, LG100268, and a Selective Estrogen Receptor Modulator, Either Arzoxifene or Acolbifene, Synergizes in the Prevention and Treatment of Mammary Tumors in an Estrogen Receptor–Negative Model of Breast Cancer*. *Clinical Cancer Research*, 2006. **12**(19): p. 5902-5909.
66. Kim, E.S., et al., *The BATTLE trial: personalizing therapy for lung cancer*. *Cancer Discov*, 2011. **1**(1): p. 44-53.
67. Kiser, P.D., M. Golczak, and K. Palczewski, *Chemistry of the retinoid (visual) cycle*. *Chem Rev*, 2014. **114**(1): p. 194-232.
68. During, A. and E.H. Harrison, *Mechanisms of provitamin A (carotenoid) and vitamin A (retinol) transport into and out of intestinal Caco-2 cells*. *J Lipid Res*, 2007. **48**(10): p. 2283-94.
69. Shirakami, Y., et al., *Hepatic metabolism of retinoids and disease associations*. *Biochim Biophys Acta*, 2012. **1**: p. 124-36.
70. Uray, I.P., E. Dmitrovsky, and P.H. Brown, *Retinoids and rexinoids in cancer prevention: from laboratory to clinic*. *Semin Oncol*, 2016. **43**(1): p. 49-64.
71. Kedishvili, N.Y., *Retinoic Acid Synthesis and Degradation*. *Subcell Biochem*, 2016. **81**: p. 127-161.
72. Ghyselinck, N.B. and G. Duyster, *Retinoic acid signaling pathways*. *Development*, 2019. **146**(13).
73. Theodosiou, M., V. Laudet, and M. Schubert, *From carrot to clinic: an overview of the retinoic acid signaling pathway*. *Cellular and Molecular Life Sciences*, 2010. **67**(9): p. 1423-1445.
74. Kongsbak, M., et al., *The Vitamin D Receptor and T Cell Function*. *Frontiers in Immunology*, 2013. **4**(148).
75. Prüfer, K., et al., *Dimerization with retinoid X receptors promotes nuclear localization and subnuclear targeting of vitamin D receptors*. *J Biol Chem*, 2000. **275**(52): p. 41114-23.
76. Sharma, V., et al., *Effects of Retinoids on Thyrotrope Function and the Hypothalamic-Pituitary-Thyroid Axis*. *Endocrinology*, 2006. **147**(3): p. 1438-1451.
77. Apfel, R., et al., *A novel orphan receptor specific for a subset of thyroid hormone-responsive elements and its interaction with the retinoid/thyroid hormone receptor subfamily*. *Mol Cell Biol*, 1994. **14**(10): p. 7025-35.
78. Li, H., et al., *Characterization of receptor interaction and transcriptional repression by the corepressor SMRT*. *Mol Endocrinol*, 1997. **11**(13): p. 2025-37.
79. Jones, P.L. and Y.B. Shi, *N-CoR-HDAC corepressor complexes: roles in transcriptional regulation by nuclear hormone receptors*. *Curr Top Microbiol Immunol*, 2003. **274**: p. 237-68.
80. Kao, H.Y., et al., *Isolation of a novel histone deacetylase reveals that class I and class II deacetylases promote SMRT-mediated repression*. *Genes Dev*, 2000. **14**(1): p. 55-66.
81. Lösel, R. and M. Wehling, *Nongenomic actions of steroid hormones*. *Nature Reviews Molecular Cell Biology*, 2003. **4**(1): p. 46-55.
82. Aggarwal, S., et al., *Nonclassical action of retinoic acid on the activation of the cAMP response element-binding protein in normal human bronchial epithelial cells*. *Mol Biol Cell*, 2006. **17**(2): p. 566-75.
83. Berry, D.C., et al., *Cross talk between signaling and vitamin A transport by the retinol-binding protein receptor STRA6*. *Mol Cell Biol*, 2012. **32**(15): p. 3164-75.
84. Morriss-Kay, G.M. and N. Sokolova, *Embryonic development and pattern formation*. *Faseb J*, 1996. **10**(9): p. 961-8.
85. Peck, G.L., et al., *Prolonged remissions of cystic and conglobate acne with 13-cis-retinoic acid*. *N Engl J Med*, 1979. **300**(7): p. 329-33.

86. Oliveira, L.d.M., F.M.E. Teixeira, and M.N. Sato, *Impact of Retinoic Acid on Immune Cells and Inflammatory Diseases*. Mediators of inflammation, 2018. **2018**: p. 3067126-3067126.
87. Idres, N., et al., *Granulocytic differentiation of human NB4 promyelocytic leukemia cells induced by all-trans retinoic acid metabolites*. Cancer Res, 2001. **61**(2): p. 700-5.
88. Grimwade, D., et al., *Acute promyelocytic leukemia: a paradigm for differentiation therapy*. Cancer Treat Res, 2010. **145**: p. 219-35.
89. Miles, S.A., et al., *Antitumor activity of oral 9-cis-retinoic acid in HIV-associated Kaposi's sarcoma*. Aids, 2002. **16**(3): p. 421-9.
90. Lalloyer, F., et al., *Rexinoid bexarotene modulates triglyceride but not cholesterol metabolism via gene-specific permissivity of the RXR/LXR heterodimer in the liver*. Arterioscler Thromb Vasc Biol, 2009. **29**(10): p. 1488-95.
91. Li, B., S.-Y. Cai, and J.L. Boyer, *The role of the retinoid receptor, RAR/RXR heterodimer, in liver physiology*. Biochimica et Biophysica Acta (BBA) - Molecular Basis of Disease, 2021. **1867**(5): p. 166085.
92. Billings, S.E., et al., *The retinaldehyde reductase DHRS3 is essential for preventing the formation of excess retinoic acid during embryonic development*. Faseb J, 2013. **27**(12): p. 4877-89.
93. Li, Y., et al., *The rexinoid, bexarotene, prevents the development of premalignant lesions in MMTV-erbB2 mice*. Br J Cancer, 2008. **98**(8): p. 1380-8.
94. Seo, H.S., et al., *Identification of biomarkers regulated by rexinoids (LGD1069, LG100268 and Ro25-7386) in human breast cells using Affymetrix microarray*. Mol Med Rep, 2015. **12**(1): p. 800-18.
95. Feldman, S.R., C.P. Werner, and A.B. Alió Saenz, *The efficacy and tolerability of tazarotene foam, 0.1%, in the treatment of acne vulgaris in 2 multicenter, randomized, vehicle-controlled, double-blind studies*. J Drugs Dermatol, 2013. **12**(4): p. 438-46.
96. Hind, M., et al., *Retinoid induction of alveolar regeneration: from mice to man?* Thorax, 2009. **64**(5): p. 451-7.
97. Roth, M.D., et al., *Feasibility of retinoids for the treatment of emphysema study*. Chest, 2006. **130**(5): p. 1334-45.
98. Yamanaka, M., et al., *PPAR $\gamma$ /RXR $\alpha$ -induced and CD36-mediated microglial amyloid- $\beta$  phagocytosis results in cognitive improvement in amyloid precursor protein/presenilin 1 mice*. J Neurosci, 2012. **32**(48): p. 17321-31.
99. McFarland, K., et al., *Low dose bexarotene treatment rescues dopamine neurons and restores behavioral function in models of Parkinson's disease*. ACS Chem Neurosci, 2013. **4**(11): p. 1430-8.
100. Guo, Y., et al., *Blockade of the ubiquitin protease UBP43 destabilizes transcription factor PML/RAR $\alpha$  and inhibits the growth of acute promyelocytic leukemia*. Cancer Res, 2010. **70**(23): p. 9875-85.
101. Atzpodien, J., et al., *Interleukin-2- and Interferon Alfa-2a-Based Immunochemotherapy in Advanced Renal Cell Carcinoma: A Prospectively Randomized Trial of the German Cooperative Renal Carcinoma Chemoimmunotherapy Group (DGCIN)*. Journal of Clinical Oncology, 2004. **22**(7): p. 1188-1194.
102. Matthay, K.K., et al., *Long-term results for children with high-risk neuroblastoma treated on a randomized trial of myeloablative therapy followed by 13-cis-retinoic acid: a children's oncology group study*. J Clin Oncol, 2009. **27**(7): p. 1007-13.
103. Arrieta, O., et al., *Randomized phase II trial of All-trans-retinoic acid with chemotherapy based on paclitaxel and cisplatin as first-line treatment in patients with advanced non-small-cell lung cancer*. J Clin Oncol, 2010. **28**(21): p. 3463-71.
104. Kong, G., et al., *The retinoid X receptor-selective retinoid, LGD1069, down-regulates cyclooxygenase-2 expression in human breast cells through transcription factor*

- crosstalk: implications for molecular-based chemoprevention. Cancer Res, 2005. 65(8): p. 3462-9.*
105. Liu, H., et al., *Bexarotene Attenuates Focal Cerebral Ischemia-Reperfusion Injury via the Suppression of JNK/Caspase-3 Signaling Pathway. Neurochem Res, 2019. 44(12): p. 2809-2820.*
  106. Xu, L., et al., *Bexarotene reduces blood-brain barrier permeability in cerebral ischemia-reperfusion injured rats. PLoS One, 2015. 10(4).*
  107. Quéreux, G., et al., *Bexarotene in cutaneous T-cell lymphoma: third retrospective study of long-term cohort and review of the literature. Expert Opin Pharmacother, 2013. 14(13): p. 1711-21.*
  108. Dragnev, K.H., et al., *A proof-of-principle clinical trial of bexarotene in patients with non-small cell lung cancer. Clin Cancer Res, 2007. 13(6): p. 1794-800.*
  109. Han, J., et al., *Evaluation of N-4-(hydroxycarbophenyl) retinamide as a cancer prevention agent and as a cancer chemotherapeutic agent. In Vivo, 1990. 4 3: p. 153-60.*
  110. Moon, R.C., et al., *N-(4-Hydroxyphenyl)retinamide, a new retinoid for prevention of breast cancer in the rat. Cancer Res, 1979. 39(4): p. 1339-46.*
  111. Anzano, M.A., et al., *Prevention of breast cancer in the rat with 9-cis-retinoic acid as a single agent and in combination with tamoxifen. Cancer Res, 1994. 54(17): p. 4614-7.*
  112. Pushpakom, S., et al., *Drug repurposing: progress, challenges and recommendations. Nature Reviews Drug Discovery, 2019. 18(1): p. 41-58.*
  113. Deeks, E.D. and S.J. Keam, *Rosiglitazone : a review of its use in type 2 diabetes mellitus. Drugs, 2007. 67(18): p. 2747-79.*
  114. Shankaranarayanan, P., et al., *Growth factor-antagonized rexinoid apoptosis involves permissive PPARGgamma/RXR heterodimers to activate the intrinsic death pathway by NO. Cancer Cell, 2009. 16(3): p. 220-31.*
  115. Hirota, K., *Adrenoceptor modulators and cancer progression. Journal of Anesthesia, 2016. 30(3): p. 365-368.*
  116. Barron, T.I., L. Sharp, and K. Visvanathan, *Beta-adrenergic blocking drugs in breast cancer: a perspective review. Ther Adv Med Oncol, 2012. 4(3): p. 113-25.*
  117. Waxenbaum, J.A., V. Reddy, and M. Varacallo, *Anatomy, Autonomic Nervous System.*
  118. Alshak, M.N. and M.D. J, *Neuroanatomy, Sympathetic Nervous System.*
  119. Dean II JS, R.A., *Alpha 1 Receptor Agonists. StatPearls, 2021.*
  120. Michel T, H.B., *Treatment of myocardial ischemia and hypertension, in Goodman & Gilman's the pharmacological basis of therapeutics., B.L. In, Chabner BA, Knollman BC, eds, Editor. 2011: New York: McGraw-Hill.*
  121. Spiss, C.K. and M. Maze, *[Adrenoreceptors]. Anaesthetist, 1985. 34(1): p. 1-10.*
  122. Ruffolo, R.R., Jr. and J.P. Hieble, *Alpha-adrenoceptors. Pharmacol Ther, 1994. 61(1-2): p. 1-64.*
  123. Giovannitti, J.A., Jr., S.M. Thoms, and J.J. Crawford, *Alpha-2 adrenergic receptor agonists: a review of current clinical applications. Anesth Prog, 2015. 62(1): p. 31-9.*
  124. Bylund, D.B., *Beta-1 Adrenoceptor\**, in *xPharm: The Comprehensive Pharmacology Reference*, S.J. Enna and D.B. Bylund, Editors. 2007, Elsevier: New York. p. 1-12.
  125. Bylund, D.B., *Beta-2 Adrenoceptor\**, in *xPharm: The Comprehensive Pharmacology Reference*, S.J. Enna and D.B. Bylund, Editors. 2007, Elsevier: New York. p. 1-12.
  126. Wachter, S.B. and E.M. Gilbert, *Beta-Adrenergic Receptors, from Their Discovery and Characterization through Their Manipulation to Beneficial Clinical Application. Cardiology, 2012. 122(2): p. 104-112.*
  127. Bylund, D.B., *Beta-3 Adrenoceptor\**, in *xPharm: The Comprehensive Pharmacology Reference*, S.J. Enna and D.B. Bylund, Editors. 2007, Elsevier: New York. p. 1-11.

128. Yamaguchi, O. and C.R. Chapple, *Beta3-adrenoceptors in urinary bladder*: *Neurourol Urodyn.* 2007;26(6):752-6. doi: 10.1002/nau.20420.
129. Quốc Lu'o'ng, K.V. and L.T. Nguyễn, *The roles of beta-adrenergic receptors in tumorigenesis and the possible use of beta-adrenergic blockers for cancer treatment: possible genetic and cell-signaling mechanisms.* *Cancer Manag Res*, 2012. **4**: p. 431-45.
130. Shan, T., et al.,  *$\beta$ 2-adrenoceptor blocker synergizes with gemcitabine to inhibit the proliferation of pancreatic cancer cells via apoptosis induction.* *Eur J Pharmacol*, 2011. **665**(1-3): p. 1-7.
131. Zhang, D., et al.,  *$\beta$ 2-adrenergic antagonists suppress pancreatic cancer cell invasion by inhibiting CREB, NF $\kappa$ B and AP-1.* *Cancer Biol Ther*, 2010. **10**(1): p. 19-29.
132. Montoya, A., et al., *Use of non-selective  $\beta$ -blockers is associated with decreased tumor proliferative indices in early stage breast cancer.* *Oncotarget*, 2017. **8**(4): p. 6446-6460.
133. Cole, S.W., et al., *Sympathetic nervous system regulation of the tumour microenvironment.* *Nat Rev Cancer*, 2015. **15**(9): p. 563-72.
134. Zheng, G., et al., *Beta-Blockers Use and Risk of Breast Cancer in Women with Hypertension.* *Cancer Epidemiol Biomarkers Prev*, 2021. **30**(5): p. 965-973.
135. Powe, D.G., et al., *Alpha- and beta-adrenergic receptor (AR) protein expression is associated with poor clinical outcome in breast cancer: an immunohistochemical study.* *Breast Cancer Res Treat*, 2011. **130**(2): p. 457-63.
136. *Carvedilol*, in *Meyler's Side Effects of Drugs (Sixteenth Edition)*, J.K. Aronson, Editor. 2016, Elsevier: Oxford. p. 167-169.
137. Lin, C.S., et al., *Carvedilol use is associated with reduced cancer risk: A nationwide population-based cohort study.* *Int J Cardiol*, 2015. **184**: p. 9-13.
138. Gillis, R.D., et al., *Carvedilol blocks neural regulation of breast cancer progression in vivo and is associated with reduced breast cancer mortality in patients.* *European Journal of Cancer*, 2021. **147**: p. 106-116.
139. de Araújo Júnior, R.F., et al., *Carvedilol decrease IL-1 $\beta$  and TNF- $\alpha$ , inhibits MMP-2, MMP-9, COX-2, and RANKL expression, and up-regulates OPG in a rat model of periodontitis.* *PLoS One*, 2013. **8**(7).
140. Costantino, S., et al., *Epigenetics and precision medicine in cardiovascular patients: from basic concepts to the clinical arena.* *European Heart Journal*, 2017. **39**(47): p. 4150-4158.
141. Handy, D.E., R. Castro, and J. Loscalzo, *Epigenetic modifications: basic mechanisms and role in cardiovascular disease.* *Circulation*, 2011. **123**(19): p. 2145-56.
142. Nina Parker, M.S., Anh-Hue Thi Tu, Philip Lister, Brian M. Forster, *Microbiology.* 2016, OpenStax: Houston, Texas.
143. Teif, V.B. and K. Bohinc, *Condensed DNA: Condensing the concepts.* *Progress in biophysics and molecular biology*, 2011. **105**(3): p. 208-222.
144. Tyagi, M., et al., *Chromatin remodelers: We are the drivers!!* *Nucleus (Austin, Tex.)*, 2016. **7**(4): p. 388-404.
145. Saha, A., J. Wittmeyer, and B.R. Cairns, *Chromatin remodelling: the industrial revolution of DNA around histones.* *Nat Rev Mol Cell Biol*, 2006. **7**(6): p. 437-47.
146. Mani, U., et al., *SWI/SNF Infobase-An exclusive information portal for SWI/SNF remodeling complex subunits.* *PLoS One*, 2017. **12**(9).
147. Tyagi, M., et al., *Chromatin remodelers: We are the drivers!!* *Nucleus*, 2016. **7**(4): p. 388-404.
148. Clapier, C.R. and B.R. Cairns, *The biology of chromatin remodeling complexes.* *Annu Rev Biochem*, 2009. **78**: p. 273-304.

149. Sawicka, A. and C. Seiser, *Histone H3 phosphorylation – A versatile chromatin modification for different occasions*. *Biochimie*, 2012. **94**(11): p. 2193-2201.
150. Swygert, S.G. and C.L. Peterson, *Chromatin dynamics: interplay between remodeling enzymes and histone modifications*. *Biochim Biophys Acta*, 2014. **8**: p. 728-36.
151. Bannister, A.J. and T. Kouzarides, *Regulation of chromatin by histone modifications*. *Cell Res*, 2011. **21**(3): p. 381-95.
152. Tellez, C.S., et al., *Chromatin remodeling by the histone methyltransferase EZH2 drives lung pre-malignancy and is a target for cancer prevention*. *Clinical Epigenetics*, 2021. **13**(1): p. 44.
153. Cusack, M., et al., *Distinct contributions of DNA methylation and histone acetylation to the genomic occupancy of transcription factors*. *Genome Res*, 2020. **30**(10): p. 1393-1406.
154. Zhong, Z., et al., *DNA methylation-linked chromatin accessibility affects genomic architecture in *Arabidopsis**. *Proceedings of the National Academy of Sciences*, 2021. **118**(5): p. e2023347118.
155. Haggarty, S.J. and L.H. Tsai, *Probing the role of HDACs and mechanisms of chromatin-mediated neuroplasticity*. *Neurobiol Learn Mem*, 2011. **96**(1): p. 41-52.
156. Sharma, A., K. Singh, and A. Almasan, *Histone H2AX phosphorylation: a marker for DNA damage*. *Methods Mol Biol*, 2012. **920**: p. 613-26.
157. Tsuda, M., et al., *The role of the SWI/SNF chromatin remodeling complex in pancreatic ductal adenocarcinoma*. *Cancer Science*, 2021. **112**(2): p. 490-497.
158. Le Quang, M., D. Ranchère-Vince, and F. Le Loarer, *[Pathological and molecular features of malignancies underlined by BAF complexes inactivation]*. *Annales de pathologie*, 2019. **39**(6): p. 399-413.
159. Zhang, P., et al., *An Overview of Chromatin-Regulating Proteins in Cells*. *Curr Protein Pept Sci*, 2016. **17**(5): p. 401-10.
160. Alver, B.H., et al., *The SWI/SNF chromatin remodelling complex is required for maintenance of lineage specific enhancers*. *Nature communications*, 2017. **8**(1): p. 14648.
161. Smith, C.L. and C.L. Peterson, *A conserved Swi2/Snf2 ATPase motif couples ATP hydrolysis to chromatin remodeling*. *Mol Cell Biol*, 2005. **25**(14): p. 5880-92.
162. Pagliaroli, L. and M. Trizzino, *The Evolutionary Conserved SWI/SNF Subunits ARID1A and ARID1B Are Key Modulators of Pluripotency and Cell-Fate Determination*. *Frontiers in cell and developmental biology*, 2021. **9**.
163. Wu, J.N. and C.W. Roberts, *ARID1A mutations in cancer: another epigenetic tumor suppressor?* *Cancer Discov*, 2013. **3**(1): p. 35-43.
164. Wu, R.C., T.L. Wang, and M. Shih le, *The emerging roles of ARID1A in tumor suppression*. *Cancer Biol Ther*, 2014. **15**(6): p. 655-64.
165. Mamo, A., et al., *An integrated genomic approach identifies ARID1A as a candidate tumor-suppressor gene in breast cancer*. *Oncogene*, 2012. **31**(16): p. 2090-100.
166. Takao, C., et al., *Downregulation of ARID1A, a component of the SWI/SNF chromatin remodeling complex, in breast cancer*. *J Cancer*, 2017. **8**(1): p. 1-8.
167. Mariotti, V., H.L. McLeod, and H.H. Soliman, *ARID1a as a marker of prognosis and increased sensitivity to CDK4/6, mTOR 1/2 and Src homology region 2 phosphatase (SHP 1/2) inhibitors in breast cancer (BC)*. *Journal of Clinical Oncology*, 2019. **37**(15\_suppl): p. 1082-1082.
168. Sun, X., et al., *Suppression of the SWI/SNF Component Arid1a Promotes Mammalian Regeneration*. *Cell Stem Cell*, 2016. **18**(4): p. 456-66.
169. Shen, J., et al., *ARID1A Deficiency Impairs the DNA Damage Checkpoint and Sensitizes Cells to PARP Inhibitors*. *Cancer Discov*, 2015. **5**(7): p. 752-67.

170. Zhao, B., et al., *ARID1A promotes genomic stability through protecting telomere cohesion*. Nature communications, 2019. **10**(1): p. 019-12037.
171. Kelso, T.W.R., et al., *Chromatin accessibility underlies synthetic lethality of SWI/SNF subunits in ARID1A-mutant cancers*. eLife, 2017. **2**(6): p. 30506.
172. Cho, H.D., et al., *Loss of Tumor Suppressor ARID1A Protein Expression Correlates with Poor Prognosis in Patients with Primary Breast Cancer*. J Breast Cancer, 2015. **18**(4): p. 339-46.
173. Nagarajan, S., et al., *ARID1A influences HDAC1/BRD4 activity, intrinsic proliferative capacity and breast cancer treatment response*. Nature Genetics, 2020. **52**(2): p. 187-197.
174. Trizzino, M., et al., *The Tumor Suppressor ARID1A Controls Global Transcription via Pausing of RNA Polymerase II*. Cell reports, 2018. **23**(13): p. 3933-3945.
175. Bitler, B.G., et al., *Synthetic lethality by targeting EZH2 methyltransferase activity in ARID1A-mutated cancers*. Nat Med, 2015. **21**(3): p. 231-8.
176. Guan, B., T.L. Wang, and M. Shih Ie, *ARID1A, a factor that promotes formation of SWI/SNF-mediated chromatin remodeling, is a tumor suppressor in gynecologic cancers*. Cancer Res, 2011. **71**(21): p. 6718-27.
177. Suryo Rahmanto, Y., et al., *Inactivating ARID1A Tumor Suppressor Enhances TERT Transcription and Maintains Telomere Length in Cancer Cells*. J Biol Chem, 2016. **291**(18): p. 9690-9.
178. Bui, C.B., et al., *ARID1A-SIN3A drives retinoic acid-induced neuroblastoma differentiation by transcriptional repression of TERT*. Mol Carcinog, 2019. **58**(11): p. 1998-2007.
179. Nagl, N.G., Jr., et al., *Distinct mammalian SWI/SNF chromatin remodeling complexes with opposing roles in cell-cycle control*. Embo J, 2007. **26**(3): p. 752-63.
180. Takaku, M., et al., *GATA3-dependent cellular reprogramming requires activation-domain dependent recruitment of a chromatin remodeler*. Genome Biology, 2016. **17**(1): p. 36.
181. Kelso, T.W.R., et al., *Chromatin accessibility underlies synthetic lethality of SWI/SNF subunits in ARID1A-mutant cancers*. eLife, 2017. **6**: p. e30506.
182. Xu, J., S. Lamouille, and R. Derynck, *TGF-beta-induced epithelial to mesenchymal transition*. Cell Res, 2009. **19**(2): p. 156-72.
183. Zhang, H., et al., *Forkhead transcription factor foxq1 promotes epithelial-mesenchymal transition and breast cancer metastasis*. Cancer Res, 2011. **71**(4): p. 1292-301.
184. Sung, H., et al., *Global Cancer Statistics 2020: GLOBOCAN Estimates of Incidence and Mortality Worldwide for 36 Cancers in 185 Countries*. CA Cancer J Clin, 2021. **71**(3): p. 209-249.
185. Jordan, V.C., *Tamoxifen: a most unlikely pioneering medicine*. Nat Rev Drug Discov, 2003. **2**(3): p. 205-13.
186. Lv, S., et al., *Overall Survival Benefit from Trastuzumab-Based Treatment in HER2-Positive Metastatic Breast Cancer: A Retrospective Analysis*. Oncol Res Treat, 2018. **41**(7-8): p. 450-455.
187. Rimawi, M.F., C.D. Angelis, and R. Schiff, *Resistance to Anti-HER2 Therapies in Breast Cancer*. American Society of Clinical Oncology Educational Book, 2015(35): p. e157-e164.
188. Fan, P. and V. Craig Jordan, *Acquired resistance to selective estrogen receptor modulators (SERMs) in clinical practice (tamoxifen & raloxifene) by selection pressure in breast cancer cell populations*. Steroids, 2014. **90**: p. 44-52.
189. Li, F., et al., *The selective estrogen receptor modulators in breast cancer prevention*. Cancer Chemother Pharmacol, 2016. **77**(5): p. 895-903.

190. Putti, T.C., et al., *Estrogen receptor-negative breast carcinomas: a review of morphology and immunophenotypical analysis*. *Modern Pathology*, 2005. **18**(1): p. 26-35.
191. Wainwright, L.J., A. Lasorella, and A. Iavarone, *Distinct mechanisms of cell cycle arrest control the decision between differentiation and senescence in human neuroblastoma cells*. *Proceedings of the National Academy of Sciences*, 2001. **98**(16): p. 9396-9400.
192. Querfeld, C., et al., *Bexarotene in the treatment of cutaneous T-cell lymphoma*. *Expert Opin Pharmacother*, 2006. **7**(7): p. 907-15.
193. Liu, J.Y., et al., *FOXQ1 promotes cancer metastasis by PI3K/AKT signaling regulation in colorectal carcinoma*. *Am J Transl Res*, 2017. **9**(5): p. 2207-2218.
194. Lu, W.C., et al., *miR-31 targets ARID1A and enhances the oncogenicity and stemness of head and neck squamous cell carcinoma*. *Oncotarget*, 2016. **7**(35): p. 57254-57267.
195. Baldi, S., et al., *Downregulated ARID1A by miR-185 Is Associated With Poor Prognosis and Adverse Outcomes in Colon Adenocarcinoma*. *Front Oncol*, 2021. **11**(679334).
196. Zhu, Y., et al., *miR-223-3p promotes cell proliferation and invasion by targeting Arid1a in gastric cancer*. *Acta Biochimica et Biophysica Sinica*, 2020. **52**(2): p. 150-159.
197. Yang, Y., X. Zhao, and H.X. Li, *MiR-221 and miR-222 simultaneously target ARID1A and enhance proliferation and invasion of cervical cancer cells*. *Eur Rev Med Pharmacol Sci*, 2016. **20**(8): p. 1509-15.
198. Wang, L., A.P. Rohatgi, and Y.Y. Wan, *Retinoic acid and microRNA*. *Methods Enzymol*, 2020. **637**: p. 283-308.
199. Sen, M., et al., *ARID1A facilitates KRAS signaling-regulated enhancer activity in an AP1-dependent manner in colorectal cancer cells*. *Clinical epigenetics*, 2019. **11**(1): p. 92-92.
200. Wierstra, I., *The transcription factor FOXM1 (Forkhead box M1): proliferation-specific expression, transcription factor function, target genes, mouse models, and normal biological roles*. *Adv Cancer Res*, 2013. **118**: p. 97-398.
201. Nandi, D., et al., *FoxM1: Repurposing an oncogene as a biomarker*. *Seminars in Cancer Biology*, 2018. **52**: p. 74-84.
202. Lee, W., et al., *Activation of transcription by two factors that bind promoter and enhancer sequences of the human metallothionein gene and SV40*. *Nature*, 1987. **325**(6102): p. 368-72.
203. Wagner, E.F., *AP-1 – Introductory remarks*. *Oncogene*, 2001. **20**(19): p. 2334-2335.
204. Zhang, Y., et al., *ARID1A is downregulated in non-small cell lung cancer and regulates cell proliferation and apoptosis*. *Tumour Biol*, 2014. **35**(6): p. 5701-7.
205. Guan, B., T.-L. Wang, and I.-M. Shih, *ARID1A, a Factor That Promotes Formation of SWI/SNF-Mediated Chromatin Remodeling, Is a Tumor Suppressor in Gynecologic Cancers*. *Cancer Research*, 2011. **71**(21): p. 6718-6727.
206. Allard, J.B. and C. Duan, *IGF-Binding Proteins: Why Do They Exist and Why Are There So Many?* *Frontiers in Endocrinology*, 2018. **9**.
207. Uray, I.P., et al., *Rexinoid-induced expression of IGFBP-6 requires RARbeta-dependent permissive cooperation of retinoid receptors and AP-1*. *The Journal of biological chemistry*, 2009. **284**(1): p. 345-353.
208. Kim, S.-M., et al., *Retinoic acid-stimulated ERK1/2 pathway regulates meiotic initiation in cultured fetal germ cells*. *PLoS One*, 2019. **14**(11): p. e0224628.
209. Wit, J.M. and M.J. Walenkamp, *Role of insulin-like growth factors in growth, development and feeding*. *World Rev Nutr Diet*, 2013. **106**: p. 60-5.
210. Baserga, R., *The IGF-I receptor in cancer research*. *Exp Cell Res*, 1999. **253**(1): p. 1-6.
211. Samani, A.A., et al., *The role of the IGF system in cancer growth and metastasis: overview and recent insights*. *Endocr Rev*, 2007. **28**(1): p. 20-47.

212. Playford, M.P., et al., *Insulin-like growth factor 1 regulates the location, stability, and transcriptional activity of  $\beta$ -catenin*. Proceedings of the National Academy of Sciences, 2000. **97**(22): p. 12103-12108.
213. Delafontaine, P., Y.-H. Song, and Y. Li, *Expression, Regulation, and Function of IGF-1, IGF-1R, and IGF-1 Binding Proteins in Blood Vessels*. Arteriosclerosis, Thrombosis, and Vascular Biology, 2004. **24**(3): p. 435-444.
214. Fagan, D.H. and D. Yee, *Crosstalk between IGF1R and estrogen receptor signaling in breast cancer*. J Mammary Gland Biol Neoplasia, 2008. **13**(4): p. 423-9.
215. Novosyadlyy, R., et al., *Crosstalk between PDGF and IGF-I receptors in rat liver myofibroblasts: implication for liver fibrogenesis*. Laboratory Investigation, 2006. **86**(7): p. 710-723.
216. Huo, X., et al., *GSK3 protein positively regulates type I insulin-like growth factor receptor through forkhead transcription factors FOXO1/3/4*. J Biol Chem, 2014. **289**(36): p. 24759-70.
217. Schayek, H., et al., *Transcription factor E2F1 is a potent transactivator of the insulin-like growth factor-I receptor (IGF-IR) gene*. Growth Horm IGF Res, 2010. **20**(1): p. 68-72.
218. Yang, Y., et al., *Loss of ARID1A promotes proliferation, migration and invasion via the Akt signaling pathway in NPC*. Cancer management and research, 2019. **11**: p. 4931-4946.
219. Xie, C., et al., *Decreased ARID1A expression facilitates cell proliferation and inhibits 5-fluorouracil-induced apoptosis in colorectal carcinoma*. Tumour Biol, 2014. **35**(8): p. 7921-7.
220. Yang, Y., et al., *Loss of ARID1A promotes proliferation, migration and invasion via the Akt signaling pathway in NPC*. Cancer Manag Res, 2019. **11**: p. 4931-4946.
221. Suryo Rahmanto, Y., et al., *Inactivation of Arid1a in the endometrium is associated with endometrioid tumorigenesis through transcriptional reprogramming*. Nature communications, 2020. **11**(1): p. 020-16416.
222. Sheng, N., et al., *Retinoic acid regulates bone morphogenic protein signal duration by promoting the degradation of phosphorylated Smad1*. Proc Natl Acad Sci U S A, 2010. **107**(44): p. 18886-91.
223. Elian, F.A., et al., *FOXQ1 is Differentially Expressed Across Breast Cancer Subtypes with Low Expression Associated with Poor Overall Survival*. Breast Cancer, 2021. **13**: p. 171-188.
224. Feng, J., et al., *FoxQ1 overexpression influences poor prognosis in non-small cell lung cancer, associates with the phenomenon of EMT*. PLoS One, 2012. **7**(6): p. 28.
225. Qiao, Y., et al., *FOXQ1 Regulates Epithelial-Mesenchymal Transition in Human Cancers*. Cancer Research, 2011. **71**(8): p. 3076-3086.
226. Xia, L., et al., *Forkhead box Q1 promotes hepatocellular carcinoma metastasis by transactivating ZEB2 and VersicanV1 expression*. Hepatology, 2014. **59**(3): p. 958-73.
227. Zhu, Z., et al., *Short hairpin RNA targeting FOXQ1 inhibits invasion and metastasis via the reversal of epithelial-mesenchymal transition in bladder cancer*. Int J Oncol, 2013. **42**(4): p. 1271-1278.
228. Yang, G. and X. Yang, *Smad4-mediated TGF-beta signaling in tumorigenesis*. Int J Biol Sci, 2010. **6**(1): p. 1-8.
229. Lim, S.K. and F.M. Hoffmann, *Smad4 cooperates with lymphoid enhancer-binding factor 1/T cell-specific factor to increase c-<i>myc</i> expression in the absence of TGF- $\beta$  signaling*. Proceedings of the National Academy of Sciences, 2006. **103**(49): p. 18580-18585.
230. Freeman, T.J., et al., *Smad4-mediated signaling inhibits intestinal neoplasia by inhibiting expression of  $\beta$ -catenin*. Gastroenterology, 2012. **142**(3): p. 562-571.

231. Peng, X., et al., *FOXQ1 mediates the crosstalk between TGF- $\beta$  and Wnt signaling pathways in the progression of colorectal cancer*. *Cancer Biol Ther*, 2015. **16**(7): p. 1099-109.
232. He, M., et al., *KLF4 mediates the link between TGF- $\beta$ 1-induced gene transcription and H3 acetylation in vascular smooth muscle cells*. *Faseb J*, 2015. **29**(9): p. 4059-70.
233. Yu, T., et al., *KLF4 regulates adult lung tumor-initiating cells and represses K-Ras-mediated lung cancer*. *Cell Death & Differentiation*, 2016. **23**(2): p. 207-215.
234. Ferralli, J., R. Chiquet-Ehrismann, and M. Degen, *KLF4 $\alpha$  stimulates breast cancer cell proliferation by acting as a KLF4 antagonist*. *Oncotarget*, 2016. **7**(29): p. 45608-45621.
235. Yu, F., et al., *Kruppel-like factor 4 (KLF4) is required for maintenance of breast cancer stem cells and for cell migration and invasion*. *Oncogene*, 2011. **30**(18): p. 2161-72.
236. Pandya, A.Y., et al., *Nuclear localization of KLF4 is associated with an aggressive phenotype in early-stage breast cancer*. *Clin Cancer Res*, 2004. **10**(8): p. 2709-19.
237. Wei, D., et al., *Drastic down-regulation of Krüppel-like factor 4 expression is critical in human gastric cancer development and progression*. *Cancer Res*, 2005. **65**(7): p. 2746-54.
238. Dang, D.T., et al., *Overexpression of Krüppel-like factor 4 in the human colon cancer cell line RKO leads to reduced tumorigenicity*. *Oncogene*, 2003. **22**(22): p. 3424-30.
239. Katsuta, E., et al., *High expression of bone morphogenetic protein (BMP) 6 and BMP7 are associated with higher immune cell infiltration and better survival in estrogen receptor -positive breast cancer*. *Oncol Rep*, 2019. **42**(4): p. 1413-1421.
240. Hu, F., et al., *BMP-6 inhibits cell proliferation by targeting microRNA-192 in breast cancer*. *Biochimica et Biophysica Acta (BBA) - Molecular Basis of Disease*, 2013. **1832**(12): p. 2379-2390.
241. Takahashi, M., et al., *Bone morphogenetic protein 6 (BMP6) and BMP7 inhibit estrogen-induced proliferation of breast cancer cells by suppressing p38 mitogen-activated protein kinase activation*. *J Endocrinol*, 2008. **199**(3): p. 445-55.
242. Kalluri, R. and R.A. Weinberg, *The basics of epithelial-mesenchymal transition*. *The Journal of clinical investigation*, 2009. **119**(6): p. 1420-8.
243. Massagué, J., *TGF $\beta$  in Cancer*. *Cell*, 2008. **134**(2): p. 215-30.
244. Kimura, N., et al., *BMP2-induced apoptosis is mediated by activation of the TAK1-p38 kinase pathway that is negatively regulated by Smad6*. *J Biol Chem*, 2000. **275**(23): p. 17647-52.
245. Kim, S.-H., et al., *Novel mechanistic targets of forkhead box Q1 transcription factor in human breast cancer cells*. *Molecular Carcinogenesis*, 2020. **59**(10): p. 1116-1128.

## 10. List of Publications



UNIVERSITY of  
DEBRECEN

UNIVERSITY AND NATIONAL LIBRARY  
UNIVERSITY OF DEBRECEN

H-4002 Egyetem tér 1, Debrecen  
Phone: +3652/410-443, email: publikaciok@lib.unideb.hu

Registry number: DEENK/418/2022.PL  
Subject: PhD Publication List

Candidate: Sham Jdeed  
Doctoral School: Doctoral School of Molecular Cellular and Immune Biology

### List of publications related to the dissertation

1. **Jdeed, S.**, Lengyel, M., Uray, I. P.: Redistribution of the SWI/SNF Complex Dictates Coordinated Transcriptional Control over Epithelial-Mesenchymal Transition of Normal Breast Cells through TGF- $\beta$  Signaling.  
*Cells*. 11 (17), 1-15, 2022.  
DOI: <http://dx.doi.org/10.3390/cells11172633>  
IF: 7.666 (2021)
2. **Jdeed, S.**, Erdős, E., Bálint, B. L., Uray, I. P.: The Role of ARID1A in the Nonestrogenic Modulation of IGF-1 Signaling.  
*Mol. Cancer Res.* 20 (7), 1071-1082, 2022.  
DOI: <http://dx.doi.org/10.1158/1541-7786.MCR-21-0961>  
IF: 6.333 (2021)

**Total IF of journals (all publications): 13,999**

**Total IF of journals (publications related to the dissertation): 13,999**

The Candidate's publication data submitted to the iDEa Tudóstér have been validated by DEENK on the basis of the Journal Citation Report (Impact Factor) database.

05 September, 2022



## 11. Acknowledgment

I would like to express my gratitude to Hungary, Tempus Public Foundation, and the Stipendium Hungaricum scholarship for giving me the chance to peruse my Ph.D. studies.

I am truly thankful to my supervisor Dr. Iván P. Uray for the unlimited support throughout my PhD journey. I am grateful for the valuable time discussing scientific topics, for being available all the time for questions and suggestions, for his trust and encouragement.

I would like to express my thanks to Dr. Bálint L Bálint for being open and available for any work-related discussion and for his valuable suggestions.

I would like to thank Dr. Beáta Scholtz for introducing me and many students to the Galaxy platform.

I would like to thank Dr. Szilárd Póliska and Erzsébet Mátyás for their professional work in regards of sequencing ChIP DNA samples

I am thankful to my colleague Dr. Edina Erdős for being available for discussion overseas and particularly for her help in learning the ChIP experiment

Many thanks to Dr. Éva Csósz and Dr. Gergő Kalló for giving me the chance to learn and work with Mass Spectrometry in the proteomic core facility University of Debrecen

I would like to express my thanks to my current and previous colleagues Máté Lengyel, Patrícia Kálmán, and Júlia Buslig, and all the other OTREL members for their support and for introducing me to many techniques in the lab.

I would like to express my thanks to all the professors and colleagues of the doctoral school of Molecular Cellular and Immune Biology for the unlimited support.

A big thank to all the workers in the Invitro diagnostic building, 3rd floor for being one big family.

I would like to thank my friends all over the world for their support.

Last but not least, I am grateful for the great support in my life; my parents, my father Nedal Jdeed, and my mother Mona Ebraheem, for their love, trust and for believing in me which gave me the strength to survive and enjoy this wonderful journey. Much gratitude is to my elder sisters Leen and Rama who paved the way for me to reach this level.

**While you are thanking amazing people in your life, remember to thank yourself!**

**Thank you, Sham!**

**06.09.2022**

## 12. Keywords

Breast cancer

Rexinoids

Bexarotene

Carvedilol

Chemoprevention

Chromatin Remodeling

SWI/SNF SWItch/Sucrose Non-Fermentable

ARID1A AT-rich interactive domain-containing protein 1A

IGF1R Insulin-like growth factor1 receptor

IRS1 Insulin receptor substrate-1

FOXQ1 Forkhead Box Q1

TGF- $\beta$  Transforming growth factor beta

EMT Epithelial–Mesenchymal Transition